NPFXD MOTIF-CONTAINING PROTEINS IN *Aspergillus nidulans*

A Dissertation

by

BLAKE ERIN COMMER

Submitted to the Office of Graduate and Professional Studies of
Texas A&M University
in partial fulfillment of the requirements for the degree of

DOCTOR OF PHILOSOPHY

Chair of Committee,	Brian D. Shaw
Committee Members,	Heather H. Wilkinson
	Herman B. Scholthof
	Beiyan Nan
Head of Department,	Leland S. Pierson III

May 2020

Major Subject: Plant Pathology

ABSTRACT

Filamentous fungi grow by producing tubular, thread-like structures called hyphae. These hyphal cells elongate in a unidirectional, polarized manner, by synthesizing and adding new cell wall and membrane exclusively at the apex. Until recently, the model of hyphal growth had been based solely on exocytosis through the Spitzenkörper (SPK), an organized body of secretory vesicles found only in growing fungal hyphae. However, it is now generally presumed that endocytosis is also required, and that a mechanism called apical recycling maintains a balance between the coupled processes of endocytosis and exocytosis. This equilibrium requires both the SPK and a sub-apical collar, which is enriched for endocytosis and originates approximately 1-5 μm distal to the SPK. As new membrane is added and cell wall is synthesized at the apex of each hypha, cargo is also internalized in the sub-apical collar. Here, a bioinformatics approach was utilized to methodically identify 39 *Aspergillus nidulans* proteins predicted to contain an NPFxD peptide motif, which is a necessary endocytic signal sequence in yeast. I hypothesized that some of these NPFxD motif-containing proteins in *A. nidulans* would localize to at least one of three apical regions where cargoes are typically observed (the SPK, the sub-apical collar, and the apical crescent). Those with apical localizations are also likely to be associated with the establishment or maintenance of polarized growth, and could even be cargo for endocytosis. In order to test this hypothesis, the expression and localization of motif-containing proteins in *A. nidulans* was evaluated by endogenously inserting GFP or mCherry and imaging during polarized growth. The localization patterns of confirmed

GFP proteins studied thus far supported the hypothesis that this motif is likely to mark proteins for localization to one or more of the three predicted regions near the growing fronts of hyphae. When apical localization was observed, a gene deletion strain was then constructed to further investigate the function of each protein. Mutants from initial deletion experiments demonstrated an inability to maintain polarization and displayed atypical development in various cell types, which also suggests that the genes in question could be involved in membrane turnover.

DEDICATION

This dissertation and the work completed toward the fulfillment of the requirements for a Doctorate of Philosophy in Plant Pathology and Microbiology are dedicated to Dr. Salomon Bartnicki-Garcia, Investigator Emeritus at the Department of Microbiology, Ensenada Center for Scientific Research and Higher Education in Baja California, Mexico. This dissertation is also dedicated to Dr. Zachary Schultzhaus, Research Biologist II at the U.S. Naval Research Laboratory in Fort Washington, Maryland.

ACKNOWLEDGEMENTS

I would like to again acknowledge the members of my graduate academic committee, including former members of the committee (Dr. Kevin Ong and Dr. Xiaorong Lin). Each member of this committee offered invaluable assistance, advice, and knowledge throughout my doctoral studies and toward the completion of this dissertation.

I would also like to acknowledge my Shaw lab siblings, Dr. Zach Schultzhaus and Joe Vasselli, for their endless encouragement and entertainment throughout my graduate career. Zach was an incredibly patient teacher and instrumental to my success in tagging and deleting proteins. Joe served as a consistent source of encouragement and laughter, for which I am truly grateful.

Additionally, I would like to acknowledge my colleagues at Texas A&M University and elsewhere that assisted through thoughtful discussions and inspirations, including: Dr. Rosa Mouriño-Pérez, Dr. Salomon Bartnicki-Garcia, Marisela Garduño-Rosales, Dr. Thomas Isakeit, Dr. Daniel Ebbole, Dr. Michelle Momany, Dr. Eli Borrego, Dr. Stanislav Vitha, and Dr. Robert Roberson.

I would also like to acknowledge my family members for their unconditional love, support, and encouragement throughout my life, as well as my time in graduate school: my parents Kathy and David Commer, my sister Samantha Fahrney, my brother-in-law Chris Fahrney, and my grandparents Jeanie Hill, Sam Hill, Frankey Commer, and Dr.

William (Bill) J. Commer. My dogs (Riley and Lilly) have also been unbelievably supportive and loving on a daily basis throughout this process.

Finally, I would like to acknowledge all of the students who spent time working on this project, including Grace Cunningham, Stephon Warren, Will Porter, Alison Donovan, Nicholas Allinson, Changzhi Han (visiting scientist), Joseph Vasselli, Caroline Burks, and Alexis Romero.

Thanks also go to my friends, colleagues, and the PLPM departmental faculty at Texas A&M University.

CONTRIBUTORS AND FUNDING SOURCES

Contributors

This work was supervised by a dissertation committee consisting of Professor Brian D. Shaw (chair), Professor Herman Scholthof, and Professor Heather H. Wilkinson of the Department of Plant Pathology and Microbiology, and Professor Beiyan Nan of the Department of Biology. Previous committee members include Dr. Kevin Ong of the Department of Plant Pathology and Microbiology, and Dr. Xiaorong Lin of the Department of Biology.

All work conducted for this dissertation was completed independently by the student.

Funding Sources

Graduate study was supported by an Excellence Fellowship from Texas A&M University College of Agriculture and Life Sciences, a Curriculum Enhancement Grant from the Texas A&M Instructional Technology Services, and a Teaching Assistantship from the Department of Plant Pathology and Microbiology.

Funding was also received from the Mycological Society of America, including an MSA Graduate Student Fellowship and the Salomon Bartnicki-Garcia Award in Cell Biology.

This work was also supported in part by USDA NIFA under Project Number TEX0-1-9018. Its contents are solely the responsibility of the authors and do not necessarily represent the official views of the United States Department of Agriculture.

NOMENCLATURE

aa	Amino Acid
EE	Early Endosome
FF	Filamentous Fungi
GFP	Green Fluorescent Protein
MM	Minimal Medium
MW	Molecular Weight
SPK	Spitzenkörper
TGN	*trans*-Golgi network
TMD	Transmembrane Domain

TABLE OF CONTENTS

Page

LIST OF FIGURES

Page

CHAPTER I

INTRODUCTION: CURRENT VIEWS ON ENDOCYTOSIS IN FILAMENTOUS FUNGI*

SUMMARY

Filamentous fungi grow by adding cell wall and membrane exclusively at the apex of tubular structures called hyphae. Growth was previously believed to occur only through exocytosis at the Spitzenkörper, an organized body of secretory macro- and microvesicles found only in growing hyphae. More recent work has indicated that an area deemed the sub-apical collar is enriched for endocytosis and is also required for hyphal growth. It is now generally believed that polarity of filamentous fungi is achieved through the balancing of the processes of endocytosis and exocytosis at these two areas. This review is an update on the current progress and understanding surrounding the occurrence of endocytosis and its spatial regulation as they pertain to growth and pathogenicity in filamentous fungi.

INTRODUCTION

Filamentous fungi (FF) uniquely produce tubular cells called hyphae in a polarized manner. This occurs through the synthesis and addition of new cell wall and membrane exclusively at the apex (Riquelme et al., 2018; Steinberg et al., 2017). The paradigm of

*Reprinted with permission from "Current Views on Endocytosis in Filamentous Fungi" by Blake Commer and Brian D. Shaw, 2020. *Mycology an International Journal on Fungal Biology* (2150-1211), DOI: 10.1080/21501203.2020.1741471, Copyright 2020 by Taylor & Francis Group.

hyphal growth has previously been to focus on exocytosis through the Spitzenkörper (SPK), an organized body of secretory macro- and microvesicles which is found only in growing fungal hyphae (Bartnicki-Garcia et al., 1995; Bartnicki-Garcia et al., 1989; Reynaga-Peña et al., 1997; Virag and Harris, 2006). An early hypothesis proposed that the establishment of polarity is a stochastic process that autonomously transpires without the need for membrane markers (Harris, 2006). However, the evidence provided since then indicates that the series of events is much less random. More recent work has forced reconsideration due to the discovery of an area that is enriched for endocytosis. This work has indicated that the area distal to the SPK, deemed the sub-apical collar, is also required for hyphal growth (Taheri-Talesh et al., 2008; Upadhyay and Shaw, 2008). It is now generally understood that polarity of FF is achieved through the balancing of the processes of endocytosis and exocytosis.

Endocytosis in yeast has been thoroughly characterized (Goode et al., 2015); however, comparatively little is known about endocytosis in FF (**Figure I.1**). In particular, little attention has been paid to proteins whose localizations and functions border between endocytosis and exocytosis in the growing hyphal apex. While a variety of process are conserved from yeasts to FF, not all components are identical, and some must be compensated for in order to afford the multiple axes of polarity and increased extension rates observed in FF. The most well-studied single-cell yeasts, *Saccharomyces cerevisiae* and *Schizosaccharomyces pombe*, also display polarized growth. However, this budding or fission growth is limited by the cell cycle, while hyphae of FF are able to continuously

extend in an unrestricted unidirectional manner (Takeshita, 2016). Evidence that endocytosis itself varies between yeasts and FF has also been provided through studies on clathrin localization. While clathrin is observed both internally as well as at the cortex of *S. cerevisiae* cells, a corresponding localization to the endocytic collar is not observed in *A. nidulans* (Newpher et al., 2005; Schultzhaus et al., 2017a).

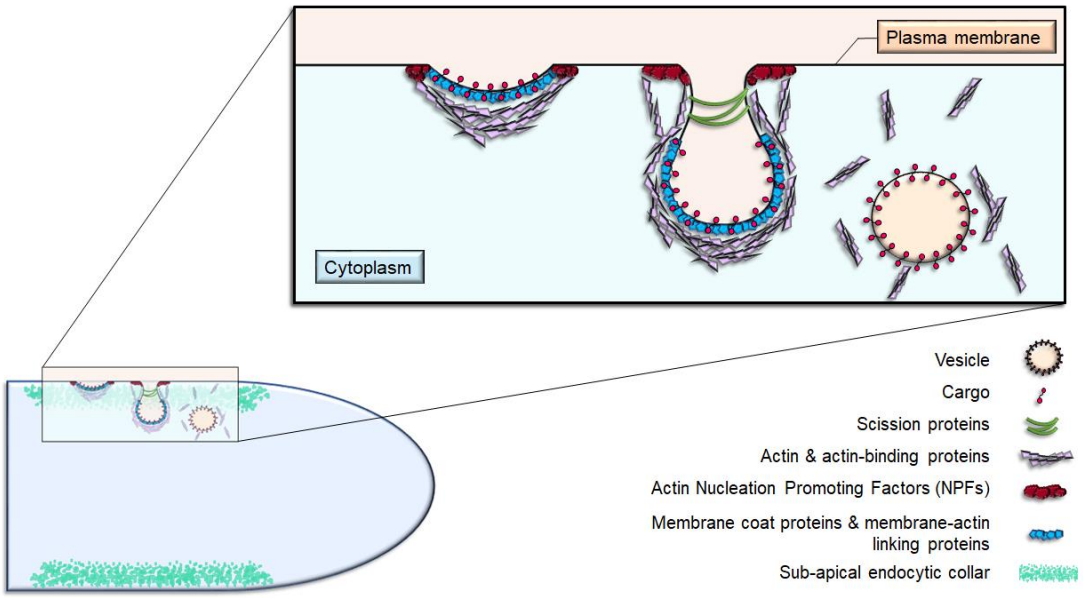

Figure I.1 – The Endocytic Process at the Sub-apical Collar of FF.
Schematic depiction of the process of endocytosis as elucidated from *Saccharomyces cerevisiae* (Lu et al., 2016). A hyphal apex is shown in the lower left corner, with a close-up partial representation of membrane bending, invagination, and scission of a vesicle. General components are highlighted as the specific proteins involved may vary from one species to another. One major difference from *S. cerevisiae* is that clathrin has been shown not to localize to endocytic sites in the sub-apical collar in some filamentous fungi (Schultzhaus et al., 2017a). *Note: image was inspired by (Lu et al., 2016), and is not drawn to scale.*

Several reviews have summarized the various aspects of polarized growth and hyphal morphogenesis in FF over the past decade (Harris, 2011; Peñalva, 2010; Riquelme et al., 2018; Shaw et al., 2011; Steinberg, 2014; Steinberg et al., 2017; Takeshita, 2016; Verdín et al., 2019). For a more comprehensive review on the process of endocytosis itself, see (Steinberg, 2014; Steinberg et al., 2017). The priority of this review is to update the current progress and understanding surrounding the occurrence of endocytosis as it pertains to growth in FF. Evidence to support the necessity of endocytosis for the maintenance of normal hyphal extension and shape in FF is provided here, as well as various theories behind its spatial regulation. Our understanding of this process as well as hyphal growth is crucial, as each one is required for the disease progression of plants, animals, and humans (Köhler et al., 2014; Riquelme et al., 2018; Zeilinger et al., 2016).

DOES ENDOCYTOSIS OCCUR IN FILAMENTOUS FUNGI?

It has been demonstrated that many proteins associated with membrane turnover (such as adapter proteins, cargoes, endocytic machinery, etc.) localize to three different apical regions of growing hyphae: the SPK, the apical crescent, and the sub-apical collar (**Figure I.2**) (Araujo-Bazan et al., 2008; Sudbery, 2011; Upadhyay and Shaw, 2008). Since endocytosis is a vital life process in FF, it is imperative that it is evaluated based on studies which implement live cell imaging. Fluorescently tagging proteins to evaluate localization patterns was a rather arduous process at the turn of the century, and it still can be in many organisms, particularly those without sequenced or publicly available genomes. Alternatively, select vital stains or dyes that had been created for use in live cell imaging

were instrumental in allowing more comprehensive studies at the time. It was through the use of these dyes that endocytosis was first discovered in FF (Hoffmann and Mendgen, 1998). The former belief behind the mechanisms of hyphal growth was based solely on the notion of exocytosis, which predominantly occurs through the SPK. However, FM4-64 staining, combined with the discovery of the sub-apical collar and genomic data, forced reevaluation of the commonly accepted notion of the vesicle supply center.

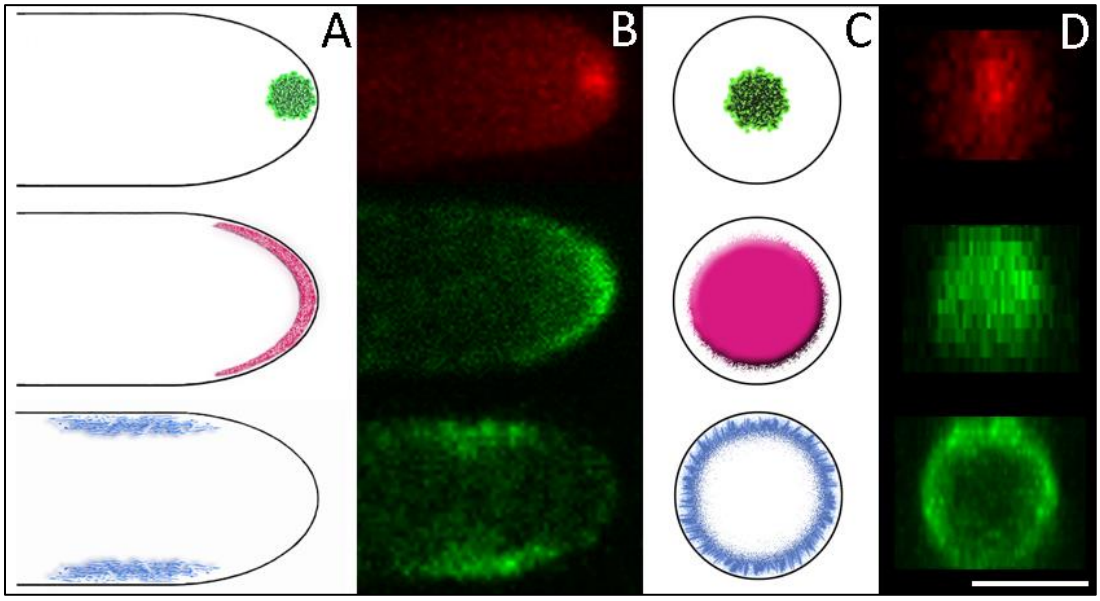

Figure I.2 – Three Apical Areas to which Proteins Associated with Membrane Turnover Localize.
(**A**) Schematic depiction of the three areas associated with endocytosis at the apices of growing hyphae, viewed from the side. (**A, top**) The Spitzenkörper (SPK) stains readily with the vital stain FM4-64, suggesting that it functions in the recycling of endocytic vesicles that are produced at the hyphal tip. (**A, middle**) Cell-end markers line the apical crescent, or dome, and localize growth machinery to hyphal tips. (**A, bottom**) The sub-apical collar is an area enriched for endocytosis where apical recycling takes place. (**B**) Fluorescence images of each of the three areas, represented by *Aspergillus nidulans* DnfB::GFP (Schultzhaus et al., 2015), HapA::GFP (unpublished data), and EcoA::GFP (unpublished data), respectively. (**C-D**) Schematic depiction & fluorescence images of the three areas as viewed from the apex of the hypha. *Scale bar 2.5 µm.*

History of Markers for Endocytosis

Several membrane-selective dyes and markers have previously been utilized in order to investigate the countless processes and pathways occurring within living fungi. For example, Lucifer Yellow, TMA-DPH, FITC-dextran, FM1-43, and FM4-64 were all utilized in an attempt to visualize internalization and subsequent trafficking (Fischer-Parton et al., 2000; Peñalva, 2005). Of the various dyes used, the lipophilic marker dye FM4-64 was particularly instrumental in revolutionizing the current understanding of endocytosis in FF.

FM4-64 was initially shown to be endocytosed at the plasma membrane in *S. cerevisiae* (Vida and Emr, 1995), and it subsequently became a vital stain which was, and still is, considered a marker for endocytosis in the yeasts. This discovery was soon-after followed by the application of FM4-64 to FF. In *Uromyces fabae*, FM4-64 uptake was observed within seconds of its application, and the most intense localization was to the membrane at the hyphal apex, making it the first evidence for endocytosis in a fungal germ tube (Hoffmann and Mendgen, 1998). This sparked an interest in using it to study FF, and shortly thereafter, endocytosis was also demonstrated in ungerminated and germinated spores of the FF *M. grisea* (Atkinson et al., 2002). In addition to labeling the apical hyphal membrane, FM4-64 uptake was also observed in the SPK (Fischer-Parton et al., 2000). This evidence was rather controversial, particularly because the SPK was believed to be involved only with apical secretion through Golgi-derived exocytic vesicles (Reynaga-Peña et al., 1997). These new data, however, indicated that the SPK functions additionally

in recycling endocytic vesicles produced at the hyphal tip (Upadhyay and Shaw, 2008). Furthermore, it suggested that endocytosis is also vital for hyphal growth, which has since been corroborated by numerous studies.

In the years following this discovery, FM4-64 was applied to a multitude of filamentous species (Atkinson et al., 2002; Fischer-Parton et al., 2000). While the use of FM4-64 in FF was still relatively limited in the early 2000s (Peñalva, 2005), its use is now considered standard practice for experiments involving endocytic or apically localized proteins in FF.

The Discovery of the Sub-apical Collar

The evidence provided from various experiments involving FM4-64 made it clear that the internalization of membranes also contributes to apical growth. This was subsequently reinforced by the discovery of the sub-apical collar in *A. nidulans* (Araujo-Bazan et al., 2008; Taheri-Talesh et al., 2008; Upadhyay and Shaw, 2008), which is an area enriched for endocytosis that lies 1-5 µm distal to the SPK. The location of the collar in the sub-apex is maintained over time during hyphal growth, and dissipates with the cessation of growth, similar to the maintenance of the SPK. Prior to this discovery, it was primarily believed that fungal growth occurred due to secretion through the SPK.

Theories Regarding the Need for Endocytosis in the Collar

It was previously shown that endocytosis in *S. pombe* is spatially associated with the actin cytoskeleton during polarized growth (Gachet and Hyams, 2005). Therefore, it does not

come as a surprise that the “zone of endocytosis” in FF also happens to be where actin is predominantly and intensely localized (Delgado-Alvarez et al., 2010; Schultzhaus et al., 2016; Upadhyay and Shaw, 2008). However, it is still unclear why endocytosis is enriched in the sub-apical collar. At this time, several theories have been proposed to elucidate the reasoning behind the presence and spatial regulation of the collar in FF. The original hypothesis for tip growth proposed that the SPK was comprised of Golgi-derived exocytic vesicles which were destined to fuse with the apex. However, this vesicle supply center concept needed to be expanded to account for the function of endocytosis at the apex and sub-apical collar once it was identified in FF (Gierz and Bartnicki-Garcia, 2001).

One explanation is provided by the apical recycling model, which indicates endocytosis at the sub-apical collar maintains the polarization of apically localized membrane proteins (Hernandez-Gonzalez et al., 2018; Shaw et al., 2011). These membrane proteins would in turn be marking areas of polarization at the apices of hyphae, and they would be displaced along the membrane during growth. These proteins would therefore need to then be removed by the sub-apical collar in order for the hyphoid shape to be maintained.

Recently, another hypothesis suggested that endocytosis in the collar acts as a means for removing excess secreted plasma membrane, which has recently been quantified in *Neurospora crassa* (Bartnicki-Garcia et al., 2018; Riquelme et al., 2018). Based on the data provided by Bartnicki-Garcia et al. in 2018, an estimated 9800 vesicles per minute are needed in order to maintain hyphal growth and cell wall expansion. This is likely on

the higher end compared to many other FF due to the large size and fast growth rate of *N. crassa* hyphae. Nonetheless, the number of vesicles discharged is estimated, on the lower end, to be around 59,000 vesicles per minute (Bartnicki-Garcia et al., 2018). Some of these proteins must therefore be recycled at the sub-apical collar in turn. In this model, endocytosis acts primarily to remove the excess membrane provided through secretion, and does so efficiently due to its close proximity to the apex. While the idea of removing excess plasma membrane was proposed as an explanation for reducing the sheer quantity of secreted membrane, it also parallels the apical recycling model.

Another comparable hypothesis is that the apex is lined with proteins which localize to the plasma membrane and are deemed "cell-end markers" or "polarity markers." Cell-end markers, such as *A. nidulans* KipA, TeaA, and TeaR, have been shown to be involved in localizing growth machinery to hyphal tips (Konzack et al.; Takeshita et al., 2013). These polarized proteins are cytoskeleton-dependent, and subsequently direct cell polarity. Secretion at the hyphal apex dilutes the accumulation of polarity markers, creating a cyclical process of assembling and disseminating cell-end markers in a pulse-like pattern (Takeshita, 2016). This proposed circulation of proteins also bares striking similarities to the apical recycling model. These are not mutually exclusive theories, as each one was proposed through the perspective of a different area at the hyphal apex.

EXPERIMENTAL EVIDENCE

Regardless of the reasoning for the location and maintenance of the sub-apical collar in FF, there is now little doubt about its existence. Countless experiments have shown that a sub-apical area enriched for endocytosis arises during growth. Further studies have provided evidence for the recycling of various polarized proteins. For example, the essential *A. nidulans* chitin-synthase ChsB is polarized through indirect endocytic recycling, which involves both exocytosis at the apex and endocytosis at the sub-apical collar. ChsB is subsequently trafficked to the *trans*-Golgi Network (TGN) cisternae and then ultimately re-delivered to the apex (Hernandez-Gonzalez et al., 2018). Additional evidence is discussed in more detail below.

Fimbrin Mutant in *Aspergillus*

The processes of endocytosis and exocytosis are synchronized and regularly maintain a spatial and temporal relationship during growth. Evidence for this relationship has been provided in the form of multiple mutational studies. When a gene involved in one of the two processes is disrupted, so too is normal hyphal elongation and the uniquely notable hyphoid shape. For example, when the *A. nidulans* F-actin cross-linking gene and endocytic marker fimbrin (*fimA*) was disrupted, cells displayed abnormal isotropic swelling and an inability to otherwise maintain polarity. Furthermore, FimA and the secretory vesicle marker GsaA were fused with mCherry and localized using the conditional *niiA* promoter in *A. nidulans*. Aberrant growth was evident when endocytosis was disrupted, and neither the SPK nor the standard zone of endocytosis at the collar could

be seen (Upadhyay and Shaw, 2008). This evidence highlighted the partnership of these two associated processes, and the aforementioned apical recycling model was proposed as a result of these findings.

NPFxD Motif

One of only two endocytic signal sequences discovered in yeast to date is the $NPFX_{(1,2)}D$ motif (and the similar but less effective variations, DPFxD, NPF, or DPF), which was shown to mark proteins for endocytosis and is required for polarity in yeast (Howard et al., 2002; Piao et al., 2007; Tan et al., 1996). This motif is found in multiple membrane proteins, and is recognized by the adapter protein Sla1p through an interaction with the SHD1 (Sla1p Homology Domain) region (Costa et al., 2005). Mutating one or more of the initial three residues in this motif to Alanine (A) has been shown to halt endocytic uptake of the protein (Tan et al., 1996). Studies have shown that the contribution of the motif to the function and localization of specific endocytic cargo proteins (Liu et al., 2007; Schultzhaus et al., 2015). For example, yeast proteins Drs2p and Dnf1p each contain at least one NPFxD motif. In wild-type (WT) cells, Drs2p localizes to the TGN and Dnf1p localizes both to the plasma membrane and to endo-membranes. When the NPFxD-dependent endocytic mechanisms were inactivated, the localization of each protein was altered (Liu et al., 2007). To further test the motif, as well as the apical recycling model, the orthologous NPFxD-containing protein DnfA in *Aspergillus nidulans* was also mutated. DnfA::GFP displayed polarized localization to the apical plasma membrane and the SPK; however, this polarized localization was also lost upon mutating the motif to

AAFxD (Schultzhaus et al., 2015). The re-localization of DnfA::GFP upon disruption of the motif corroborates the notion that apical recycling maintains the polarization of the protein. These studies also reinforce the proposition that the peptide motif is essential for proper endocytic uptake in a variety of cargo proteins.

The Requirement of Endocytosis for Pathogenicity

Recent studies have also provided evidence that the endocytic pathway is important for pathogenicity in many plant pathogens. For example, a multitude of proteins in *Magnaporthe oryzae* have been shown to be involved in both endocytosis and pathogenicity. It was recently found that *M. oryzae* protein MoEnd3 is critical for development and virulence due to its role in mediating receptor endocytosis (Li et al., 2017b). Additionally, MoRab5A and MoRab5B, both of which are Rab5 homologs in *M. oryzae*, are critical for endocytosis and plant pathogenesis, among other things (Yang et al., 2017). Other studies have linked MoArk1, MoAbp1, MoAct1, and MoCAP proteins (among others) to endocytosis, growth, the actin cytoskeleton, and therefore, pathogenicity (Li et al., 2017a; Li et al., 2019). Investigation of *Ustilago maydis* protein Yup1 similarly demonstrated that endocytosis is essential for the beginning stages of pathogenesis (Fuchs et al., 2006). This requirement has been further demonstrated in multiple species of *Fusarium* as well. For example, *Fusarium graminearum* proteins FgMon1 and FgRab7 have been shown to play critical roles in modulating vesicle trafficking, endocytosis, and plant infection (Li et al., 2015). Deletions of FgSnc1,

FgSnx41, or FgSnx4 also affect endosomal sorting, polarized growth, and ultimately pathogenicity (Zheng et al., 2018).

Genome-wide Studies and Bioinformatic Analysis

An invaluable tool made widely available to fungal biologists in recent years is bioinformatic analysis. Combined with genome-wide studies, these analyses allow for evolutionary relationships and dynamics to be revealed and reconsidered. Examples of this include the recently elucidated origin of fungal hyphae and adaptation mechanisms in dimorphic fungi (Kiss et al., 2019; Muñoz et al., 2018). Trends within and between organisms have been made visible with the availability of databases of information, and the field has been able to utilize this information to expand the current understanding of signaling networks and orthologous relationships. Bioinformatic analysis of fungal genomes has also provided overwhelming evidence that endocytosis and endocytic recycling are important life processes for FF. For example, sequencing and annotating the *A. nidulans* genome revealed that there were many more genes implicated in vegetative growth and morphogenesis than in yeast (Harris et al., 2009). In addition, genomic studies using expressed sequence tag (EST) analyses and whole-genome sequencing in *A. oryzae* have elucidated genes involved in growth and secretion (Abe et al., 2006). In *A. niger*, a transcriptomic fingerprint was also developed for apical branching and hyphal elongation (Meyer et al., 2009).

CONCLUSIONS & OUTSTANDING QUESTIONS

Both endocytosis and the spatial coupling of endocytosis with secretion have now been shown to be of great importance for hyphal extension in several FF. In the last two decades, our understanding of how FF grow has been entirely revolutionized by the discovery of endocytosis and the areas in which it occurs. Since then, many questions have been answered, and even more have been posed.

Single particle tracking, fluorescence recovery after photobleaching (FRAP), and various other advanced microscopy techniques have provided a means for scientists to answer pressing questions about endocytosis. For example, data on the quantification of endocytosis was previously very limited (Thilo, 1985); however, Bartnicki *et. al* were able to implement a comprehensive FRAP protocol in 2018 and better estimate the number of vesicles that are endocytosed in the sub-apical collars of *N. crassa* hyphae. This impressive milestone serves as a baseline on which others in the field can build. This also answered multiple questions posed by Penalva *et. al* in 2010 regarding whether or not the apex contains an excess of membrane for which endocytosis compensates. It was found that, while endocytosis does partially compensate for the excess membrane, there is still far more membrane produced at the apex than endocytosis can account for. This result was somewhat unexpected and suggests that perhaps these secreted proteins function in additional ways that we have yet to identify. It is possible that there are additional routes of endocytosis that are not adequately measured by this method, or that the overwhelming amounts of molecules which are recycled cannot be captured in their entirety by FRAP

data alone. A reverse genetics approach to identify genes which encode the endocytosis peptide motif NPFxD is currently underway. In addition, whole genome sequencing provides an opportunity to identify genes from mutant collections created in the classical genetics era that are involved in endocytosis.

It was also recently suggested that "endocytic components are underexplored targets for engineering fungal cell factories" (Cairns et al., 2019). Many species of fungi are industrially utilized and harvested in mass for useful molecules such as enzymes, proteins, secondary metabolites, and organic acids (Cairns et al., 2018; Cairns et al., 2019). Since many enzymes and molecules are secreted at the apex, the amount produced tends to initially correspond to the number of hyphal tips. However, an increased number of hyphal tips does not always correlate to an elevation in protein concentration. A recent explanation for this is that unconventional protein secretion pathways are activated during the fermentation process, meaning secretion is no longer predominantly occurring at the apex, but instead through the cell membrane or septa (Veiter et al., 2018). Little work has been done to investigate the role of endocytosis in the fermentation process, even though we know that the processes of exocytosis and endocytosis are tightly coupled. It is entirely possible that the decrease in overall secretion could instead be due to an increase in endocytosis, or an alteration of the specific cargo which is endocytosed. The preference for recycled products could fluctuate with various environmental conditions, such as diauxic shifts, for example. If this is elucidated, the fermentation environment could

potentially be manipulated or optimized based on an ideal organismal ratio, or by first increasing endocytosis.

Furthermore, the dynamic localization of GFP-fusion proteins must continue to be tested. Researchers should take advantage of organisms that cooperate in large-scale studies so that curated databases such as FungiDB can consolidate and distribute these data (Stajich et al., 2012). Not only do we need to characterize and localize multiple proteins, but we also need to investigate the relationships among them and focus on those whose roles vary between yeast-like and hyphal growth. Since many pathogenic fungi are dimorphic, priority should also be given to signaling networks and proteins that do not follow the typical yeast model of life and growth, or that are specific to FF altogether.

As the availability and affordability of advanced technology increases, so too will the discoveries in this field. The development of advanced microscopic tools and methods for bioinformatic analysis will continue to significantly contribute to our current knowledge on filamentous fungal growth, as well as its interconnectedness with the environment.

CHAPTER II

LOCALIZATION OF NPFXD MOTIF-CONTAINING PROTEINS IN *Aspergillus nidulans*

SUMMARY

During growth, filamentous fungi produce polarized cells called hyphae. It is generally presumed that polarization of hyphae is dependent upon secretion through the Spitzenkörper, as well as a mechanism called apical recycling, which maintains a balance between the tightly coupled processes of endocytosis and exocytosis. Endocytosis predominates in an annular domain called the sub-apical endocytic collar, which is located in the region of plasma membrane 1-5 μm distal to the Spitzenkörper. It has previously been proposed that one function of the sub-apical endocytic collar is to maintain the apical localization of polarization proteins. These proteins mark areas of polarization at the apices of hyphae. However, as hyphae grow, these proteins are displaced along the membrane and some must then be removed at the sub-apical endocytic collar in order to maintain the hyphoid shape. While endocytosis is fairly well characterized in yeast, comparatively little is known about the process in filamentous fungi. Here, a bioinformatics approach was utilized to identify 39 *Aspergillus nidulans* proteins that are predicted to be cargo of endocytosis based on the presence of an NPFxD peptide motif. This motif is a necessary endocytic signal sequence first established in *Saccharomyces cerevisiae*, where it marks proteins for endocytosis through an interaction with the adapter protein Sla1p. It is hypothesized that some proteins that contain this NPFxD peptide

sequence in *A. nidulans* will be potential targets for endocytosis, and therefore will localize either to the endocytic collar or to more proximal polarized regions of the cell, e.g. the apical dome or the Spitzenkörper. To test this, a subset of the motif-containing proteins in *A. nidulans* was tagged with GFP and the dynamic localization was evaluated. The documented localization patterns support the hypothesis that the motif marks proteins for localization to the polarized cell apex in growing hyphae.

INTRODUCTION

Filamentous fungi (FF) produce hyphae that elongate in a unidirectional, polarized manner, by synthesizing and adding new cell wall and membrane exclusively at the apex (Riquelme et al., 2018; Steinberg et al., 2017). Until recently, the paradigm of hyphal growth has been to focus on exocytosis through the Spitzenkörper (SPK), which is an organized body of secretory vesicles found only in growing fungal hyphae (Bartnicki-Garcia et al., 1989; Reynaga-Peña et al., 1997; Virag and Harris, 2006). However, more recent work has indicated that the sub-apical collar, an area enriched for endocytosis distal to the apex, is also required for hyphal growth (Taheri-Talesh et al., 2008; Upadhyay and Shaw, 2008). Why endocytosis is enriched in the sub-apical collar remains a topic of uncertainty. The phenomenon has been shown to act, in part, as a means of removing excess plasma membrane in the filamentous fungus *Neurospora crassa* (Bartnicki-Garcia et al., 2018; Riquelme et al., 2018). A similar explanation that has been proposed is the apical recycling model, which suggests that polarization of apically localized membrane proteins is maintained through endocytosis at the sub-apical collar (Hernandez-Gonzalez

et al., 2018; Shaw et al., 2011). A prediction of the model would be that these proteins mark areas of polarization at the apices of hyphae. Furthermore, these proteins would be displaced along the membrane as hyphae grow, and some would therefore need to be removed by the sub-apical endocytic collar in order to maintain the hyphoid shape (**Figure II.1A**), which parallels the idea of plasma membrane removal. This has been substantiated by disrupting the F-actin cross-linking gene and endocytic marker fimbrin (*fimA*), which resulted in abnormally distended and lobed cells, apical swelling, and an inability to maintain hyphal polarity (Upadhyay and Shaw, 2008). Additionally, the dynamic localizations of GsaA::mCherry, a secretory vesicle marker, and FimA::mCherry were observed when endocytosis was disrupted through the use of the conditional *niiA* promoter (Schultzhaus et al., 2015). In this experiment, aberrant growth was observed in the absence of a noticeable SPK, and a standard zone of endocytosis could not be defined, highlighting the partnership of these two associated processes.

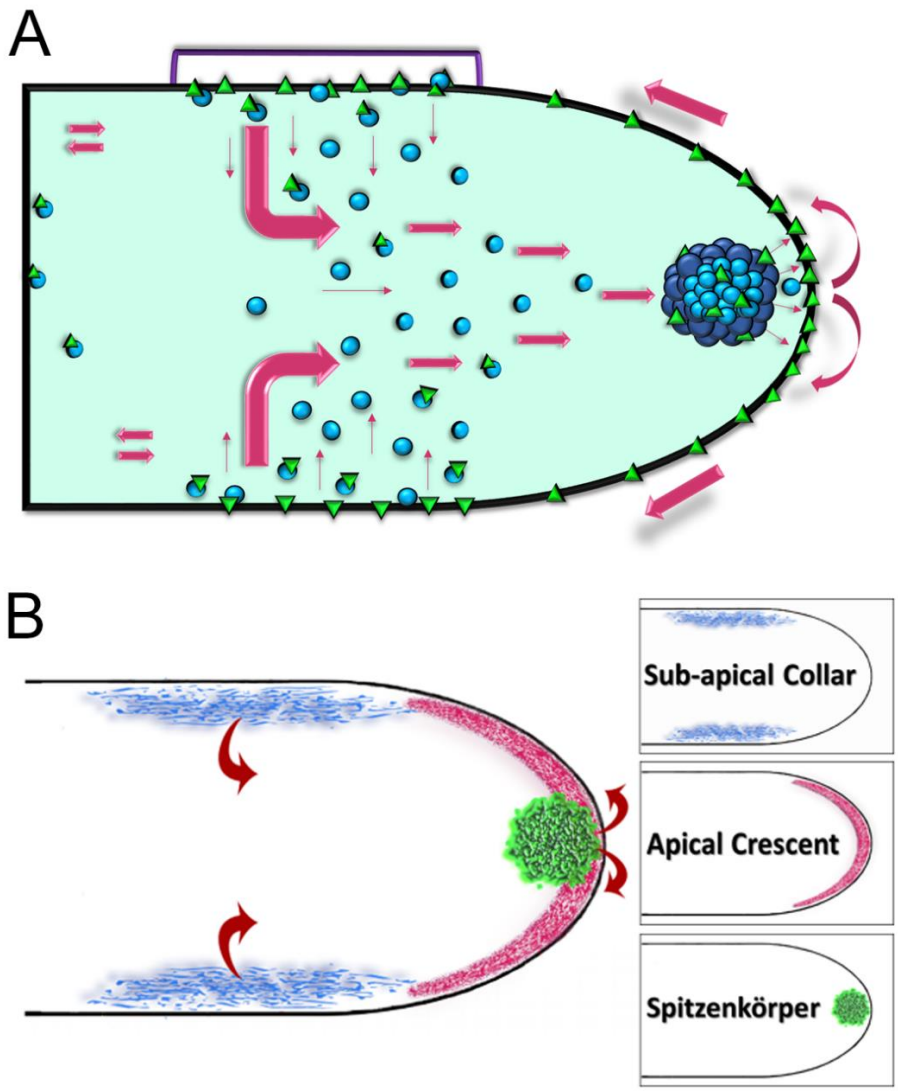

Figure II.1 – Apical Recycling Model & Predicted Localization Patterns.
(**A**) The arrows represent the cyclic flow of endocytic traffic. As secretion occurs at the apex through the Spitzenkörper (SPK), some proteins are subsequently removed from the membrane through endocytosis in the sub-apical collar, which is located in the region of plasma membrane 1-5 µm distal to the SPK. While the majority of the observed trafficking is toward the apex, some retrograde trafficking occurs as well. Here, vesicles are represented by blue circles, while cargoes are represented by green triangles. The SPK is a represented by a collection of blue vesicles at the apex. (**B**) Three areas are depicted here: the sub-apical endocytic collar, the apical crescent, or dome, and the Spitzenkörper (SPK). It is predicted that endocytic cargo proteins which contain the NPFxD peptide sequence in *A. nidulans* will localize to one or more of these areas.

The endocytic signal sequences NPFX$_{(1,2)}$D (hereafter referred to as NPFxD), and the less specific NPF and DPFxD motifs, were identified in *Saccharomyces cerevisiae* (Howard et al., 2002; Tan et al., 1996). This motif is recognized by the SHD1 (Sla1p Homology Domain) region of the adapter protein Sla1p, and is required for maintaining polarity of various proteins (Howard et al., 2002; Mahadev et al., 2007; Piao et al., 2007; Schultzhaus et al., 2015). The motif has also been found in numerous integral membrane proteins that transit the plasma membrane (Costa et al., 2005). Mutating one or more of the residues Arginine (N), Proline (P), or Phenylalanine (F) to Alanine (A) in this motif has been shown to halt endocytic uptake (Tan et al., 1996). Additional studies have tested whether this motif contributes to the function and localization of specific proteins that are cargo of endocytosis (Liu et al., 2007; Schultzhaus et al., 2015). The *S. cerevisiae* proteins Drs2p and Dnf1p each contain at least one NPFxD motif. Drs2p localizes to the TGN and Dnf1p localizes to the plasma membrane and to endo-membranes in wild-type cells. Localization of both Drs2p and Dnf1p was altered when the NPFxD-dependent endocytic mechanisms were inactivated (Liu et al., 2007). Furthermore, internalization of the cell wall stress sensor Wsc1 was blocked and polarized localization was lost upon mutation of NPFxD or expression of Sla1p lacking SHD1 (Piao et al., 2007). To test the apical recycling model in *Aspergillus nidulans*, NPFxD-containing protein DnfA was also mutated. The wild-type localization of this protein was polarized to the apical plasma membrane as well as the SPK; however, polarization was lost when the motif was mutated to AAFxD (Schultzhaus et al., 2015). These studies demonstrate the necessity of the peptide motif for proper

endocytic uptake. Furthermore, the mislocalization of DnfA upon disruption of the motif corroborates the concept of the apical recycling model.

While endocytosis in yeast is fairly well characterized (Goode et al., 2015), comparatively little is known about the proteins involved in endocytosis in FF. In particular, proteins at the interface of endocytosis and exocytosis in the growing hyphal apex have received little attention. For example, clathrin does not predominantly localize to the endocytic collar in *A. nidulans*, and the AP-2 complex plays a clathrin-independent role in endocytosis and polarized growth (Martzoukou et al., 2017; Schultzhaus et al., 2017a). These studies indicate that the intricacies of endocytosis, at least as they relate to hyphal growth, are different in FF. For this reason, it is not only necessary to identify the cargo of endocytosis, but also to prioritize the proteins being screened.

Recently, fluorescent proteins have been shown to be highly beneficial for elucidating structures at the hyphal tip (Lorang et al., 2001; Sudbery, 2011). The focus of this manuscript is to establish the conservation of the NPFxD motif as marker for apical localization in *A. nidulans* by performing an initial survey of a subset of motif-containing proteins and evaluating the dynamic localization of each. By investigating proteins which contain this motif, several previously unknown polarized proteins were identified here. A comprehensive list of the NPFxD motif-containing proteins in *A. nidulans* was established (**Table A-1**) and categorized based on predicted functions. The dynamic localization of GFP-fusion proteins was then tested. It is hypothesized that some proteins that contain the

NPFxD peptide sequence in *A. nidulans* will be targets for endocytic recycling, and therefore will localize either to the endocytic collar or to more proximal polarized regions of the cell, e.g. the apical dome or the SPK (**Figure II.1B**).

MATERIALS AND METHODS

Identifying NPFxD Motif-containing Proteins in *A. nidulans*

The *Aspergillus nidulans* proteome was queried on FungiDB (Stajich et al., 2012) using protein motif search for NPFxD, or NPF.D in Perl script. The resulting genes were then placed in functional categories based on their annotated gene ontology (GO) terms and the functions of known orthologs in other model organisms. Proteins were prioritized for this study in order to achieve representation from each functional category. Particular interest was given to proteins associated with growth and development as well as proteins specific to FF. Each gene tagged was first verified to be present as a single copy in the *A. nidulans* genome.

Strains and Culture Conditions

Strains of *A. nidulans* used or created in this study are listed in **Table A-2**. All strains were maintained on solid minimal medium (MM) with the necessary nutritional supplements, as previously described (Kaminskyj, 2001). All cultures were incubated at 30°C throughout the course of these experiments. For transformations, 1 mL of 1 x 10^6 freshly harvested conidia were grown overnight in liquid complete medium with appropriate supplements. Selection occurred on solid MM with 1.2 M sorbitol and appropriate

supplements. Crosses were prepared on MM according to standard *A. nidulans* mating techniques (Kaminskyj, 2001) with appropriate supplements as needed.

Molecular Techniques

All constructs used to create GFP strains through transformation were formed via fusion PCR (Szewczyk et al., 2007). Constructs were designed to insert eGFP in frame at the 3' end of the coding sequence of the native locus, followed by *Aspergillus fumigatis pyr*G, which was used for selection. Further details on primer and construct design were previously published (Schultzhaus et al., 2017a) and a visual representation is provided in **Figure II.2**. Prior to performing the fusion PCR, three fragments were individually amplified: a fragment containing 1 kb of the gene upstream from the insertion point (not including the stop codon), a fragment containing eGFP::*AfpyrG* from plasmid pFNO3 (Yang et al., 2004), and a fragment containing 1 kb downstream from the insertion point. Amplification of the final fused construct utilized nested primers P7 and P8 (**Figure II.2**). Phusion™ Flash High-Fidelity PCR Master Mix (Thermo Fisher Scientific™, Waltham, MA, USA) was used for each amplification. All PCR reactions were carried out using a PTC-100 Programmable Thermal Cycler (MJ Research, Inc., Waltham, MA, USA) or a T1000 Thermal Cycler (Bio-Rad Laboratories, Inc., Hercules, CA, USA). All primers were ordered from Integrated DNA Technologies Inc. (Integrated DNA Technologies, Inc., Coralville, IA, USA). A complete list of primers designed for this study can be found in **Table A-3**, and each is named corresponding to **Figure II.2**.

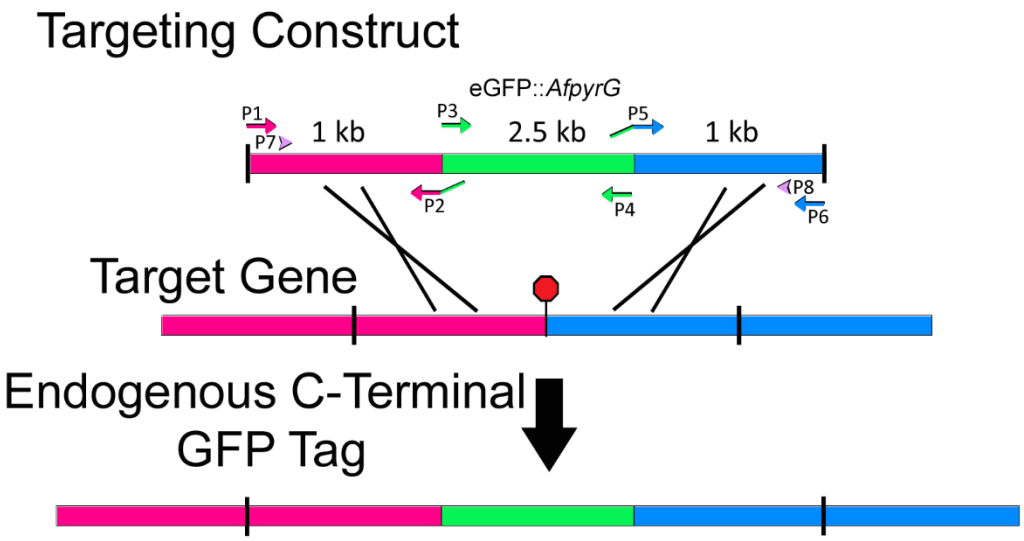

Figure II.2 – Primer Design & Layout of Construct
Constructs were designed to insert eGFP in frame at the 3' end of the coding sequence of the native locus, followed by *Aspergillus fumigatis pyr*G for selection. The stop codon (red octagon) was removed prior to primer design. Three fragments were individually amplified prior to performing the fusion PCR: a fragment containing 1 kb of the gene upstream from the insertion point (pink), a fragment containing eGFP::*pyrG* (green), and a fragment containing 1 kb downstream from the insertion point (blue). Separate sets of primers were designed for each fragment. For example, primers P1 (forward) and P2 (reverse) were utilized for the first fragment. Primers P2 and P5 contained an overhang of P3 or P4, respectively, which later acted as the primers in the overall fusion reaction. Once fused, a final amplification utilized nested primers P7 and P8. PCR verification of tagged genes was performed using outermost primers, P1 and P6.

Polyethylene-glycol mediated transformation was performed according to a previously described protocol (Szewczyk et al., 2007) using protoplasts of strain NkuNU (Schultzhaus et al., 2015). A minimum of eight transformants were screened for each target of interests using the following criteria. A homokaryon was established for each

transformant by single-spore streaking. Colonies that were pyrimidine prototrophs were evaluated for morphological similarity to wild type and screened for expression of GFP on a fluorescence microscope (described below). For each transformation experiment, all eight observed strains expressed eGFP at similar levels with similar localization patterns. This methodology was followed to ensure native levels of expression for all fluorescent constructs, and all GFP fusions discussed here were constructed in the same manner. An elite strain was then selected for all subsequent experiments and confirmed to carry the endogenous tag using PCR primers P1 and P6, which flank the construct insertion site. Template DNA was acquired by following standard phenol-chloroform procedures with lyophilized mycelium (Sambrook and Russell, 2001).

Microscopy

Imaging was performed using an Olympus BX51 microscope (Olympus America, Inc., Melville, NY, USA) outfitted for DIC optics and the Olympus DSU (Disk Scanning Unit) spinning disk confocal imaging system as previously described (Schultzhaus et al., 2016; Upadhyay and Shaw, 2008). A 100x oil objective with a numerical aperture of 1.4, working distance of 100µm, and index of refraction of 1.518 was used unless otherwise stated. Wide-field fluorescent images were acquired with a Hamamatsu Flash Orca-ER cooled CCD (Hamamatsu Photonics, Hamamatsu City, Japan). This microscope interfaced with a Windows 8 based desktop using SlideBook version 5.2.12 imaging and deconvolution software (Intelligent Imaging Innovations, Inc./3i, Denver, CO, USA). All

images and movies were prepared for publication using Photoshop CC 2019 (Adobe, Mountain View, CA, USA).

Slide Preparation and Staining Techniques

After 24 hours of growth, agar blocks (roughly 1 square inch in size) were cut at the leading edge of the hyphal growth and placed upright on a slide. 20 µL of liquid MM was then pipetted on top of the growth, and the coverslip was gently applied. All slides were incubated at 30°C for approximately 15-20 minutes prior to imaging. When FM4-64 was used, a final concentration of 5 µM FM4-64 in 20 µL liquid MM was applied to agar blocks, then immediately rinsed with another 20 µL liquid MM twice before the coverslip was gently placed.

RESULTS

The *A. nidulans* genome encodes more than 10,000 proteins total, and 509 of those proteins are predicted to encode a truncated 'NPF.' Only 39 genes are predicted to encode a full NPFxD motif, though, and an even smaller pool of 26 genes are predicted to encode the similar, but less efficient, DPFxD motif (one of which contains both an NPFxD and DPFxD motif). An initial assessment of the 39 proteins was conducted to determine the number of times each of the 13 represented amino acids occurred as the fourth residue in the motif (**Figure II.3**). Aside from leucine being present over twice as many times as any other residue, this did not provide additional insight into prioritization of the proteins.

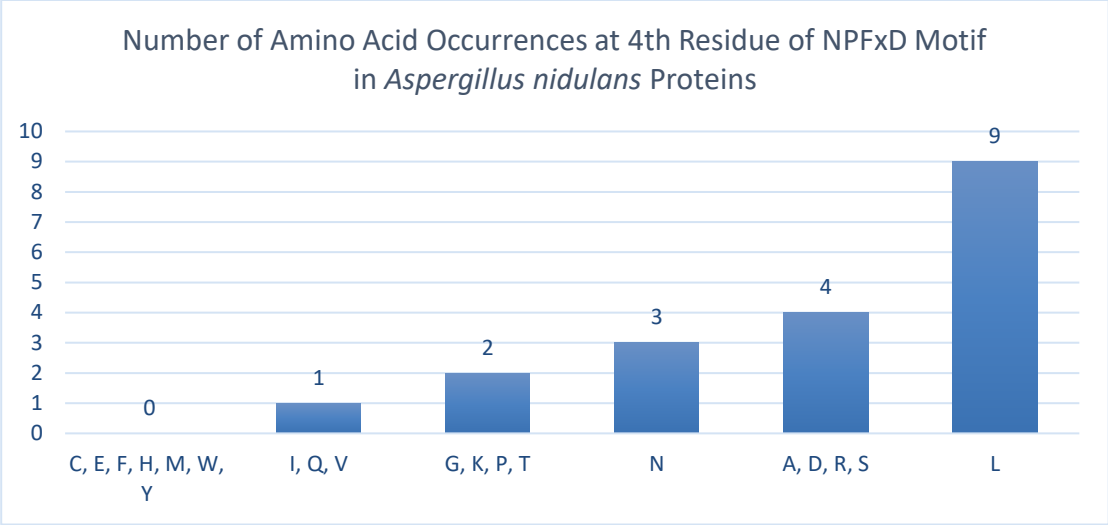

Figure II.3 – Occurrence of Amino Acids Occupying the Fourth Residue of the NPFxD Motif.
The 39 NPFxD motif-containing proteins were initially assessed to determine the number of times each amino acid occurred as the fourth residue in the motif. Only 13 amino acids were represented in total by these proteins. The most frequently occurring residue was leucine, which was present over twice as many times as any other. Residues are organized here by the number of times they appear in an NPFxD motif in *Aspergillus nidulans* proteins.

In order to focus on a more manageable number of genes and to prioritize those that are most likely to be marked for endocytosis or apical localization, the NPFxD motif-encoding genes were further categorized. Gene ontology (GO) terms were electronically curated and assigned to many of the proteins on the list based on the functions and localization patterns of orthologous proteins in various other model organisms, particularly if there was a shared or unique domain present. The predicted functions of these *A. nidulans* proteins range from calcium ion channeling and FAD-transporters to cytoskeleton organization, endocytosis, and maintenance of polarity. Based on these predicted functions, the 39 proteins were sorted into four basic functional categories: 1) ion binding and related channels, 2) cell morphogenesis and cytoskeleton, 3) membrane modification,

and 4) uncharacterized (**Figure II.4**). Over half of the proteins (21) were placed into the 'ion binding and related channels' category, seven proteins were placed in the 'cell morphogenesis and cytoskeleton' category, and two were placed in the 'membrane modification' category. The remaining nine proteins were categorized as 'uncharacterized.' At least one representative protein was selected from each of the categories for subsequent localization analysis.

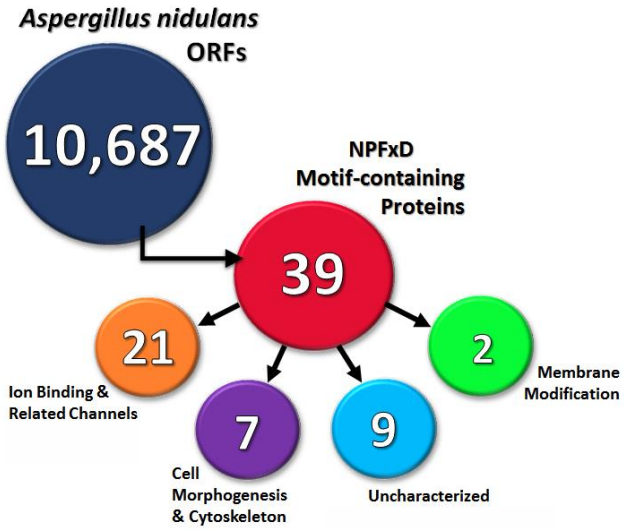

Figure II.4 – Categories of Predicted Functions.
The predicted roles of 39 NPFxD motif-containing proteins in *Aspergillus nidulans* were sorted into categories based on assigned gene ontologies (GO terms) and the roles of orthologous proteins. The predicted functions of these *A. nidulans* proteins range from calcium ion channeling and FAD-transporters to cytoskeleton organization, endocytosis, and maintenance of polarity. Based on these predicted functions, the 39 proteins were sorted into four basic functional categories: 1) ion binding and related channels, 2) cell morphogenesis and cytoskeleton, 3) membrane modification, and 4) uncharacterized. Over half of the proteins (21) were placed into the 'ion binding and related channels' category, seven proteins were placed in the 'cell morphogenesis and cytoskeleton' category, and two were placed in the 'membrane modification' category. The remaining nine proteins were categorized as 'uncharacterized,' as they do not contain predicted functions or orthologs in *Saccharomyces cerevisiae*, *Schizosaccharomyces pombe*, or *Candida albicans*. A comparison of the number of times the motif is encoded in each of four model organisms is provided in **Figure A-1**.

Further reasoning on protein selection is provided in the results section. Here, the GFP localization of a subset of these proteins was investigated. It is hypothesized that some proteins which contain the NPFxD peptide sequence in *A. nidulans* will localize either to the endocytic collar or to more proximal polarized regions of the cell, e.g. the apical dome or the SPK (**Figure II.1**). Based on this hypothesis, the results of the proteins investigated here were subcategorized based on the presence of apical or non-apical localization.

NPFxD Proteins That Localize to the Hyphal Apex or Membrane

AN0594 – TaoA

AN0594 is the presumed ortholog of *S. cerevisiae tao3* based on a reciprocal best BLAST between the two genomes on NCBI. Therefore, AN0594 is hereafter referred to as *taoA*. *taoA* is predicted to encode a 2591 amino acid (aa) protein with a MW of 289.0 kDa, which is similar in size to the 2376 aa size of *tao3*. An NPFxD motif is predicted to be encoded 740 aa from the N terminus. Based on characterization of Tao3p in *S. cerevisiae* and the orthologs CaCas4p in *Candida albicans* and Mor2 in *S. pombe*, functions associated with this component of the RAM signaling network include establishment or maintenance of cell polarity, regulation of cell shape, and bud site selection (Bruno et al., 2006; Du and Novick, 2002; Hirata et al., 2002; Nelson et al., 2003; Song et al., 2008). For these reasons, TaoA was chosen for this study.

In hyphae, TaoA::GFP localized to the apical crescent proximal to the collar, but was absent from the apex (**Figure II.5A, arrow**) and terminated in an area that would

correspond to the sub-apical endocytic collar. Puncta of TaoA::GFP were dispersed around the perimeter of the plasma membrane of (non-germinated) conidia. Prior to the appearance of a discernable germ tube, the localization concentrated to the site at which the eventual germ tube would emerge (**Figure II.5B**). Once the germ tube emerged, TaoA::GFP localization was maintained at the apical crescent (**Figure II.5C**). The apical crescent was also apparent immediately after a new branch emerged from the main hypha (**Figure II.5D**).

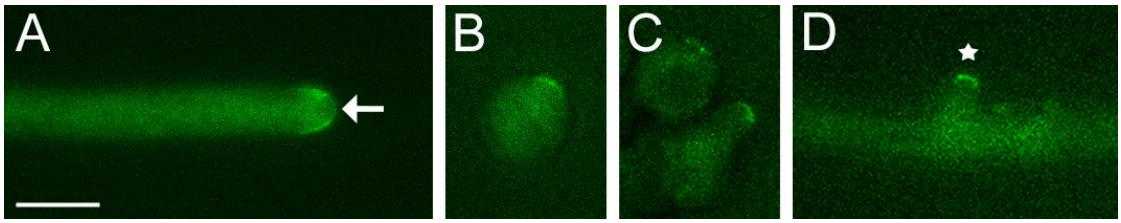

Figure II.5 – TaoA::GFP Localization.
(**A**) TaoA::GFP localization was observed in the apical crescent of a hypha, but was absent from the apex (**arrow**); (**B**) The localization of TaoA::GFP concentrated to predict the location of germ tube emergence; (**C**) Once the germ tube emerged, TaoA::GFP localization was maintained at the apical crescent; (**D**) TaoA::GFP was also apparent in the apical crescent immediately after a new branch emerged from the main hypha (new branch is denoted by the **star**). Scale bar is 5 µm.

AN2492 – EcoA

AN2492 is a homolog of *S. cerevisiae pal1* based on a reciprocal best BLAST between the two genomes on NCBI. The pH signal transduction pathway gene AN4351 was previously assigned the name *palA* (Negrete-Urtasun et al., 1997), so AN2492 is instead

referred to as *ecoA* based on its localization in the *e*ndocytic *co*llar. e*coA* is predicted to encode a 500 aa protein with a MW of 55.4 kDa, which is nearly identical in size to the 499 aa protein encoded by *pal1*. In additional to the presence of two truncated 'NPF' motifs and one 'DPF' motif, the peptide NPFLD is predicted to be encoded 65 aa from the N terminus of EcoA. Based on the characterization of Pal1p in *S. cerevisiae* and Pal1 in *S. pombe*, EcoA is also predicted to be associated with the regulation of polar cellular morphology (Ge et al., 2005; Swartzman et al., 1996). For these reasons, EcoA was chosen for this study.

EcoA::GFP localization was observed in the endocytic sub-apical collar, where endocytosis is enriched at the membrane, and was absent at the apical crescent (**Figure II.6A**). EcoA::GFP localization remained near the apex of germ tubes (**Figure II.6B**) until the hypha was mature enough for the collar to be evident. During conidiophore development, polarized growth was reduced and the apex swelled isotropically to form a vesicle. As this occurred, the intense localization of EcoA::GFP in the collar was again repositioned around the perimeter of the apex and the spatial distribution of the localization spread evenly throughout the plasma membrane of the vesicle (**Figure II.6C**). As the conidiophore developed further, the localization was observed at the leading edge or apex of the outermost cells (**Figure II.6D,E**). In hyphal tips, distinct puncta of EcoA::GFP could be seen internalizing from the plasma membrane, and were observed trafficking both toward and away from the apex (**Figure II.6F, Figure II.7**).

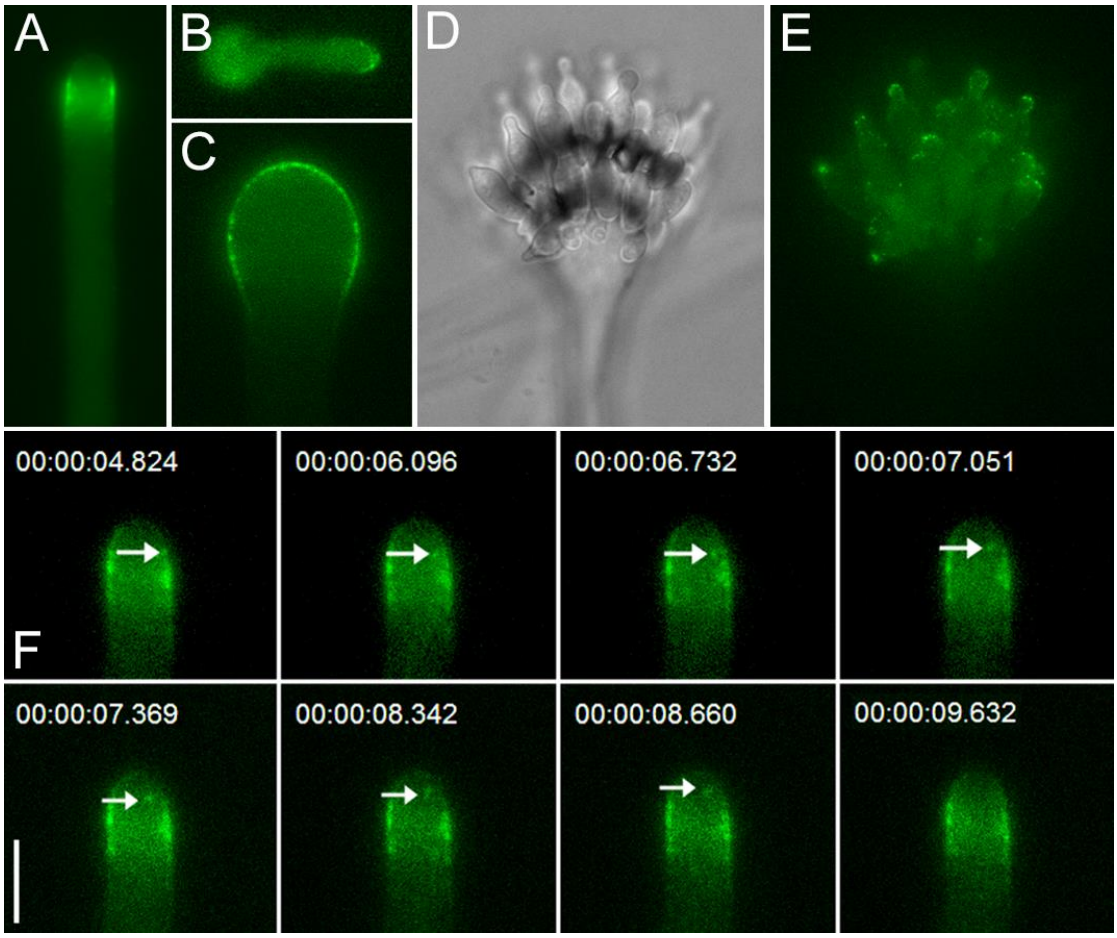

Figure II.6 – EcoA::GFP Localization.
(**A**) EcoA::GFP localization observed in the sub-apical collar; (**B**) Localization remained near the apex of germ tubes while hyphae were immature; (**C**) During vesicle development, the localization in the collar was redistributed throughout the perimeter of the vesicle; (**D**,**E**) As the conidiophore continued to develop, EcoA::GFP localization was observed at the leading edge of the outermost cells (in this case, the first layer of conidia); (**F**) Time-lapse panels depicting an individual puncta of EcoA::GFP being internalized and trafficked toward the apex. Time is in hh:mm:ss. Scale bar is 5 µm.

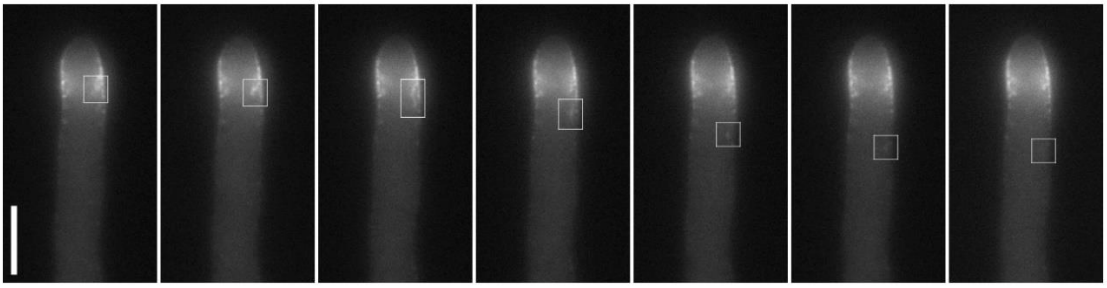

Figure II.7 - EcoA::GFP Retrograde Trafficking.
Retrograde trafficking of individual EcoA::GFP puncta (**box**) was observed. Scale bar is 5 µm.

AN0777 – EcoB

AN0777 is one of 10 proteins that both contains the NPFxD motif and is encoded only by FF. It is predicted to consist of 435 aa with a MW of 48.7 kDa, and the peptide NPFAD is predicted to begin at aa 395. AN0777 lacks a characterized ortholog in other model organisms, and is named EcoB based on the pattern of localization observed here. EcoB contains a VHS and a GAT domain, each of which is associated with intracellular trafficking and endocytosis. Based on the functions of proteins containing these domains, as well as the presence of an NPFxD motif and the fact that *ecoB* occurs only in FF, it was selected for this study.

EcoB::GFP localization was most intense at the sub-apical collar, but was also present in diminishing concentrations at and internal to the plasma membrane over distances of 50 µm or more distal to the apex. EcoB::GFP was also frequently observed localizing to septa (**Figure II.8B**). When the lipophilic dye and endocytic marker FM4-64 was applied, partial colocalization was observed with EcoB::GFP, particularly in the sub-apical collar

(**Figure II.8C-E**). This colocalization was not observed in the puncta distal to the collar. Similar to the localization of EcoA::GFP, EcoB::GFP was also absent at the apex (**Figure II.8A**), and individual puncta were observed trafficking in a bidirectional manner.

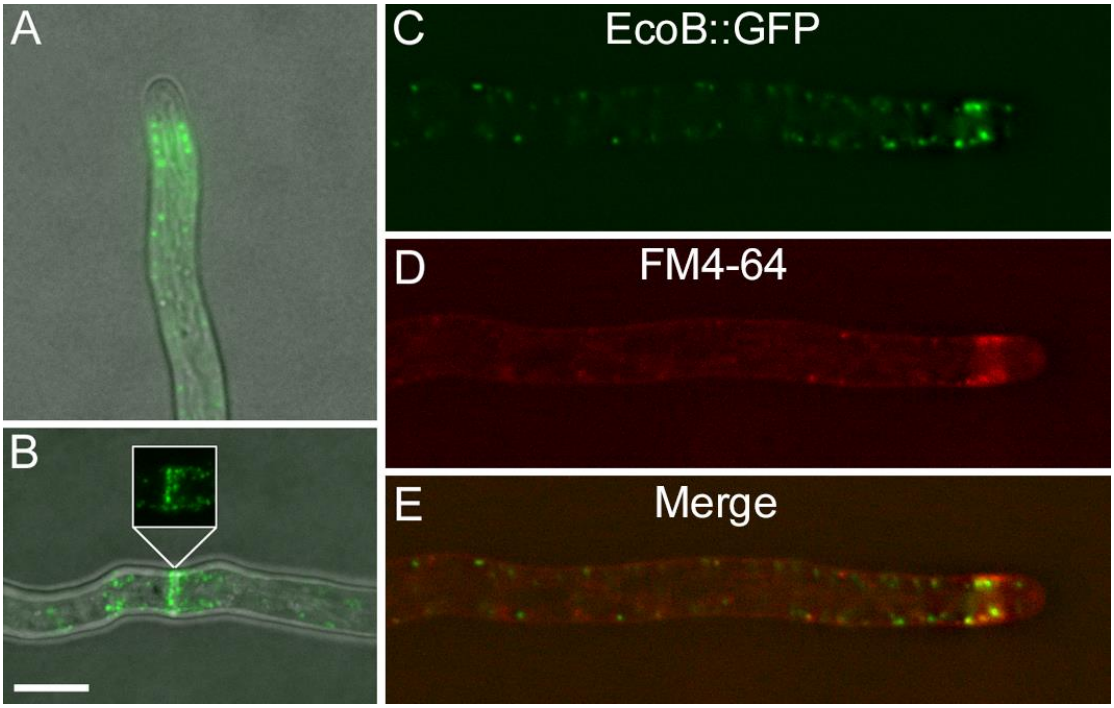

Figure II.8 – EcoB::GFP Localization.
(**A**) Growing hypha that shows intense localization of EcoB::GFP to the sub-apical collar, and absence of EcoB::GFP at the apex; (**B**) Brightfield overlay of the maximum projection of a Z-stack through a septum (shown in box without brightfield overlay); (**C, D, E**) A single hypha with (**C**) EcoB::GFP, (**D**) FM4-64, and (**E**) merged channels showing partial colocalization of EcoB::GFP and FM4-64 in region of sub-apical collar. Less colocalization was observed in puncta distal to the collar. Scale bar is 5 µm.

AN6341 – CorA

AN6341 is predicted to encode a 611 aa protein with a MW of 66.5 kDa. Reciprocal best BLASTs with both *S. cerevisiae* and *N. crassa* revealed that AN6341 is the ortholog of coronin (*crn1*) in each of the organisms. For this reason, AN6341 will now be referred to as CorA. The peptide NPFND is predicted to be encoded 90 aa from the N-terminus. CorA was selected for this study based on the increased likelihood of having similar functions with various orthologs based on the high conservation of the coronin family of proteins and related domains (Eckert et al., 2011; Xavier et al., 2008).

Localization of CorA::GFP was predominantly observed in the sub-apical collar, and many puncta were also seen diffusing away from the apex (**Figure II.9A,B**). CorA::GFP localization was also absent in the apical crescent, but was observed throughout the formation of septa, first as a diffuse cloud of localization (**Figure II.9C**), then as a distinct double ring around the site of the future septum (**Figure II.9D**), and finally as a single ring once the septum was completed (**Figure II.9E,F**).

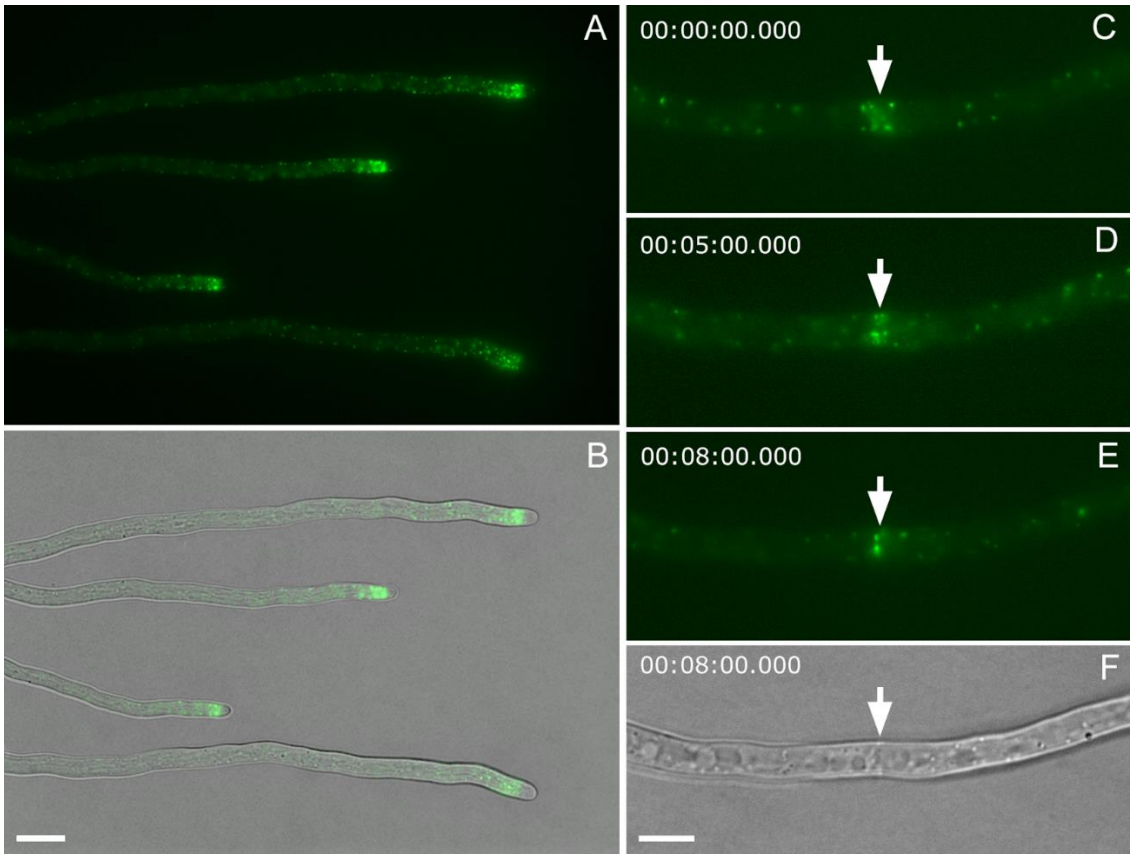

Figure II.9 – CorA::GFP Localization.
(**A,B**) CorA::GFP localization to the sub-apical collar, as well as to multiple puncta diffusing away from the collar; (**C-E**) Time-lapse image series during septum formation. CorA::GFP localized in a diffuse area near the site where a septum would eventually form (**C**), then to a distinct double-ring formation on either side of the future septum (**D**), and finally to a single line as the septum was completed (**E**,**F**). Time is in hh:mm:ss. Scale bar is 5 µm in **A-B** and 2.5 µm in **C-F**.

AN1950 – HapA

AN1950 is predicted to encode a 732 aa protein with a MW of 79.5 kDa. A reciprocal best BLAST with *S. cerevisiae* predicted the ortholog *flc1*, which transports flavin adenine dinucleotide (FAD) and is required for the uptake of FAD into the endoplasmic reticulum (Protchenko et al., 2006). Additional orthologs listed at FungiDB include *C. albicans*

CaFLC2 and *S. pombe pkd2* (Palmer et al., 2005; Protchenko et al., 2006; Stajich et al., 2012). The name *hapA* was assigned to this gene based on the localization of HapA::GFP to the *h*yphal *ap*ex. HapA contains one signal peptide, seven transmembrane domains (TMDs), and a TRP-like family domain. TRP domain-containing proteins are typically ion channels that are found on the plasma membrane or organelle membranes where they direct cation transport (Nilius and Owsianik, 2011; Zhu, 2011). The peptide NPFDD is predicted to be encoded beginning with aa 637. HapA was selected for this study for these reasons.

Localization of HapA::GFP was observed in the apical crescent, as well as the SPK (**Figure II.10A**); however, the apical localization of HapA::GFP terminated in an area that corresponded to the beginning of the sub-apical collar. Immediately after the emergence of a new branch, HapA::GFP clearly labeled the apical crescent (**Figure II.10B,C**); however, a distinct SPK was not labeled until each branch was mature enough to contain one. In addition, HapA::GFP localization to the SPK was frequently rearranged in coordination with changes in directionality and dissipated as growth ceased (**Figure II.10D-G**). HapA-GFP also localized to round intracellular structures approximately 500 nm wide, and uniform localization was observed in the entirety of the conidial membranes (**Figure II.11A**).

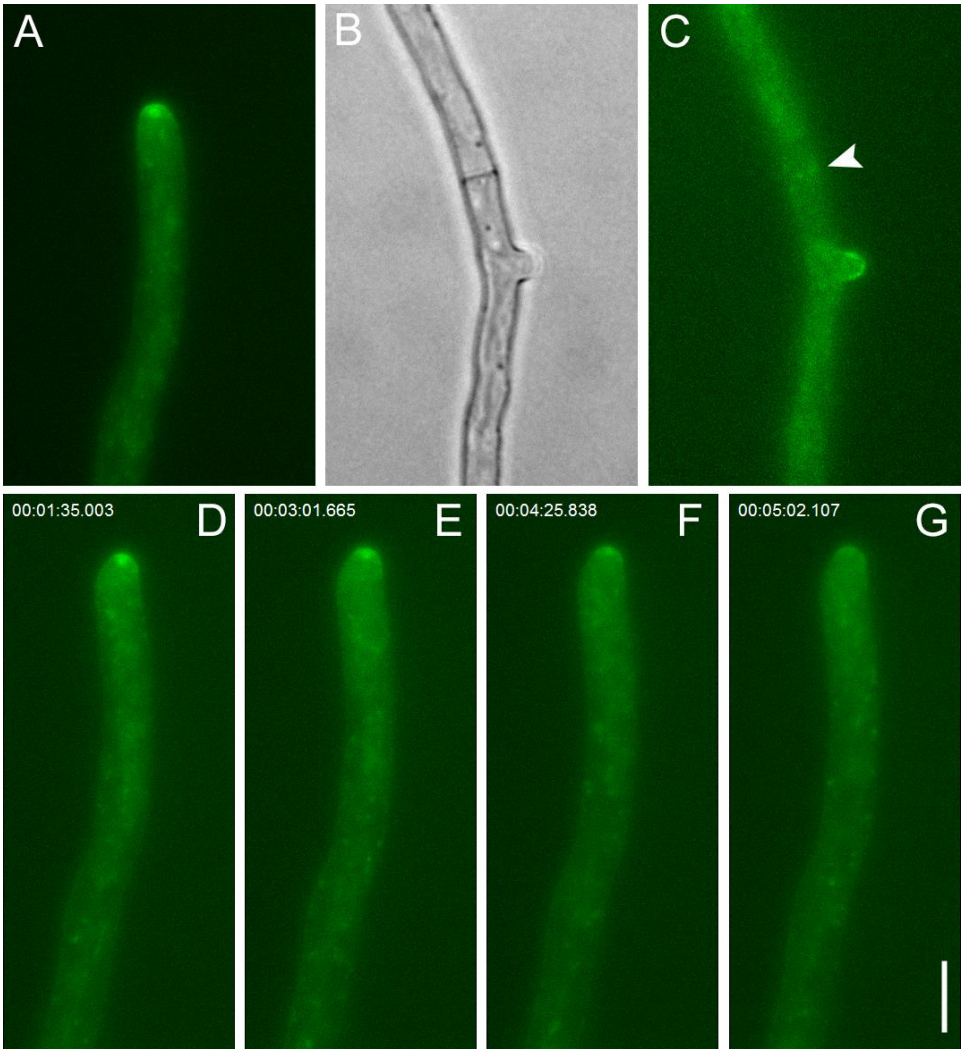

Figure II.10 – HapA::GFP Localization.
(**A**) Localization of HapA::GFP to the SPK as well as the apical crescent. (**B**) Brightfield view of new branch and septum represented in (**C**), where faint localization was observed to septa (arrowhead); (**D-G**) time-lapse series of a hypha during growth (**D-E**), and once growth ceases (**F-G**). The localization to the SPK diffuses with the cessation of growth (**G**). Scale bar is 5 μm.

AN12305 – LsbA

AN12305 is predicted to encode a 398 aa protein with a MW of 45 kDa. The peptide NPFND is predicted to be encoded beginning with aa 375 near the C terminus. AN12305 also contains domains associated with endocytosis and intracellular protein transport, such as the VHS and GAT domains. The name *lsbA* was given to this gene because it is the ortholog of *lsb5* (*L*as *S*eventeen *B*inding) in *S. pombe* and *S. cerevisiae*.

LsbA::GFP localization was faint; however, distinct puncta were observed along the length of the hyphal membrane (**Figure II.11F**). These puncta remained stationary as hyphae continued to grow. LsbA::GFP predominantly localized to actively growing cells. LsbA::GFP also localized to newly forming septa (**Figure II.11F, arrow**) in a pattern similar to that of CorA::GFP, and mostly dissipated once the septum matured. Dormant conidia showed little cytoplasmic localization of LsbA::GFP; however, upon breaking dormancy and swelling, puncta were observed localizing to the perimeter of the conidia (**Figure II.11E**).

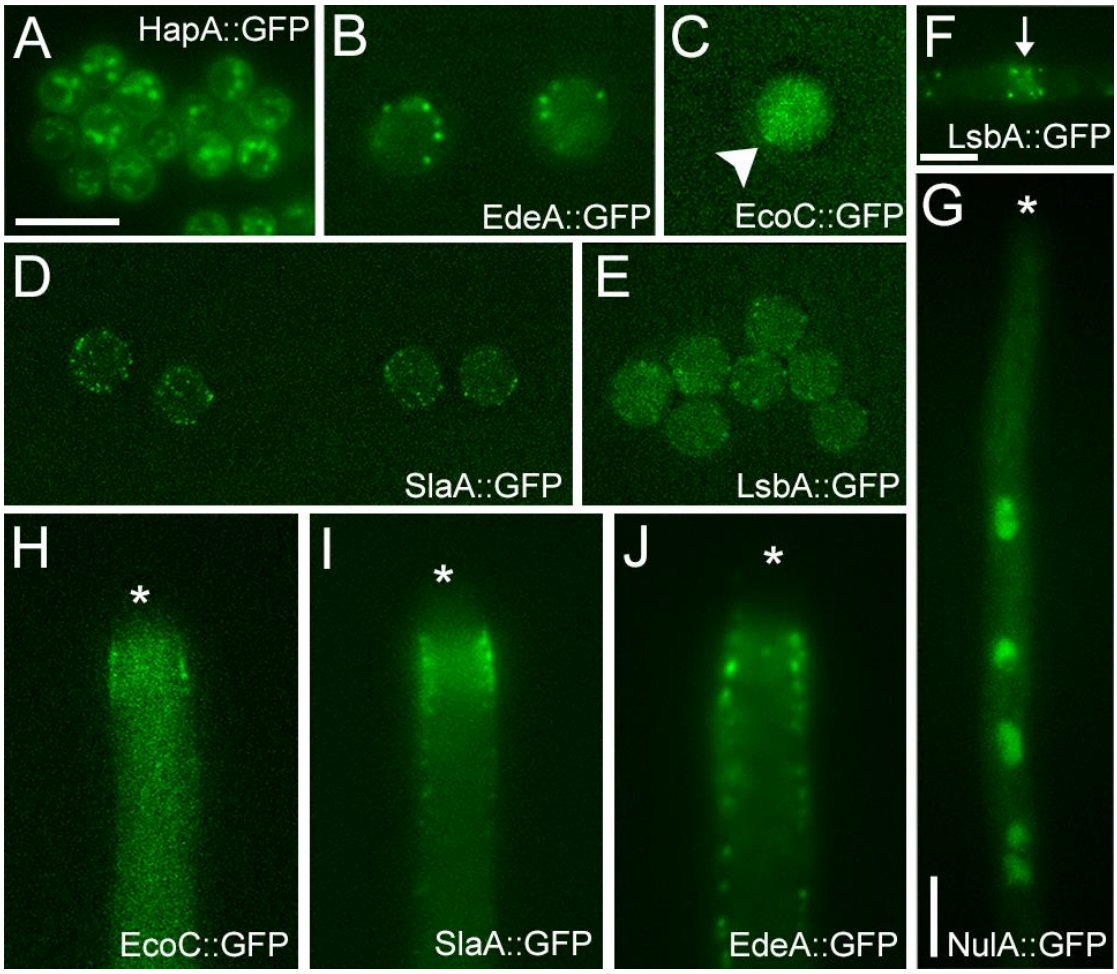

Figure II.11 – Additional Proteins & Areas of Localization.
(**A**) HapA::GFP localization to the membranes of conidia and as individual puncta within the conidia; (**B**) EdeA::GFP punctate localization in conidia; (**C**) EcoC::GFP in a single conidium. Arrow marks the area of concentrated localization; (**D**) SlaA::GFP localization in conidia; (**E**) LsbA faint localization to conidial membranes; (**F**) LsbA localization during septum formation (**arrow** denotes site of septum establishment); (**G**) NulA::GFP localization to nuclei; (**H**) EcoC::GFP localization to sub-apical collar in a growing hypha; (**I**) SlaA::GFP localization to sub-apical collar; (**J**) EdeA::GFP localization to sub-apical collar, and to puncta on the membrane diffusing away from the apex. Due to low signals, images C, D, E, and H were each deconvolved to reduce background noise. Asterisks represent the apex of each hypha in panels G-J. All scale bars represent 5 µm. The scale bar in image A is standard for all images except F and G, which have separate scale bars due to a difference in magnification.

Proteins with a Variation of the Motif and Apical Localization

AN0697 – EcoC

AN0697 is predicted to encode an 853 aa protein with a MW of 93.3 kDa. AN0697 is named *ecoC* here based on the observed localization of the tagged protein to the endocytic collar, similar to that seen with EcoA::GFP and EcoB::GFP. The ortholog is *syp1* in both *S. cerevisiae* and *S. pombe*. Syp1p negatively regulates WASp-Arp2/3 complex activity during endocytic patch formation (Boettner et al., 2009) and is required for septin cytoskeleton dynamics in yeast (Qiu et al., 2008). Syp1p was recently shown to regulate both clathrin-mediated and clathrin-independent endocytosis of multiple cargo proteins, and localization was observed in endocytic patches as well as at the cellular bud tip (Apel et al., 2017). Additionally, the knockout phenotype of the *N. crassa* ortholog (NCU04427) displays slightly reduced aerial hyphal extension and linear growth rates (Collopy et al., 2010; Colot et al., 2006). EcoC contains the less common but similarly functioning DPFxD motif (Tan et al., 1996), as well as one signal peptide. For all of these reasons, EcoC was also selected for investigation.

EcoC::GFP localization was observed faintly in conidia, in particular immediately before germ tube emergence (**Figure II.11C, arrow**). EcoC::GFP was predominantly observed localizing to the sub-apical collar, and the localization terminated immediately adjacent to the tail end of the apical crescent (**Figure II.11H**). The localization was not observed in the apical crescent (**Figure II.11H, asterisk**). This protein is presumed to be less concentrated than EcoA or EcoB based on the lower intensity of fluorescence observed.

AN1462 – SlaA

Sla1p is the well-characterized yeast adapter protein that recognizes the NPFxD (or the similar but less common DPFxD) motif. Sla1p is able to bind to activators of actin dynamics as well as to cargo proteins, and forms a complex with Pan1p and End3p (Mahadev et al., 2007; Tuo et al., 2013; Zeng et al., 2012). It is also the ortholog of *A. nidulans* SlaA, which contains a truncated NPF motif as well as four copies of the SH3 (src Homology-3) domain. Multiple (2-4) copies of this domain are typically only present in adaptor proteins. SlaA has a predicted role in actin patch assembly (Harris et al., 2009), which is not surprising given the role of Sla1p in the regulation of actin dynamics and functioning of the endocytic machinery. In *A. nidulans*, SlaA::GFP localized to the sub-apical endocytic collar of growing hyphae (**Figure II.11I**), as well as to cortical patches in conidia (**Figure II.11D**). This localization was also not observed at the apex (**Figure II.11I, asterisk**).

AN0317 – EdeA

EdeA contains two truncated motifs, one each of NPF and DPF, which have also been shown to function in association with endocytosis (Brett et al., 2002; de Beer et al., 2000). It is the ortholog of Ede1, which is one of five proteins in yeast which contains an epsin-homology (EH) domain. Ede1p is a scaffold for the organization of the early stages of endocytosis (Boeke et al., 2014), and localized in punctate cortical spots around the perimeter of the cells (Gagny et al., 2000). This localization was identical to what was seen when EdeA::GFP was observed in conidia (**Figure II.11B**). Localization of

EdeA::GFP was primarily observed in the sub-apical collar of growing hyphae (**Figure II.11J**); however, patches could be seen throughout the membrane for distances over 50 µm distal to the apex. When viewed over time during growth, it is clear that the puncta can be found throughout the cortical membrane of the hypha.

NPFxD Motif-containing Proteins with Non-apical Localizations

Two of the investigated motif-containing proteins did not localize to the hyphal apex. Possible reasons for this are considered in the discussion. These proteins were not studied intensively due to the non-apical localization patterns observed.

AN1557 – FmlA

FmlA (*f*aint *m*itochondrial *l*ocalization) is present only in some FF, and has no ortholog in *N. crassa*. It does, however, contain a signal peptide and seven TMDs, each of which increases the likelihood of membrane interactions. Localization of FmlA::GFP was sporadic and observed in all cell types. FmlA::GFP localization was observed in tubular structures that ran parallel with the hypha. These structures were not uniform, but instead seemed to be comprised of many pieces of different sizes, at times resembling mitochondria (**Figure II.12**). One unforeseen phenomenon observed in FmlA::GFP was an increase in both the number and the intensity of puncta along the membrane when two hyphae were in close proximity to one another. When two hyphae came into contact (**Figure II.12, arrow**), a spike in fluorescent intensity could be seen either at the site of contact or at the apex of the leading hypha (**Figure II.12, arrowhead**).

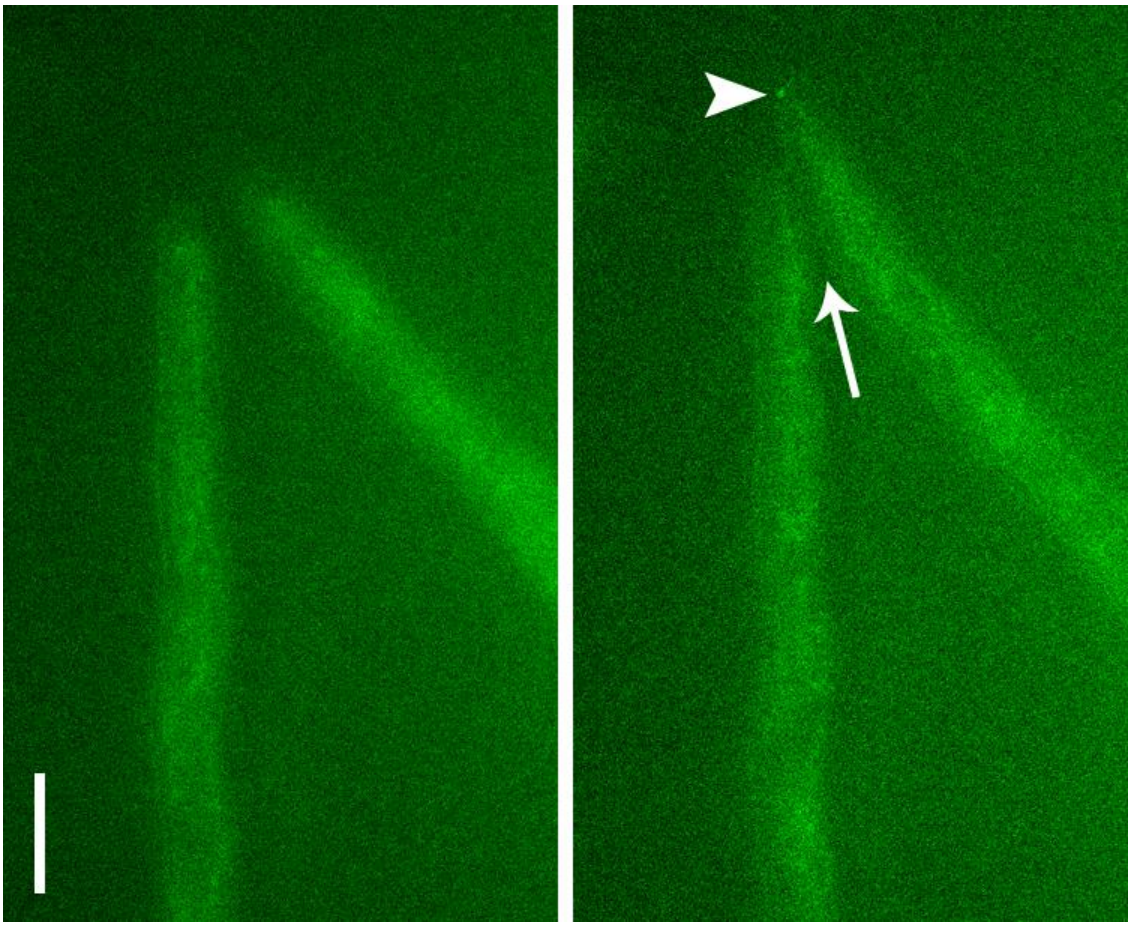

Figure II.12 – FmlA::GFP Localization.
An increase in both the number and the intensity of puncta along the membrane was observed when two hyphae tagged with FmlA::GFP were in close proximity to one another. When two hyphae came into contact (**arrow**), a spike in fluorescent intensity could be seen either at the site of contact or at the apex of the leading hypha (**arrowhead**). Scale bar is 5μm.

AN6164 – NulA

AN6164 is predicted to encode a 2510 aa protein with a MW of 284.1 kDa. The truncated NPF is predicted to be encoded starting at aa 331, followed by the complete peptide

NPFID starting at aa 864. The *N. crassa* ortholog (NCU00320) has not yet been localized, but the knockout phenotype includes decreased aerial hyphae extension (05-10 mm/day), smaller protoperithecia with fewer ascospores formed, and a slightly reduced linear growth rate (Collopy et al., 2010; Colot et al., 2006). The top match in both *S. cerevisiae* and *S. pombe* is UPB15. AN6164 contains domains with predicted thiol-dependent ubiquitinyl hydrolase activity and roles in protein deubiquitination, as well as ubiquitin-dependent protein catabolic processes. Ubiquitin carboxyl-terminal hydrolases are thiol proteases that recognize and hydrolyze the peptide bond at the C-terminal glycine of ubiquitin. These enzymes are involved in processing poly-ubiquitin precursors as well as ubiquinated proteins (Jentsch et al., 1991). Here, AN6164 was given the name NulA because of the observed *n*uclear *l*ocalization (**Figure II.11G**). NulA::GFP scarcely localized outside of the nuclei of growing hyphae; however, at times faint localization was observed in punctate structures along the membrane.

NPFxD Motif-containing Proteins with Low Levels of Expression

A localization pattern could not be established for seven of the endogenously tagged motif-containing proteins and, therefore, these proteins were analyzed only minimally (see **Table A-1**). These include AN4106, AN8621, AN10090, AN10296, AN2669, AN4945, and AN5302. While the proteins in this category could very well localize to an area near the growing fronts of hyphae, and could also be involved in membrane turnover, the lack of observable fluorescence implies that the proteins are present or expressed in too low a number to accurately quantify or visualize. Another explanation could be that each of these

proteins is not highly expressed during growth, and therefore does not fit this model. Furthermore, one or more of the proteins could be expressed during specific instances of growth for short durations of time, or only when interacting with other hyphae (i.e. during hyphal anastomosis).

DISCUSSION

It has already been established that proteins which are cargo for endocytosis are also likely to be associated with the establishment or maintenance of polarized hyphal growth, characteristics which remain unique to FF (Riquelme et al., 2018; Steinberg et al., 2017). This study corroborates that NPFxD is a reliable motif for localizing proteins to the cell apex in growing hyphae. This localization is likely due to the importance of endocytosis at the hyphal tip. An initial survey of motif-containing proteins in *A. nidulans* was conducted here, and the dynamic localization of each tagged protein was evaluated.

It was previously believed that clathrin was required for endocytosis to occur. We now know that there are clathrin dependent and clathrin independent modes of endocytosis, and that clathrin is not found in great amounts in the sub-apical endocytic collar of *A. nidulans* or *N. crassa* (Delgado-Alvarez et al., 2010; Epp et al., 2013; Martzoukou et al., 2017; Mayor and Pagano, 2007; Miaczynska and Stenmark, 2008; Robinson et al., 1996; Schultzhaus et al., 2017a). Various adapter proteins, such as Sla1p, are innately programmed to recognize specific peptide sequences and deliver cargo to the membrane (Mahadev et al., 2007; Tolsma et al., 2018). While the NPFxD motif is required for this

specific route of endocytosis, it is also possible that some proteins contain this motif and do not function as cargo for endocytosis or associate with the apical plasma membrane. Similarly, not all proteins with an endocytic function will contain this motif; however, the evidence provided here suggests that the presence of at least one copy of the NPFxD endocytic internalization signal alone could increase the likelihood that a protein will localize to the apex of growing hyphae and, therefore, one of its functions could also be an involvement in endocytosis and/or polarized growth. It is unclear at this time if the presence of more than one copy of the truncated NPF or DPF motif increases the likelihood of the protein localizing to the hyphal apex. For example, both EcoA and NulA contain additional, truncated NPF motifs; however, EcoA displays apical localization while NulA is observed only in the nuclei. In addition to the motif-containing proteins discussed here, eight of the 39 have previously been investigated; however, only a select few have been localized. These proteins include the aforementioned DnfA (Schultzhaus et al., 2015; Schultzhaus et al., 2017b), as well as MyoA, which is enriched in growing hyphal tips, sites of septum formation, and patches at the cell cortex (Yamashita et al., 2000).

In this study, each motif-containing protein was initially categorized and prioritized for localization analysis based on the function of its ortholog(s) in other model organisms with well annotated genomes, such as *S. cerevisiae, S. pombe, N.* crassa, and *C. albicans*. Although budding and fission yeasts are morphologically less similar to *A. nidulans*, deductions can be made in order to best predict the comparable localization in the other. For example, many of the yeast orthologs localize to the “bud tip,” “bud neck,” or areas

of "mother-daughter cell separation." These likely correspond to the hyphal tip in FF, but may also correlate to other areas where cell wall or membrane is being added, such as the sites of septum formation, sites of cell differentiation in conidiophores, or sites of germ tube emergence in conidia. Proteins found only in FF were prioritized based on alternative parameters. In this case, the presence of multiple copies of the truncated NPF or the full NPFxD peptide motif, the number of TMDs, and the presence of unique or shared domains were all variables that were considered when deciding which proteins to pursue first.

In this study, 19 proteins were tagged with GFP and their localizations were examined, including four (EcoC, SlaA, EdeA, PeaA) that contain a variation or truncated form of the NPFxD motif, and fluorescence was observed in 12. The data presented here suggest that nine of these are machinery or cargo for endocytosis and, therefore, are also likely to be associated with the establishment or maintenance of polarized growth. The remaining three appeared to localize to nuclei, mitochondria, or vesicles and organelles in mature hyphae and developing conidiophores, and therefore have not been investigated as intensively. Seven other proteins have been initially ruled out for further studies based on a lack of observable fluorescence. Six of the nine proteins contain a complete NPFxD motif and are discussed further below.

TaoA

TaoA is the ortholog of *S. cerevisiae* Tao3, an integral component of the RAM signaling network in yeast (Bogomolnaya et al., 2006; Nelson et al., 2003). This network is required

for the *r*egulation of *A*ce2p activity and cellular *m*orphogenesis, which largely governs growth and development. The RAM signaling network is comprised of Tao3p (previously referred to as Pag1p), Hym1p, Cbk1p kinase, and its binding partner Mob2p. Each of these RAM proteins localizes to cortical sites of growth during budding in yeast, and the signaling network, also known as the morphogenesis-related NDR kinase (MOR) pathway, is conserved in many different organisms (Maerz and Seiler, 2010), including *Colletotrichum orbiculare* (Kodama et al., 2017), *N. crassa* (Yarden et al., 1992), *Cryptococcus neoformans* (Walton et al., 2006), and *Ustilago maydis* (Sartorel and Pérez-Martín, 2012). The localization observed in *A. nidulans* is also consistent with that of Tao3p (previously called Pag1p) in *S. cerevisiae*, which was polarized and observed at the cell periphery (Du and Novick, 2002). It is likely that TaoA is cargo for endocytosis based on the apical localization that terminates abruptly in the area that corresponds to the sub-apical endocytic collar. A similar localization has been observed in other proteins, such as the cell-end marker TeaA, and the formin SepA (Fischer et al., 2008; Sharpless and Harris, 2002).

EcoA

It is likely that EcoA functions partly as endocytic machinery involved in the trafficking of cargo based on the areas of localization observed, the functional roles of its orthologs, and the detection of periodic bidirectional trafficking. EcoA::GFP predominantly localized to the sub-apical collar, and at times puncta could be seen trafficking either toward or away from the apex. In *S. cerevisiae*, Pal1p fused with GFP localized to the bud

neck and was also found at endocytic sites along the cell periphery during the early stages of endocytosis (Carroll et al., 2012). *S. pombe* paralog Pal1p localized to the growing tips of interphase cells, as well as to division sites in cells undergoing cytokinesis, which was similar to what was observed in SpSla2p and SpEnd4p (Ge et al., 2005). Each of these three proteins was shown to be important for the maintenance of cylindrical cellular morphology. Pal1p contains the exact same motif (NPFLD) as its paralog in *A. nidulans*, EcoA. Pal1p also shares the Pal1 homology domain with a single paralog (Pal2p) that resulted from the whole genome duplication (Byrne and Wolfe, 2005). Similarly, there is a single paralog in *A. nidulans*, AN1509, which shares this domain with EcoA. AN1509, referred to as PeaA (*p*aralog of *e*co*A*), was also tagged here; however, localization was strictly observed in mature hyphae or developing vesicles and conidiophores (**Video S13**). Since the paralog localizes to intracellular sites and is not known to interact with other endocytic machinery, it is unlikely to also contribute to endocytosis (Goode et al., 2015).

EcoB

At this time, the ortholog of EcoB in *N. crassa* (NCU01927) has not been characterized, but it already shares many similarities, including the comparable DPFxD motif and the presence of two noteworthy domains. EcoB is likely to be involved with intracellular protein transport and endocytosis based on the presence of these two important domains. One of these is the VHS domain (named based on its occurrence in VPS-27, Hrs, and STAM), which is typically found at the N-terminus and is contained in many proteins involved with endocytosis and/or vesicular trafficking (Lohi and Lehto, 1998). It has been

proposed that the VHS domain also functions in part as a multi-purpose docking adapter which interacts with the membrane and/or endocytic machinery in order to localize proteins to the membrane (Mao et al., 2000; Misra et al., 2000). The other is the GAT domain, which is found only in eukaryotic Golgi-localized, Gamma ear-containing ARF-binding proteins (GGAs). The GAT domain serves as a molecular anchor of GGAs to TGN membranes and is commonly seen in conjunction with the VHS domain (Dell'Angelica et al., 2000). Each of these domains is associated with intracellular protein transport, which was observed regularly in EcoB::GFP. It is also possible that EcoB localizes in part to an early endosome (EE) based on the frequent bidirectional movement detected. The speed of this movement varied among the individual puncta, but movement away from the apex was noticeably quicker, as was seen with EcoA::GFP retrograde trafficking. In FF, EEs display bidirectional movement along microtubules, binding to dynein for retrograde transport and kinesin-3 for anterograde transport (Abenza et al., 2009). It has also been suggested that EEs participate in endocytic recycling by sorting cargo and organelles to the subapical vacuolar system for degradation (Steinberg, 2014), and that they traffic polysomes in order to evenly distribute protein translation (Shoji et al., 2014). Preliminary experiments with benomyl, which disrupts microtubule trafficking, have shown minor disruptions to the intracellular trafficking observed in EcoB::GFP (data not shown). This supports the notion that EcoB is involved in trafficking and could partially localize to EEs. Future investigations with dynein and kinesin mutants would elucidate the exact percentage of EcoB puncta that participates in microtubule-based trafficking. Since the intent of the current manuscript is to survey the localization patterns

of NPFxD motif-containing proteins, these and other experiments will be discussed in future work. Ultimately, this protein is an ideal candidate for further investigations of endocytosis and intracellular trafficking, and may also be a promising target for antifungal drug discovery, particularly because it is unique to FF.

CorA

corA contains the highly conserved Coronin domain (PTHR10856)(Mi et al., 2018), and is further categorized into a subfamily (PTHR10856:SF0), with all of the fungi discussed here containing one copy of coronin each. This domain is associated with actin cytoskeleton organization and non-motor actin binding proteins. In addition, *corA* includes three WD40 repeats (also known as WD or beta-transducin repeats), which are roughly 40 aa long and typically repeat anywhere from three to 16 times to form a circular beta-propeller structure (Neer et al., 1994). These repeats are found in all eukaryotes and act as sites for protein-protein interactions (McArdle and Hofmann, 2008). Coronins are frequently considered to be multifunctional regulators of the cortical actin cytoskeleton and are involved in membrane trafficking (de Hostos, 1999; de Hostos et al., 1991; Rybakin and Clemen, 2005). They are evolutionarily conserved proteins that characteristically contain a DUF1899 domain, a DUF1900 domain, a C-terminal coiled-coil domain, and a series of three to ten WD40 repeats. The ortholog of CorA in *S. cerevisiae* (Crn1p) also associates with the Arp2/3 complex (Heil-Chapdelaine et al., 1998). A *Xenopus* homolog of coronin (Xcoronin) has previously been investigated, and localization was observed to the cell periphery in membrane ruffles, as well as the leading

edge of lamellipodia, specifically during extension (Asano et al., 2001; Mishima and Nishida, 1999). The peptide motif in CorA (NPFND) is identical to and in the same location as the motif in Crn1 of *N. crassa*, which further suggests a high level of conservation. In *N.* crassa, Crn1::GFP localized to the endocytic collar (Echauri-Espinosa et al., 2012), just as we observed in *A. nidulans*. The double-ring of localization detected during septum formation is also identical to what has previously been shown with actin (Berepiki et al., 2010; Schultzhaus et al., 2016). CorA has a predicted role in actin patch assembly based on its localization and its similarity to yeast Crn1p, as well as the ortholog Crn1 in *N. crassa* and best hits in *C. albicans* and *S. pombe* (both of which are also Crn1).

HapA

HapA contains one signal peptide, seven TMDs, and a TRP-like family domain. In bacteria, signal peptides target proteins directly to the cell membrane; however, it is common for signal peptides in eukaryotes to target proteins to the endoplasmic reticulum (ER), where they are subsequently directed to the secretory pathway (Rapoport, 2007). This may be the case for HapA::GFP, as it was also observed in the SPK, where secretion occurs. In addition, activated TRP channels have been linked to ion channels and altered intracellular cation concentration because they cause cellular membranes to depolarize. These channels are typically located in the plasma membrane where they direct transcellular cation transporting machinery and moderate ion entry. TRP channels are also required for the proper function of organelles, such as endosomes and lysosomes. For this reason, TRP gene mutations have been associated with a variety of human diseases, such

as polycystic kidney disease (Nilius and Owsianik, 2011). In fact, the ortholog of HapA in *S. pombe* is PKD2, which acts as a key signaling component in the regulation of yeast cell shape and cell wall synthesis, and was named for its similarities with the ion channel genes associated with polycystic kidney disease (Aydar and Palmer, 2009; Morris et al., 2019; Palmer et al., 2005). In *S. cerevisiae*, localization of FLC1 was observed to the cell periphery, bud neck, and endoplasmic reticulum (Protchenko et al., 2006). HapA::GFP similarly localized both to the apical crescent as well as the SPK. The localization to the SPK was frequently rearranged in coordination with changes in directionality and dissipated as growth ceased, which has been seen previously with various other SPK-localizing proteins (Harris, 2009; Reynaga-Peña et al., 1997; Riquelme and Sanchez-Leon, 2014; Virag and Harris, 2006). In addition to the SPK, localization of HapA::GFP was also observed to the apical crescent of growing hyphae. HapA::GFP displayed a close similarity to the localization of the previously characterized NPFxD motif-containing protein DnfA (Schultzhaus et al., 2015). DnfA::GFP labeled the plasma membrane slightly beyond the crescent, while the apical localization of HapA::GFP terminated in an area that corresponded with the beginning of the sub-apical collar. Despite this minor discrepancy, it is likely that HapA is also endocytic cargo that is recycled at hyphal tips.

LsbA

The gene AN1768 was split in 2010 during preparation of the reference annotation (Version 5), resulting in AN12304 and AN12305. Of these two, AN12305 (LsbA) contains the VHS and GAT domains, as well as an NPFxD motif, while AN12304 contains

a ubiquitin homolog domain and shares 42% structure similarity to the *S. cerevisiae* ubiquitin-like modifier protein Hub1 (Ramelot et al., 2003). In *S. cerevisiae*, Lsb5p has been shown to physically interact with the adapter proteins Sla1p and Las17p to couple actin dynamics with the plasma membrane (Costa et al., 2005). The interaction with Sla1p likely occurs between the Sla1 homology domain 1 (SHD1) and the Lsb5 NPF motif (Costa et al., 2005), which is precisely what we predict to occur in *A. nidulans* as well. Lsb5p is an Arf3 GTPase-activating protein that has been shown to play a role in membrane-trafficking events at the plasma membrane by interacting with actin cytoskeleton regulators (Goode et al., 2015); however, the late arrival of Lsb5p to sites of endocytosis indicates that it is also involved in coat disassembly (Toret et al., 2008). The localization pattern of LsbA::GFP to the cytoplasm, plasma membrane, and conidial membrane is similar to what was observed in Lsb5p (Costa et al., 2005; Toret et al., 2008). Unfortunately, localization of this protein has proven difficult to study in depth due to the low expression and faint signal. It is possible that LsbA also plays a role in coat disassembly in *A. nidulans*, and therefore is not expressed as highly in each area that it localizes. This would contribute to it being more difficult to detect than the previously discussed proteins, most of which are highly expressed. LsbA::GFP was also observed in the mature hyphae roughly as often as it was observed at the hyphal apices, suggesting that it does not function only in endocytosis, and that it may also play a role in long-distance trafficking.

CHAPTER III

CONCLUSION

The understanding of hyphal growth, as well as the secretory network at the hyphal tip, has progressed significantly in recent years. However, comparably little has focused on the process of internalization, which has been shown to be equally necessary for hyphal growth and polarity, and is the hallmark characteristic of FF. Now that it is generally accepted that endocytosis does occur in FF, priority should be given to identifying the proteins that act as cargo for endocytosis, or that participate in apical recycling. This study served as an attempt to do just that- to identify proteins in *A. nidulans* which are potentially involved in hyphal growth, membrane turnover, and/or endocytosis.

First, a list of genes predicted to encode one or more NPFxD (or similar DPFxD) motifs in *A. nidulans* was comprised. Each of the predicted proteins was then sorted and categorized based on the little information that is available for each, or for the ortholog of each in other model fungi. Once this list was established, proteins were prioritized based on the predicted function (gathered through GO terms and ortholog functions, when available), the inclusion of particular domains or motifs, and the number of TMDs. One at a time, proteins were tagged from this list, as well as a few select proteins which function in the endocytic pathway in *S. cerevisiae* and include a partial motif (NPF or DPF). If

apical localization was observed, a deletion strain was also constructed for many of the genes (see **Appendix B**). The mutant phenotypes were then observed and characterized, when possible. Three of the deletion strains (*slaA*, *hapA*, and *ecoC*) were considered lethal, and each gene is therefore required. The remainder showed a variety of growth defects, such as an inability to maintain consistent hyphal diameter, develop normal conidiophores and conidia, and generate consistently spaced septa. In addition, one deletion strain in particular (Δ*ecoA*) displayed a peculiar cell lysis phenotype, in which multiple hyphae lysed at the apex during growth, as well as an over-production of cleistothecia. These deletion phenotypes are consistent with the localization patterns observed in each protein, and indicate an involvement with hyphal growth, membrane turnover, and/or endocytosis.

The documented localization patterns (discussed in CHAPTER II) support the hypothesis that the NPFxD motif is likely to mark proteins for localization to the polarized cell apex in growing hyphae. Several polarized proteins that were previously unknown have now been identified, and investigating proteins which contain the NPFxD motif could be key to further understanding the mechanism of polarized hyphal growth.

Many of the motif-containing proteins shown here localize to at least one of three regions near the growing fronts of hyphae. These areas include 1) the SPK, which displays an intimate association with the precise growth pattern of hyphae and hyphal directionality, 2) the sub-apical collar, where endocytosis is enriched at the membrane, and 3) the apical crescent or dome, where cargo is actively recycled. The predominance of localization to

the sub-apical collar here also supports the presumption that the NPFxD motif marks proteins to areas of endocytosis, or areas where endocytosis is enriched. In addition to the prioritized list of NPFxD motif-containing proteins, three associated proteins (SlaA, EcoC, and EdeA) that contain similar or truncated motifs were also investigated. Based on the observed localization patterns and similarities to orthologs, these three proteins also fit the hypothesis and provide further evidence that the NPFxD motif, in a variety of forms, is likely to mark proteins to areas where endocytosis is enriched.

REFERENCES

Abe, K., Gomi, K., Hasegawa, F., Machida, M., 2006. Impact of *Aspergillus oryzae* genomics on industrial production of metabolites. Mycopathologia. 162, 143-153.

Abenza, J. F., Pantazopoulou, A., Rodriguez, J. M., Galindo, A., Penalva, M. A., 2009. Long-distance movement of *Aspergillus nidulans* early endosomes on microtubule tracks. Traffic. 10, 57-75.

Apel, A. R., Hoban, K., Chuartzman, S., Tonikian, R., Sidhu, S., et al., 2017. Syp1 regulates the clathrin-mediated and clathrin-independent endocytosis of multiple cargo proteins through a novel sorting motif. Mol Biol Cell. 28, 2434-2448.

Araujo-Bazan, L., Peñalva, M. A., Espeso, E. A., 2008. Preferential localization of the endocytic internalization machinery to hyphal tips underlies polarization of the actin cytoskeleton in *Aspergillus nidulans*. Mol Microbiol. 67, 891-905.

Asano, S., Mishima, M., Nishida, E., 2001. Coronin forms a stable dimer through its C-terminal coiled coil region: an implicated role in its localization to cell periphery. Genes Cells. 6, 225-235.

Atkinson, H. A., Daniels, A., Read, N. D., 2002. Live-cell imaging of endocytosis during conidial germination in the rice blast fungus *Magnaporthe grisea*. Fungal Genet Biol. 37, 233-244.

Aydar, E., Palmer, C. P., 2009. Polycystic kidney disease channel and synaptotagmin homologues play roles in *Schizosaccharomyces pombe* cell wall synthesis/repair and membrane protein trafficking. J Membr Biol. 229, 141-152.

Bartnicki-Garcia, S., Bartnicki, D. D., Gierz, G., Lopez-Franco, R., Bracker, C. E., 1995. Evidence that Spitzenkörper behavior determines the shape of a fungal hypha: a test of the hyphoid model. Exp Mycol. 19, 153-159.

Bartnicki-Garcia, S., Garduno-Rosales, M., Delgado-Alvarez, D. L., Mourino-Perez, R. R., 2018. Experimental measurement of endocytosis in fungal hyphae. Fungal Genet Biol. 118, 32-36.

Bartnicki-Garcia, S., Hergert, F., Gierz, G., 1989. Computer simulation of fungal morphogenesis and the mathematical basis for hyphal (tip) growth. Protoplasma. 46-57.

Berepiki, A., Lichius, A., Shoji, J.-Y., Tilsner, J., Read, N. D., 2010. F-actin dynamics in *Neurospora crassa*. Eukaryot Cell. 9, 547-557.

Boeke, D., Trautmann, S., Meurer, M., Wachsmuth, M., Godlee, C., et al., 2014. Quantification of cytosolic interactions identifies Ede1 oligomers as key organizers of endocytosis. Molecular Systems Biology. 10, 756.

Boettner, D. R., D'Agostino, J. L., Torres, O. T., Daugherty-Clarke, K., Uygur, A., et al., 2009. The F-BAR protein Syp1 negatively regulates WASp-Arp2/3 complex activity during endocytic patch formation. Curr Biol. 19, 1979-1987.

Bogomolnaya, L. M., Pathak, R., Guo, J., Polymenis, M., 2006. Roles of the RAM signaling network in cell cycle progression in *Saccharomyces cerevisiae*. Curr Genet. 49, 384-392.

Brett, T. J., Traub, L. M., Fremont, D. H., 2002. Accessory protein recruitment motifs in clathrin-mediated endocytosis. Structure. 10, 797-809.

Bruno, V. M., Kalachikov, S., Subaran, R., Nobile, C. J., Kyratsous, C., et al., 2006. Control of the *C. albicans* cell wall damage response by transcriptional regulator Cas5. PLoS Pathog. 2, e21.

Byrne, K. P., Wolfe, K. H., 2005. The Yeast Gene Order Browser: combining curated homology and syntenic context reveals gene fate in polyploid species. Genome Res. 15, 1456-1461.

Cairns, T. C., Nai, C., Meyer, V., 2018. How a fungus shapes biotechnology: 100 years of *Aspergillus niger* research. Fungal Biol Biotechnol. 5, 14.

Cairns, T. C., Zheng, X., Zheng, P., Sun, J., Meyer, V., 2019. Moulding the mould: understanding and reprogramming filamentous fungal growth and morphogenesis for next generation cell factories. Biotechnol Biofuels. 12, 77.

Carroll, S. Y., Stimpson, H. E., Weinberg, J., Toret, C. P., Sun, Y., et al., 2012. Analysis of yeast endocytic site formation and maturation through a regulatory transition point. Mol Biol Cell. 23, 657-668.

Collopy, P. D., Colot, H. V., Park, G., Ringelberg, C., Crew, C. M., et al., 2010. High-throughput construction of gene deletion cassettes for generation of *Neurospora crassa* knockout strains. Methods Mol Biol. 638, 33-40.

Colot, H. V., Park, G., Turner, G. E., Ringelberg, C., Crew, C. M., et al., 2006. A high-throughput gene knockout procedure for *Neurospora* reveals functions for multiple transcription factors. Proc Natl Acad Sci USA. 103, 10352-10357.

Costa, R., Warren, D. T., Ayscough, K. R., 2005. Lsb5p interacts with actin regulators Sla1p and Las17p, ubiquitin and Arf3p to couple actin dynamics to membrane trafficking processes. Biochem J. 387, 649-658.

de Beer, T., Hoofnagle, A. N., Enmon, J. L., Bowers, R. C., Yamabhai, M., et al., 2000. Molecular mechanism of NPF recognition by EH domains. Nature Structural Biology. 7, 1018-1022.

de Hostos, E. L., 1999. The coronin family of actin-associated proteins. Trends Cell Biol. 9, 345-350.

de Hostos, E. L., Bradtke, B., Lottspeich, F., Guggenheim, R., Gerisch, G., 1991. Coronin, an actin binding protein of *Dictyostelium discoideum* localized to cell surface projections, has sequence similarities to G protein beta subunits. EMBO J. 10, 4097-4104.

Delgado-Alvarez, D. L., Callejas-Negrete, O. A., Gomez, N., Freitag, M., Roberson, R. W., et al., 2010. Visualization of F-actin localization and dynamics with live cell markers in *Neurospora crassa*. Fungal Genet Biol. 47, 573-586.

Dell'Angelica, E. C., Puertollano, R., Mullins, C., Aguilar, R. C., Vargas, J. D., et al., 2000. GGAs: a family of ADP ribosylation factor-binding proteins related to adaptors and associated with the Golgi complex. J Cell Biol. 149, 81-94.

Du, L. L., Novick, P., 2002. Pag1p, a novel protein associated with protein kinase Cbk1p, is required for cell morphogenesis and proliferation in *Saccharomyces cerevisiae*. Mol Biol Cell. 13, 503-514.

Echauri-Espinosa, R. O., Callejas-Negrete, O. A., Roberson, R. W., Bartnicki-Garcia, S., Mourino-Perez, R. R., 2012. Coronin is a component of the endocytic collar of hyphae of *Neurospora crassa* and is necessary for normal growth and morphogenesis. PloS one. 7, e38237.

Eckert, C., Hammesfahr, B., Kollmar, M., 2011. A holistic phylogeny of the coronin gene family reveals an ancient origin of the tandem-coronin, defines a new subfamily, and predicts protein function. BMC Evol Biol. 11, 268.

Epp, E., Nazarova, E., Regan, H., Douglas, L. M., Konopka, J. B., et al., 2013. Clathrin- and Arp2/3-independent endocytosis in the fungal pathogen *Candida albicans*. mBio. 4, e00476-00513.

Fischer-Parton, S., Parton, R. M., Hickey, P. C., Dijksterhuis, J., Atkinson, H. A., et al., 2000. Confocal microscopy of FM4-64 as a tool for analysing endocytosis and vesicle trafficking in living fungal hyphae. J Microsc. 198, 246-259.

Fischer, R., Zekert, N., Takeshita, N., 2008. Polarized growth in fungi--interplay between the cytoskeleton, positional markers and membrane domains. Mol Microbiol. 68, 813-826.

Fuchs, U., Hause, G., Schuchardt, I., Steinberg, G., 2006. Endocytosis is essential for pathogenic development in the corn smut fungus *Ustilago maydis*. Plant Cell. 18, 2066-2081.

Gachet, Y., Hyams, J. S., 2005. Endocytosis in fission yeast is spatially associated with the actin cytoskeleton during polarised cell growth and cytokinesis. J Cell Sci. 118, 4231-4242.

Gagny, B., Wiederkehr, A., Dumoulin, P., Winsor, B., Riezman, H., et al., 2000. A novel EH domain protein of *Saccharomyces cerevisiae*, Ede1p, is involved in endocytosis. J Cell Sci. 113, 3309-3319.

Ge, W., Chew, T. G., Wachtler, V., Naqvi, S. N., Balasubramanian, M. K., 2005. The novel fission yeast protein Pal1p interacts with Hip1-related Sla2p/End4p and is involved in cellular morphogenesis. Mol Biol Cell. 16, 4124-4138.

Gierz, G., Bartnicki-Garcia, S., 2001. A three-dimensional model of fungal morphogenesis based on the vesicle supply center concept. J Theor Biol. 208, 151-164.

Goode, B. L., Eskin, J. A., Wendland, B., 2015. Actin and endocytosis in budding yeast. Genetics. 199, 315-358.

Harris, S. D., Cell polarity in filamentous fungi: shaping the mold. Elsevier Inc., 2006, pp. 41-77.

Harris, S. D., 2009. The Spitzenkörper: a signalling hub for the control of fungal development? Mol Microbiol. 73, 733-736.

Harris, S. D., 2011. Hyphal morphogenesis: an evolutionary perspective. Fungal Biol. 115, 475-484.

Harris, S. D., Turner, G., Meyer, V., Espeso, E. A., Specht, T., et al., 2009. Morphology and development in *Aspergillus nidulans*: A complex puzzle. Fungal Genet Biol. 46, S82-S92.

Heil-Chapdelaine, R. A., Tran, N. K., Cooper, J. A., 1998. The role of *Saccharomyces cerevisiae* coronin in the actin and microtubule cytoskeletons. Curr Biol. 8, 1281-1287.

Hernandez-Gonzalez, M., Bravo-Plaza, I., Pinar, M., de Los Rios, V., Arst, H. N., Jr., et al., 2018. Endocytic recycling via the TGN underlies the polarized hyphal mode of life. PLoS Genet. 14, e1007291.

Hirata, D., Kishimoto, N., Suda, M., Sogabe, Y., Nakagawa, S., et al., 2002. Fission yeast Mor2/Cps12, a protein similar to *Drosophila* Furry, is essential for cell morphogenesis and its mutation induces Wee1-dependent G(2) delay. EMBO J. 21, 4863-4874.

Hoffmann, J., Mendgen, K., 1998. Endocytosis and membrane turnover in the germ tube of *Uromyces fabae*. Fungal Genet Biol. 24, 77-85.

Howard, J. P., Hutton, J. L., Olson, J. M., Payne, G. S., 2002. Sla1p serves as the targeting signal recognition factor for NPFX(1,2)D-mediated endocytosis. J Cell Biol. 157, 315-326.

Jentsch, S., Seufert, W., Hauser, H. P., 1991. Genetic analysis of the ubiquitin system. BBA. 1089, 127-139.

Kaminskyj, S. G. W., 2001. Fundamentals of growth, storage, genetics and microscopy of *Aspergillus nidulans*. Fungal Genet Rep. 48, 25-31.

Kiss, E., Hegedüs, B., Virágh, M., Varga, T., Merényi, Z., et al., 2019. Comparative genomics reveals the origin of fungal hyphae and multicellularity. Nat Commun. 10, 4080.

Kodama, S., Ishizuka, J., Miyashita, I., Ishii, T., Nishiuchi, T., et al., 2017. The morphogenesis-related NDR kinase pathway of *Colletotrichum orbiculare* is required for translating plant surface signals into infection-related morphogenesis and pathogenesis. PLoS Pathog. 13, e1006189.

Köhler, J. R., Casadevall, A., Perfect, J., 2014. The spectrum of fungi that infects humans. Cold Spring Harb Perspect Med. 5, a019273.

Konzack, S., Rischitor, P. E., Enke, C., Fischer, R., 2005. The role of the kinesin motor KipA in microtubule organization and polarized growth of *Aspergillus nidulans*. Mol Biol Cell. 16, 497-506.

Li, L., Chen, X., Zhang, S., Yang, J., Chen, D., et al., 2017a. MoCAP proteins regulated by MoArk1-mediated phosphorylation coordinate endocytosis and actin dynamics

to govern development and virulence of Magnaporthe oryzae. PLoS Genet. 13, e1006814.

Li, L., Zhang, S., Liu, X., Yu, R., Li, X., et al., 2019. *Magnaporthe oryzae* Abp1, a MoArk1 kinase-interacting actin binding protein, links actin cytoskeleton regulation to growth, endocytosis, and pathogenesis. Molecular Plant-Microbe Interactions. 32, 437-451.

Li, X., Gao, C., Li, L., Liu, M., Yin, Z., et al., 2017b. MoEnd3 regulates appressorium formation and virulence through mediating endocytosis in rice blast fungus *Magnaporthe oryzae*. PLoS Pathog. 13, e1006449.

Li, Y., Li, B., Liu, L., Chen, H., Zhang, H., et al., 2015. FgMon1, a guanine nucleotide exchange factor of FgRab7, is important for vacuole fusion, autophagy and plant infection in *Fusarium graminearum*. Sci Rep. 5, 18101.

Liu, K., Hua, Z., Nepute, J. A., Graham, T. R., 2007. Yeast P4-ATPases Drs2p and Dnf1p are essential cargos of the NPFXD/Sla1p endocytic pathway. Mol Biol Cell. 18, 487-500.

Lohi, O., Lehto, V., 1998. VHS domain marks a group of proteins involved in endocytosis and vesicular trafficking. FEBS Lett. 440, 255-257.

Lorang, J. M., Tuori, R. P., Martinez, J. P., Sawyer, T. L., Redman, R. S., et al., 2001. Green fluorescent protein is lighting up fungal biology. Appl Environ Microbiol. 67, 1987-1994.

Lu, R., Drubin, D. G., Sun, Y., 2016. Clathrin-mediated endocytosis in budding yeast at a glance. J Cell Sci. 129, 1531-1536.

Maerz, S., Seiler, S., 2010. Tales of RAM and MOR: NDR kinase signaling in fungal morphogenesis. Curr Opin Microbiol. 13, 663-671.

Mahadev, R. K., Di Pietro, S. M., Olson, J. M., Piao, H. L., Payne, G. S., et al., 2007. Structure of Sla1p homology domain 1 and interaction with the NPFxD endocytic internalization motif. EMBO J. 26, 1963-1971.

Mao, Y., Nickitenko, A., Duan, X., Lloyd, T. E., Wu, M. N., et al., 2000. Crystal structure of the VHS and FYVE tandem domains of Hrs, a protein involved in membrane trafficking and signal transduction. Cell. 100, 447-456.

Martzoukou, O., Amillis, S., Zervakou, A., Christoforidis, S., Diallinas, G., 2017. The AP-2 complex has a specialized clathrin-independent role in apical endocytosis and polar growth in fungi. eLife. 6, 26.

Mayor, S., Pagano, R. E., 2007. Pathways of clathrin-independent endocytosis. Nat Rev Mol Cell Biol. 8, 603-612.

McArdle, B., Hofmann, A., 2008. Coronin structure and implications. Subcell Biochem. 48, 56-71.

McCluskey, K., Wiest, A., Plamann, M., 2010. The Fungal Genetics Stock Center: a repository for 50 years of fungal genetics research. J. Biosci. 35, 119-126.

Meyer, V., Arentshorst, M., Flitter, S. J., Nitsche, B. M., Kwon, M. J., et al., 2009. Reconstruction of signaling networks regulating fungal morphogenesis by transcriptomics. Eukaryot Cell. 8, 1677-1691.

Mi, H., Muruganujan, A., Ebert, D., Huang, X., Thomas, P. D., 2018. PANTHER version 14: more genomes, a new PANTHER GO-slim and improvements in enrichment analysis tools. Nucleic Acids Res. 47, D419-D426.

Miaczynska, M., Stenmark, H., 2008. Mechanisms and functions of endocytosis. J Cell Biol. 180, 7-11.

Mishima, M., Nishida, E., 1999. Coronin localizes to leading edges and is involved in cell spreading and lamellipodium extension in vertebrate cells. J Cell Sci. 112, 2833-2842.

Misra, S., Beach, B. M., Hurley, J. H., 2000. Structure of the VHS domain of human Tom1 (target of myb 1): insights into interactions with proteins and membranes. Biochemistry. 39, 11282-11290.

Morris, Z., Sinha, D., Poddar, A., Morris, B., Chen, Q., 2019. Fission yeast TRP channel Pkd2p localizes to the cleavage furrow and regulates cell separation during cytokinesis. Mol Biol Cell. 30, 1791-1804.

Muñoz, J. F., McEwen, J. G., Clay, O. K., Cuomo, C. A., 2018. Genome analysis reveals evolutionary mechanisms of adaptation in systemic dimorphic fungi. Sci Rep. 8, 4473.

Neer, E. J., Schmidt, C. J., Nambudripad, R., Smith, T. F., 1994. The ancient regulatory-protein family of WD-repeat proteins. Nature. 371, 297-300.

Negrete-Urtasun, S., Denison, S. H., Arst, H. N., Jr., 1997. Characterization of the pH signal transduction pathway gene palA of *Aspergillus nidulans* and identification of possible homologs. J Bacteriol. 179, 1832-1835.

Nelson, B., Kurischko, C., Horecka, J., Mody, M., Nair, P., et al., 2003. RAM: a conserved signaling network that regulates Ace2p transcriptional activity and polarized morphogenesis. Mol Biol Cell. 14, 3782-3803.

Newpher, T. M., Smith, R. P., Lemmon, V., Lemmon, S. K., 2005. In vivo dynamics of clathrin and Its adaptor-dependent recruitment to the actin-based endocytic machinery in yeast. Dev Cell. 9, 87-98.

Nilius, B., Owsianik, G., 2011. The transient receptor potential family of ion channels. Genome Biol. 12, 218.

Palmer, C. P., Aydar, E., Djamgoz, M. B., 2005. A microbial TRP-like polycystic-kidney-disease-related ion channel gene. Biochem J. 387, 211-219.

Peñalva, M. A., 2005. Tracing the endocytic pathway of *Aspergillus nidulans* with FM4-64. Fungal Genet Biol. 42, 963-975.

Peñalva, M. A., 2010. Endocytosis in filamentous fungi: Cinderella gets her reward. Curr Opin Microbiol. 13, 684-692.

Piao, H. L., Machado, I. M. P., Payne, G. S., 2007. NPFXD-mediated endocytosis Is required for polarity and function of a yeast cell wall stress sensor. Mol Biol Cell. 18, 57-65.

Protchenko, O., Rodriguez-Suarez, R., Androphy, R., Bussey, H., Philpott, C. C., 2006. A screen for genes of heme uptake identifies the FLC family required for import of FAD into the endoplasmic reticulum. J Biol Chem. 281, 21445-21457.

Qiu, W., Neo, S. P., Yu, X., Cai, M., 2008. A novel septin-associated protein, Syp1p, is required for normal cell cycle-dependent septin cytoskeleton dynamics in yeast. Genetics. 180, 1445-1457.

Ramelot, T. A., Cort, J. R., Yee, A. A., Semesi, A., Edwards, A. M., et al., 2003. Solution structure of the yeast ubiquitin-like modifier protein Hub1. Journal of Structural and Functional Genomics. 4, 25-30.

Rapoport, T. A., 2007. Protein translocation across the eukaryotic endoplasmic reticulum and bacterial plasma membranes. Nature. 450, 663-669.

Reynaga-Peña, C. G., Gierz, G., Bartnicki-Garcia, S., 1997. Analysis of the role of the Spitzenkörper in fungal morphogenesis by computer simulation of apical branching in *Aspergillus niger*. Proc Natl Acad Sci USA. 94, 9096-9101.

Riquelme, M., Aguirre, J., Bartnicki-Garcia, S., Braus, G. H., Feldbrugge, M., et al., 2018. Fungal morphogenesis, from the polarized growth of hyphae to complex reproduction and infection structures. Microbiol Mol Biol Rev. 82.

Riquelme, M., Sanchez-Leon, E., 2014. The Spitzenkörper: a choreographer of fungal growth and morphogenesis. Curr Opin Microbiol. 20, 27-33.

Robinson, M. S., Watts, C., Zerial, M., 1996. Membrane Dynamics in Endocytosis. Cell. 84, 13-21.

Rybakin, V., Clemen, C. S., 2005. Coronin proteins as multifunctional regulators of the cytoskeleton and membrane trafficking. Bioessays. 27, 625-632.

Sambrook, J., Russell, D. W., Purification of nucleic acids by extraction with Phenol:Chloroform. Molecular Cloning. Cold Spring Harbor Laboratory Press, Cold Spring Harbor, NY, USA, 2001.

Sartorel, E., Pérez-Martín, J., 2012. The distinct interaction between cell cycle regulation and the widely conserved morphogenesis-related (MOR) pathway in the fungus *Ustilago maydis* determines morphology. J Cell Sci. 125, 4597-4608.

Schultzhaus, Z., Johnson, T. B., Shaw, B. D., 2017a. Clathrin localization and dynamics in *Aspergillus nidulans*. Mol Microbiol. 103, 299-318.

Schultzhaus, Z., Quintanilla, L., Hilton, A., Shaw, B. D., 2016. Live cell imaging of actin dynamics in the filamentous fungus *Aspergillus nidulans*. Microsc Microanal. 22, 264-274.

Schultzhaus, Z., Yan, H., Shaw, B. D., 2015. *Aspergillus nidulans* flippase DnfA is cargo of the endocytic collar and plays complementary roles in growth and phosphatidylserine asymmetry with another flippase, DnfB. Mol Microbiol. 97, 18-32.

Schultzhaus, Z., Zheng, W., Wang, Z., Mourino-Perez, R., Shaw, B. D., 2017b. Phospholipid flippases DnfA and DnfB exhibit differential dynamics within the *A. nidulans* Spitzenkörper. Fungal Genet Biol. 99, 26-28.

Sharpless, K. E., Harris, S. D., 2002. Functional characterization and localization of the *Aspergillus nidulans* formin SepA. Mol Biol Cell. 13, 469-479.

Shaw, B. D., Chung, D. W., Wang, C. L., Quintanilla, L. A., Upadhyay, S., 2011. A role for endocytic recycling in hyphal growth. Fungal Biol. 115, 541-546.

Shoji, J. Y., Kikuma, T., Kitamoto, K., 2014. Vesicle trafficking, organelle functions, and unconventional secretion in fungal physiology and pathogenicity. Curr Opin Microbiol. 20, 1-9.

Song, Y., Cheon, S. A., Lee, K. E., Lee, S. Y., Lee, B. K., et al., 2008. Role of the RAM network in cell polarity and hyphal morphogenesis in *Candida albicans*. Mol Biol Cell. 19, 5456-5477.

Stajich, J. E., Harris, T., Brunk, B. P., Brestelli, J., Fischer, S., et al., 2012. FungiDB: an integrated functional genomics database for fungi. Nucleic Acids Res. 40, D675-D681.

Steinberg, G., 2014. Endocytosis and early endosome motility in filamentous fungi. Curr Opin Microbiol. 20, 10-18.

Steinberg, G., Peñalva, M. A., Riquelme, M., Wosten, H. A., Harris, S. D., 2017. Cell biology of hyphal growth. Microbiol Spectr. 5, 34.

Sudbery, P., 2011. Fluorescent proteins illuminate the structure and function of the hyphal tip apparatus. Fungal Genet Biol. 48, 849-857.

Swartzman, E. E., Viswanathan, M. N., Thorner, J., 1996. The PAL1 gene product is a peroxisomal ATP-binding cassette transporter in the yeast *Saccharomyces cerevisiae*. J Cell Biol. 132, 549-563.

Szewczyk, E., Nayak, T., Oakley, C. E., Edgerton, H., Xiong, Y., et al., 2007. Fusion PCR and Gene Targeting in Aspergillus nidulans. Nature protocols. 1, 3111-3120.

Taheri-Talesh, N., Horio, T., Araujo-Bazan, L., Dou, X., Espeso, E. A., et al., 2008. The tip growth apparatus of *Aspergillus nidulans*. Mol Biol Cell. 19, 1439-1449.

Takeshita, N., 2016. Coordinated process of polarized growth in filamentous fungi. Biosci Biotechnol Biochem. 80, 1693-1699.

Takeshita, N., Mania, D., Herrero, S., Ishitsuka, Y., Nienhaus, G. U., et al., 2013. The cell-end marker TeaA and the microtubule polymerase AlpA contribute to microtubule guidance at the hyphal tip cortex of *Aspergillus nidulans* to provide polarity maintenance. J Cell Sci. 126, 5400-5411.

Tan, P. K., Howard, J. P., Payne, G. S., 1996. The sequence NPFXD defines a new class of endocytosis signal in *Saccharomyces cerevisiae*. J Cell Biol. 135, 1789-1800.

Thilo, L., 1985. Quantification of endocytosis-derived membrane traffic. BBA-Biomembranes. 822, 243-266.

Tolsma, T. O., Cuevas, L. M., Di Pietro, S. M., 2018. The Sla1 adaptor-clathrin interaction regulates coat formation and progression of endocytosis. Traffic. 19, 446-462.

Toret, C. P., Lee, L., Sekiya-Kawasaki, M., Drubin, D. G., 2008. Multiple pathways regulate endocytic coat disassembly in *Saccharomyces cerevisiae* for optimal downstream trafficking. Traffic. 9, 848-859.

Tuo, S., Nakashima, K., Pringle, J. R., 2013. Role of endocytosis in localization and maintenance of the spatial markers for bud-site selection in yeast. PloS one. 8, e72123.

Upadhyay, S., Shaw, B. D., 2008. The role of actin, fimbrin and endocytosis in growth of hyphae in *Aspergillus nidulans*. Mol Microbiol. 68, 690-705.

Veiter, L., Rajamanickam, V., Herwig, C., 2018. The filamentous fungal pellet-relationship between morphology and productivity. Appl Microbiol Biotechnol. 102, 2997-3006.

Verdín, J., Sánchez-León, E., Rico-Ramírez, A. M., Martínez-Núñez, L., Fajardo-Somera, R. A., et al., 2019. Off the wall: the rhyme and reason of *Neurospora crassa* hyphal morphogenesis. Cell Surf. 5, 100020.

Vida, T. A., Emr, S. D., 1995. A new vital stain for visualizing vacuolar membrane dynamics and endocytosis in yeast. J Cell Biol. 128, 779-792.

Virag, A., Harris, S. D., 2006. The Spitzenkörper: a molecular perspective. Mycol Res. 110, 4-13.

Walton, F. J., Heitman, J., Idnurm, A., 2006. Conserved elements of the RAM signaling pathway establish cell polarity in the basidiomycete *Cryptococcus neoformans* in a divergent fashion from other fungi. Mol Biol Cell. 17, 3768-3780.

Xavier, C.-P., Eichinger, L., Fernandez, M. P., Morgan, R. O., Clemen, C. S., Evolutionary and functional diversity of coronin proteins. In: C. S. Clemen, L. Eichinger, V. Rybakin, Eds., The Coronin Family of Proteins: Subcellular Biochemistry. Springer New York, New York, NY, 2008, pp. 98-109.

Yamashita, R. A., Osherov, N., May, G. S., 2000. Localization of wild type and mutant class I Myosin proteins in *Aspergillus nidulans* using GFP-fusion proteins Cell Motil Cytoskel. 163-172.

Yang, C. D., Dang, X., Zheng, H. W., Chen, X. F., Lin, X. L., et al., 2017. Two Rab5 homologs are essential for the development and pathogenicity of the Rice Blast fungus *Magnaporthe oryzae*. Front. Plant Sci. 8, 620.

Yang, L., Ukil, L., Osmani, A., Nahm, F., Davies, J., et al., 2004. Rapid production of gene replacement constructs and generation of a green fluorescent protein-tagged centromeric marker in *Aspergillus nidulans*. Eukaryot Cell. 3, 1359-1362.

Yarden, O., Plamann, M., Ebbole, D. J., Yanofsky, C., 1992. cot-1, a gene required for hyphal elongation in *Neurospora crassa,* encodes a protein kinase. EMBO J. 11, 2159-2166.

Zeilinger, S., Gupta, V. K., Dahms, T. E. S., Silva, R. N., Singh, H. B., et al., 2016. Friends or foes? Emerging insights from fungal interactions with plants. FEMS Microbiol Rev. 40, 182-207.

Zeng, G., Wang, Y. M., Wang, Y., 2012. Cdc28-Cln3 phosphorylation of Sla1 regulates actin patch dynamics in different modes of fungal growth. Mol Biol Cell. 23, 3485-3497.

Zheng, W., Lin, Y., Fang, W., Zhao, X., Lou, Y., et al., 2018. The endosomal recycling of FgSnc1 by FgSnx41-FgSnx4 heterodimer is essential for polarized growth and pathogenicity in *Fusarium graminearum*. New Phytologist. 219, 654-671.

Zhu, M. X., 2011. TRP Channels. CRC Press/Taylor & Francis Llc., Boca Raton (FL).

APPENDIX A

SUPPLEMENTARY MATERIALS

Table A-1. Chart of NPFxD Motif-Containing Proteins in *Aspergillus nidulans*. This table is included as a separate file.

Table A-1 Notes:

[a] = N. crassa knockout references: (Collopy et al., 2010; Colot et al., 2006)

None[b] = A N. crassa knockout phenotype was not associated with the ortholog for this gene.

(N/A)[c] = A N. crassa knockout phenotype was not provided for the ortholog for this gene.

Table A-1 References:

- Ahuja, M., et al., 2012. Illuminating the diversity of aromatic polyketide synthases in *Aspergillus nidulans*. J. Am. Chem. Soc. 134, 8212-8221.
- Bauer, S., et al., 2006. Development and application of a suite of polysaccharide-degrading enzymes for analyzing plant cell walls. PNAS USA. 103, 11417-11422.
- Collopy, P. D., et al., 2010. High-throughput construction of gene deletion cassettes for generation of *Neurospora crassa* knockout strains. Methods Mol. Biol. 638, 33-40.
- Colot, H. V., et al., 2006. A high-throughput gene knockout procedure for *Neurospora* reveals functions for multiple transcription factors. PNAS USA. 103, 10352-10357.
- David, H., et al., 2008. Analysis of *Aspergillus nidulans* metabolism at the genome-scale. BMC Genomics. 9, 163.
- De Souza, C. P., et al., 2013. Functional analysis of the *Aspergillus nidulans* kinome. PLoS One. 8, e58008-e58008.
- Efimov, V. P., Morris, N. R., 1998. A screen for dynein synthetic lethals in *Aspergillus nidulans* identifies spindle assembly checkpoint genes and other genes involved in mitosis. Genetics. 149, 101-116.
- Gacek-Matthews, A., et al., 2015. KdmA, a histone H3 demethylase with bipartite function, differentially regulates primary and secondary metabolism in *Aspergillus nidulans*. Mol Microbiol. 96, 839-60.
- James, S. W., et al., 2014. Restraint of the G2/M transition by the SR/RRM family mRNA shuttling binding protein SNXAHRB1 in *Aspergillus nidulans*. Genetics. 198, 617-633.
- Schultzhaus, Z., et al., 2015. *Aspergillus nidulans* flippase DnfA is cargo of the endocytic collar and plays complementary roles in growth and phosphatidylserine asymmetry with another flippase, DnfB. Mol. Microbiol. 97, 18-32.
- Yamashita, R. A., et al., 2000. Localization of wild type and mutant class I Myosin proteins in *Aspergillus nidulans* using GFP-fusion proteins Cell Motil. Cytoskel., 163-172.

Table A-2. Strains created and used in this study.

Name	Genotype	Source
TNO2A7	*pyrG89; ΔnkuA::argB; pyroA4; riboB2*	(McCluskey et al., 2010)
NKUNU	*pyrG89; ΔnkuA::argB; pabaA1; pyroA4;*	(Schultzhaus et al., 2015)
A773	*pyrG89; wA3; pyroA4*	(McCluskey et al., 2010)
TaoA::GFP	*pyrG89; ΔnkuA::argB;* ***taoA****::GFP::pyrG; pabaA1; pyroA4*	This Study
EcoA::GFP	*pyrG89; ΔnkuA::argB;* ***ecoA****::GFP::pyrG; pabaA1; pyroA4*	This Study
EcoB::GFP	*pyrG89; ΔnkuA::argB;* ***ecoB****::GFP::pyrG; pabaA1; pyroA4*	This Study
EcoC::GFP	*pyrG89; ΔnkuA::argB;* ***ecoC****::GFP::pyrG; pabaA1; pyroA4*	This Study
CorA::GFP	*pyrG89; ΔnkuA::argB;* ***corA****::GFP::pyrG; pabaA1; pyroA4*	This Study
SlaA::GFP	*pyrG89; ΔnkuA::argB;* ***slaA****::GFP::pyrG; pabaA1; pyroA4*	This Study
HapA::GFP	*pyrG89; ΔnkuA::argB;* ***hapA****::GFP::pyrG; pabaA1; pyroA4*	This Study
LsbA::GFP	*pyrG89; ΔnkuA::argB;* ***lsbA****::GFP::pyrG; pabaA1; pyroA4*	This Study
EdeA::GFP	*pyrG89; ΔnkuA::argB;* ***edeA****::GFP::pyrG; pabaA1; pyroA4*	This Study
FmlA::GFP	*pyrG89; ΔnkuA::argB;* ***lwpA****::GFP::pyrG; pabaA1; pyroA4*	This Study
NulA::GFP	*pyrG89; ΔnkuA::argB;* ***nulA****::GFP::pyrG; pabaA1; pyroA4*	This Study
PeaA::GFP	*pyrG89; ΔnkuA::argB;* ***peaA****::mCherry::paba; pabaA1; pyroA4*	This Study
AN4106::GFP	*pyrG89; ΔnkuA::argB; AN4106::GFP::pyrG; pabaA1; pyroA4*	This Study
AN8621::GFP	*pyrG89; ΔnkuA::argB;* ***AN8621****::GFP::pyrG; pabaA1; pyroA4*	This Study
AN10090::GFP	*pyrG89; ΔnkuA::argB;* ***AN10090****::GFP::pyrG; pabaA1; pyroA4*	This Study
AN10296::GFP	*pyrG89; ΔnkuA::argB;* ***AN10296****::GFP::pyrG; pabaA1; pyroA4*	This Study
AN2669::GFP	*pyrG89; ΔnkuA::argB;* ***AN2669****::GFP::pyrG; pabaA1; pyroA4*	This Study
AN4945::GFP	*pyrG89; ΔnkuA::argB;* ***AN4945****::GFP::pyrG; pabaA1; pyroA4*	This Study

Table A-2 Continued

Name	Genotype	Source
AN5302::GFP	*pyrG89; ΔnkuA::argB; **AN5302**::GFP::pyrG; pabaA1; pyroA4*	This Study
TaoAxFimA	*pyrG89; ΔnkuA::argB; TaoA::GFP::pyrG; pabaA1; pyroA4; fimA::mCherry::pyroA*	This Study
EcoAxFimA	*pyrG89; ΔnkuA::argB; **ecoA**::GFP::pyrG; pabaA1; pyroA4; **fimA**::mCherry::pyroA*	This Study
CorAxFimA	*pyrG89; ΔnkuA::argB; cor**A**::GFP::pyrG; pabaA1; pyroA4; **fimA**::mCherry::pyroA*	This Study
Δ*taoA*	*pyrG89; ΔnkuA::argB; pyroA4; riboB2; ΔtaoA::riboB*	This Study
Δ*ecoA*	*pyrG89; ΔnkuA::argB; pyroA4; riboB2; ΔecoA::riboB*	This Study
Δ*ecoC*	*pyrG89; ΔnkuA::argB; pyroA4; riboB2; ΔecoC::riboB*	This Study
Δ*slaA*	*pyrG89; ΔnkuA::argB; pyroA4; riboB2; ΔslaA::riboB*	This Study
Δ*hapA*	*pyrG89; ΔnkuA::argB; pyroA4; riboB2; ΔhapA::riboB*	This Study
cΔ*taoA* (Complement)	*pyrG89; ΔnkuA::argB; riboB2; ΔtaoA::riboB; taoA::GFP::pyrG; pabaA1*	This Study
cΔ*ecoA* (Complement)	*pyrG89; ΔnkuA::argB; riboB2; ΔecoA::riboB; ecoA::GFP::pyrG; pabaA1*	This Study
Δ*ecoA*xDAB	*pyrG89; ΔnkuA::argB; pyroA4; riboB2; ΔecoA::riboB; DnfA::GFP::pyrG; pabaA1; DnfB::mCherry::pyroA*	This Study
Δ*taoA*xCoFm	*pyrG89; ΔnkuA::argB; pyroA4; riboB2; ΔtaoA::riboB; corA::GFP::pyrG; pabaA1; fimA::mCherry::pyroA*	This Study

Table A-3. Primers created and used in this study.

Primer Name	Primer Sequence
GFP::*AfpyrG*	
P3	GGAGCTGGTGCAGGCGCT
P4	CTGTCTGAGAGGAGGCACTGAT
mCherry::*Afpyro*	
P3	GGAGCTGGTGCAGGCGCTGG
P4	GAAGGACAAATGCACAGAACACCC
AfriboB	
P3	GAAAAAGGACACCTACCGCC
P4	CGGGGTCTCTAGTTTTCCCAAT
TaoA::GFP – AN0594	
P1	GAAAGAATACGAGCGAATCCAGAGTCT
P2	AGCGCCTGCACCAGCTCC-GTTGCACTGGAGGGAAC
P5	ATCAGTGCCTCCTCTCAGACAG-TGTGCCGATGCTGGAC
P6	GCTGTATCCCGAGCCTCT
P7	AGTTGATCGGGTAGATG
P8	CATGTTGTATCCTGTCAAT
Δ*taoA*	
ΔP1	AGACGAAGCCTTTATGCTTAC
ΔP2	GGCGGTAGGTGTCCTTTTTC-GTTGCACTGGAGGGAAC
ΔP5	ATTGGGAAAACTAGAGACCCCG-TGTGCCGATGCTGGAC
ΔP7	CACAGTGAGTTTGCTGT
Δ*taoA* Complement	
cΔtao-P7	GCGTTAGCCCCAGTCAGCC
cΔtao-P8	ATGTTGTATCCTGTCAATGTAATGTTAGCAGC
EcoA::GFP – AN2492	
P1	GTCGAAACTCTGAATCATCCA
P2	AGCGCCTGCACCAGCTCC-GTCATCGGTGACACGTCTC
P5	ATCAGTGCCTCCTCTCAGACAG-ACCGTTAAATTATATTTCCTACGC
P6	ATATGATACTCATTGAAAGGTCG
P7	ATGATGAGCGACGACGAC
P8	TGGATGTTGATGCTGACG
Δ*ecoA*	
ΔP1	CCTGGATTGGGCTTGG
ΔP2	GGCGGTAGGTGTCCTTTTTC-TTTGCCAGCAATGCG

Table A-3 Continued

Primer Name	Primer Sequence
ΔP5	ATTGGGAAAACTAGAGACCCCG-ACCGTTAAATTATATTTCCTACGC
ΔP7	GGCACAAGAATCAGGATACG
cΔecoA-P8	GCCTCTTCTGTTTGATGATGTT
EcoB::GFP – AN0777	
P1	TTGTCACAGCCATCAAGGAT
P2	AGCGCCTGCACCAGCTCC-ATAATGCTGGTGCTGCTGG
P5	ATCAGTGCCTCCTCTCAGACAG-CCGAGTATCCGATTTTGATTACTAC
P6	GATTGAAGGTTTTTTCTTATGGCT
P7	ATCTCAAGCCGCTCGT
P8	CCTGTATGAAGAGAATGTATGGTT
Δ*ecoB*	
ΔP1	GCAGCGTGGTGCTCAGAT
ΔP2	GGCGGTAGGTGTCCTTTTTC-TATGTCGGCGACTAGTAGGAATG
ΔP5	ATTGGGAAAACTAGAGACCCCG-CCGAGTATCCGATTTTGATTACTAC
ΔP7	CTGTTGTACGGAACAAATACCTG
EcoC::GFP – AN0697	
P1	CCAGTCCCAAATCAAGCT
P2	AGCGCCTGCACCAGCTCC-TGAAGAAACGTACTTCCCAA
P5	ATCAGTGCCTCCTCTCAGACAG-CTTATGATATCCACCCTGGAC
P6	GTTGGGCTACAAACTCGAC
P7	CGTCGCATACTTTGCATAG
P8	TATCTTCGATGGTGAGAACG
Δ*ecoC*	
ΔP1	GAGTTGGTAATGATGCCG
ΔP2	GGCGGTAGGTGTCCTTTTTC-TGCTTCTCACGAGACACAG
ΔP5	ATTGGGAAAACTAGAGACCCCG-CTTATGATATCCACCCTGGAC
ΔP7	GTACTAGGCACGATGGCA
SlaA::GFP – AN1462	
P1	AAGTCAAGACTCCCAAGCA
P2	AGCGCCTGCACCAGCTCC-AAAGCCAAACGGGTTG

Table A-3 Continued

Primer Name	Primer Sequence
P5	ATCAGTGCCTCCTCTCAGACAG-GTACATAGGATTTTCTTCGCAG
P6	CTACATTTGGATTGGGCA
P7	CCCACGTCTACCCCTG
P8	GCACTTGCCAGATTACCA
SlaA::mCh	
P1	GAAGTCAAGACTCCCAAGCAA
P2	CCAGCGCCTGCACCAGCTCC-AAAGCCAAACGGGTTGG
P5	GGGTGTTCTGTGCATTTGTCCTTC-GCGAAGCGTTGTGTACATAGG
P6	TGCCCAATCCAAATGTAGC
Δ*slaA*	
ΔP1	GAAGATGAAGAGGATGGGTATGA
ΔP2	GGCGGTAGGTGTCCTTTTTC-GGTGGCCGGTCAACTGAAT
ΔP5	ATTGGGAAAACTAGAGACCCCG-GCGAAGCGTTGTGTACATAGG
ΔP7	ATGGATGACAGATCGGAAG
AN1130::mCh (HOS4)	
P1	TCAAGCAGACTCTAAAGCCA
P2	GGAGCGCCTGCACCAGCTCC-GTCTTCTCGGGCGC
P5	GGGTGTTCTGTGCATTTGTCCTTC-GACTAATCCTGGTCGGGC
P6	CGTGTTGTTTCATGGAGC
P7	CAAGCAGACTGTAAGGATGG
P8	GCTCAGGCTAGGCAAAGTA
CorA::GFP – AN6341	
P1	GATACTTTGAGCTGGAGAATGACA
P2	AGCGCCTGCACCAGCTCC-GCCCAGCTTAGCCTTG
P5	ATCAGTGCCTCCTCTCAGACAG-CCTTGCGTCTGATACCTC
P6	GATCCTCATACCTTAGAGCG
P7	TGCACGAGAATGAGGTTACC
P8	CGACAGGAGCGAGCTG
Δ*corA*	
ΔP1	GGTATGGGCTTTTGTAGCTC
ΔP2	GGCGGTAGGTGTCCTTTTTC-GATGCTGGGTATCAAGGAA
ΔP5	ATTGGGAAAACTAGAGACCCCG-CCTTGCGTCTGATACCTC
ΔP7	CGGAGTTGTTGGCTACTCAC

Table A-3 Continued

Primer Name	Primer Sequence
HapA::GFP – AN1950	
P1	GGAATTTACTCGCAACGA
P2	AGCGCCTGCACCAGCTCC-ATGGTCATAACCTGCCC
P5	ATCAGTGCCTCCTCTCAGACAG-CGTTTTTTCTTCTTTTCCCG
P6	TTGTGTTGTGAGTGACATAGGG
P7	GTCATCAGCCTAGCGAAA
P8	AAGGTTAGTTGAAGAAAGATGCT
Δ*hapA*	
ΔP1	ACGATCCTATTGAATATAGAACTGTTACA
ΔP2	GGCGGTAGGTGTCCTTTTTC-TTTGGCGAGTATATGTCCTACC
ΔP5	ATTGGGAAAACTAGAGACCCCG-AAGAGTTTCGCGCGTTTT
ΔP7	GACACTCGAAAGGTAATCCTC
AN1909::GFP	
P1	CAACCTACGAGGGTAAGAAATAC
P2	AGCGCCTGCACCAGCTCC--ACCATACATTCCATCCCAC
P5	ATCAGTGCCTCCTCTCAGACAG-ATTACAAGGTATGCCAGGTCG
P6	AATGCCACCAAGAACCC
P7	GACCTCTCCACTTTCTTCG
P8	CTTCCCTCTCAACTTGTGG
PeaA::mCh – AN1509	
P1	ATGCAGCAATATCAAATGGACC
P2	CCAGCGCCTGCACCAGCTCC-CGCCGTGTTCCTGTGC
P5	GGGTGTTCTGTGCATTTGTCCTTC-TAGACGGCGTTTAAGAGCACC
P6	GCCTCACCGGGATTGAG
P7	CAACGCTTTCTTTCGCC
P8	GTACATGGAGACGGTGCTATG
AN7552::mCh	
P1	CGGTTTCAGAATGGGACG
P2	CCAGCGCCTGCACCAGCTCC-AACAGCCCCAACCCAATT
P5	GGGTGTTCTGTGCATTTGTCCTTC-TAGGGTTCAGCTCTTATCCG
P6	CCGCTCCTTCCAGTAGC
P7	CCAAGTGTAGAAGAACAAGCG
P8	CCATCATCTCAGCCAGC

Table A-3 Continued

Primer Name	Primer Sequence
FmlA::mCh – AN1557	
P1	GTGTGCGTCATTCCATTGTTTCT
P2	AGCGCCTGCACCAGCTCC-GCCTGCGGCACTGTCACT
P5	ATCAGTGCCTCCTCTCAGACAG-GGCTCAATCGGGAAGG
P6	TCCTATAACTTTGCTTCGGC
P7	GACCCTGACTATCTTTGTATGTCTT
P8	TTCCTGTTTCTTGTTGGTCT
AN6228::GFP (SYH1)	
P1	AGATCCAGGAAGCTGAGGC
P2	AGCGCCTGCACCAGCTCC-CCGCTTGCCCTTCTTG
P5	ATCAGTGCCTCCTCTCAGACAG-TTTCCGAGCTGTGACTCA
P6	CGCTCGGGAACGTATAAG
P7	CTCAGGCTCAGCAATCC
P8	AAGACTCAGCACACCCTCT
NulA::GFP – AN6164	
P1	CGTTGACGGAACACGACCTC
P2	AGCGCCTGCACCAGCTCC-TGGCGTTCCGGCCAT
P5	ATCAGTGCCTCCTCTCAGACAG-AAAGCAGAACAGTGAGAACG
P6	CCACTAGCCAATGGCTTAT
P7	CCAGTACAACAACCCACAA
P8	TCACGTCTGGTGGTATCG
LsbA::GFP – AN12305	
P1	AGACGAACCTTTGCTTGA
P2	AGCGCCTGCACCAGCTCC--AACTTCCTTACTGAGAGAACGT
P5	ATCAGTGCCTCCTCTCAGACAG-ATGAATTATCCTTTCTGCGG
P6	ATAGTCGCCTCTGTATCTATCATG
P7	GGCAATGGGCAGTTTCTTA
P8	GTCGCCTTCATTCTGGC
EdeA::GFP – AN0317	
P1	CGATAACTTTACGCCTGTC
P2	AGCGCCTGCACCAGCTCCCGATTTGGACGTGAGATG
P5	ATCAGTGCCTCCTCTCAGACAGTTCCACCTATGCACCGAATC
P6	CGTTGGTGGACAGACTTCG
P7	CATCGCAACTTGATGCTTTC
P8	TCTCCAGAAAAGGGACTCTG

Table A-3 Continued

Primer Name	Primer Sequence
AN10090::GFP	
P1	CGATCACGAATCAGTCG
P2	AGCGCCTGCACCAGCTCC-GTACCCCCACATATCATCC
P5	ATCAGTGCCTCCTCTCAGACAG-ATAGTCTACACCATCTCTCTGGTT
P6	ATCTAGTCCACGACTTTATGGA
P7	GGTTAGTCCAACGGACG
P8	GATCTCTGCTTGGTCGG
AN4106::GFP	
P1	TGTTAAGGGACGATCCGT
P2	AGCGCCTGCACCAGCTCC-ATGAGCGAACCGAAAGTC
P5	ATCAGTGCCTCCTCTCAGACAG-ATATCCCAATAAACGGGTACTTT
P6	GAAAGTGGGAATTTACGGG
P7	CAAGCAATAACCCTCTCGG
P8	CGC TAC GGC TGT CTG AAT
AN8621::GFP (TPO1)	
P1	GATGGAGAGGAAATCCCC
P2	AGCGCCTGCACCAGCTCC-CTTACCGCACAAGTGTTCAT
P5	ATCAGTGCCTCCTCTCAGACAG-TCACGAGTGTAGTCGGCAT
P6	GACAGCCTCAGCCCG
P7	ATTGCCCCTAGATGTAGAGTG
P8	TTGAGCACCAGTACCACAG
AN10296::GFP (FRD1)	
P1	TTATTGGGTCATTATTGGACAAA
P2	AGCGCCTGCACCAGCTCC-ATGCCCACTGTCAGAAACA
P5	ATCAGTGCCTCCTCTCAGACAG-GTGGCGATAGAGTGCAGC
P6	AAAAACGCCATGAAGTTGG
P7	TCGTCGGCGTTGAGTAC
P8	GAGAGGGCGGGATCTG

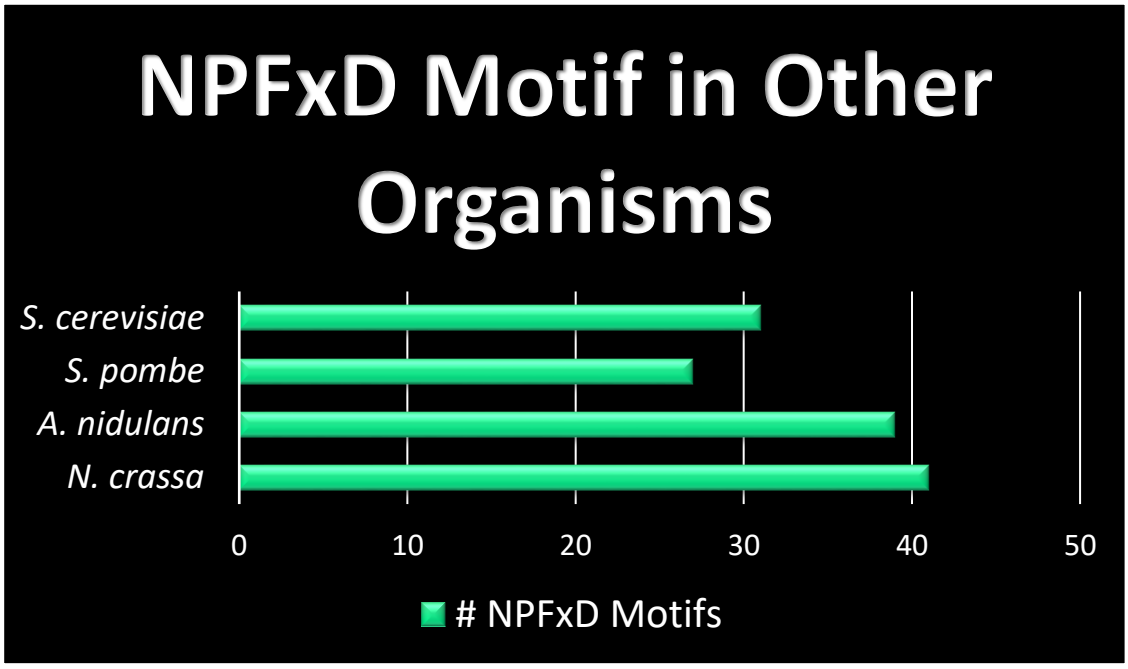

Figure A-1. NPFxD Motif Occurrences in Other Model Organisms.
Each of the four model organisms shown here was surveyed for the NPFxD motif, and the number of occurrences is represented by the graph. *Saccharomyces cerevisiae* and *Schizosaccharomyces pombe* are predicted to encode the motif 31 and 27 times, respectively. Alternatively, the two filamentous fungi (*Aspergillus nidulans* and *Neurospora crassa*) are predicted to encode the motif 39 and 41 times, respectively. It is likely that some of the proteins which contain this motif in filamentous fungi are involved in hyphal growth.

APPENDIX B

GENE DELETIONS

The basis of this study was to systematically tag NPFxD motif-containing proteins in *A. nidulans* with a fluorescent protein. When apical localization was observed, a deletion strain was also constructed for many of the genes. The mutant phenotypes were then observed and characterized, when possible. Three of the deletion strains (*slaA*, *hapA*, and *ecoC*) were lethal, and each gene is therefore considered to be required. The remainder of the deletion strains showed a variety of growth defects, such as an inability to maintain consistent hyphal diameter, develop normal conidiophores and conidia, and generate consistently spaced septa. In addition, one deletion strain in particular (Δ*ecoA*) displayed a peculiar cell lysis phenotype, in which multiple hyphae lysed at the apex during growth. The deletion phenotypes are consistent with the localization patterns observed in each protein, and indicate that the genes of interest may play roles in hyphal growth, membrane turnover, and/or endocytosis. A summary of deleted genes and observed phenotypes is provided in **Table B-1**.

Table B-1. Gene Deletions & Observed Phenotypes.

Aspergillus nidulans Gene/Name:	TMD:	Predicted function:	Area of Localization:	Deleted	Is Deletion Lethal? Null Phenotype(s) Observed, if any:	Complemented	# of NPF* Motifs	NPFxD Motif:
AN0594/TaoA	No	Actin filament reorganization, cell morphogenesis	Apical crescent only; abruptly stops where endocytic collar is predicted to begin; predicting site of germ tube emergence in conidia; membrane of outermost cells during conidiophore development.	**YES**	Viable	**YES - all phenotypes restored by complement.**	1	P **NPFTD** P
AN2492/EcoA	No	None (best hits and orthologs are both unknown)	Sub-apical collar (strong signal); not present at apical crescent; internalization can be observed from membrane at collar and near apex, minor bidirectional trafficking	**YES**	Viable	**YES - all phenotypes restored by complement.**	3 (2*)	T **NPFLD** D
AN1950/HapA	7	FAD transmembrane transporter activity; Ca^{2+} channel activity; Cell wall involvement; cellular bud neck in yeast (junction for polarization); *S. pombe* ortholog localizes to the cleavage furrow, PM, PM of cell tip, ER, Golgi apparatus, and transport vesicles; null deletion is inviable (as seen here)	Apical crescent; macrovesicles of SPK; septa	**YES**	Lethal; extremely small colonies; unable to transfer or grow tissue in liquid medium.	NO	1	A **NPFDD** E
AN0697/EcoC	No	Actin cortical patch assembly, septin cytoskeleton organization, enzyme inhibitor activity, negative regulation of catalytic activity; 1 signal peptide	Sub-apical collar (weak signal) - not observed in apical crescent or extending distal to apex much at all	**YES**	Lethal; Very small, tight colonies with excessive hyperbranching. Unable to transfer.	NO	1*	S **DPFAD**
AN1462/SlaA	No	Predicted role in actin patch assembly	Concentrated in the sub-apical collar in actin-like patches; punctate; extended away from tip similar to localization of FimA.	**YES**	Lethal; Very small (avg. 0.5-5 mm in diameter) white colonies with no asexual reproduction; unable to transfer. Hülle cells present at times, but no cleistothecia observed.	NO	1*	**NPF** near C terminus
AN6341/CorA	No	Coronin; Protein with similarity to *Saccharomyces cerevisiae* Crn1p; predicted role in actin patch assembly	Concentrated in the collar in actin patches; punctate; extended away from tip like Fim/Sla	NO	Final construct (P7/8) has been created and is ready for transformation.	N/A	1	W **NPFND** D
AN0777/EcoB	No	Intracellular protein transport; contains VHS domain (which is found @ N-term. of proteins associated w/ endocytosis and/or vesicular trafficking/might function as a multi-purpose docking adapter that localizes proteins to the membrane through interactions with the membrane or endocytic machinery); Also contains GAT domain (found only in eukaryotic GGAs), which serves as a molecular anchor of GGA to TGN membranes.	Concentrated in the collar in actin patches; punctate; extended away from tip like Fim/Sla/CorA	NO	Primers have been ordered, but construct is not yet complete or ready for transformation.	N/A	1	Q **NPFAD** N

* = Truncated motifs (NPF or DPF) or full DPFxD motif present

MATERIALS AND METHODS

Strains and Culture Conditions

Deletion strains of *A. nidulans* created in this study were maintained on solid minimal medium (MM) with the necessary nutritional supplements, as described in CHAPTER II. All cultures were incubated at 30°C throughout the course of these experiments. For transformations, 1 mL of 1 x 10^6 freshly harvested conidia were grown overnight in liquid complete medium (CM) with appropriate supplements. Selection occurred on solid MM with 1.2 M sorbitol and appropriate supplements.

Molecular Techniques

All constructs used to create deletion strains through transformation were created via fusion PCR (Szewczyk et al., 2007). Three fragments were individually amplified prior to performing the fusion PCR: a fragment containing the native promoter (1 Kb upstream from the gene of interest), a fragment containing *A. fumigatus riboB* (as a selectable marker to replace the complete coding sequence of the gene), and a fragment containing 1 kb downstream from the gene (**Figure B-1B**). Amplification of the fused construct utilized nested primers (**Figue B-1**), and GFP primers P6 and P8 were also used for the deletion since both constructs included the same third fragment. Phusion™ Flash High-Fidelity PCR Master Mix (Thermo Fisher Scientific™, Waltham, MA, USA) was used for all amplifications. PCR reactions either occurred on a PTC-100 Programmable Thermal

Cycler (MJ Research, Inc., Waltham, MA, USA) or on a T1000 Thermal Cycler (Bio-Rad Laboratories, Inc., Hercules, CA, USA). Further details on construct design were previously published (Schultzhaus et al., 2017a) and discussed in CHAPTER II. All primers were ordered from Integrated DNA Technologies Inc. (Integrated DNA Technologies, Inc., Coralville, IA, USA). A complete list of primers used in this study can be found in **Table A-3**, and each primer is named corresponding to **Figure B-1**.

Complementation

For complementation, a construct was created using existing primers and DNA from the original GFP-tagged strain as a template. Primers ΔP1/7 and GFP-P6/8 were used to amplify the entire gene with GFP::*pyrG*, in addition to 1 Kb up- and down-stream from the gene. This construct was then transformed into protoplasts of the deletion strain. In this case, the complement could also be verified by screening for fluorescence and ensuring that the exact same localization patterns were observed. Both Δ*taoA* and Δ*ecoA* were complemented. All phenotypes observed in the mutants were restored, and each exhibited the same localization patterns as the GFP-tagged strain.

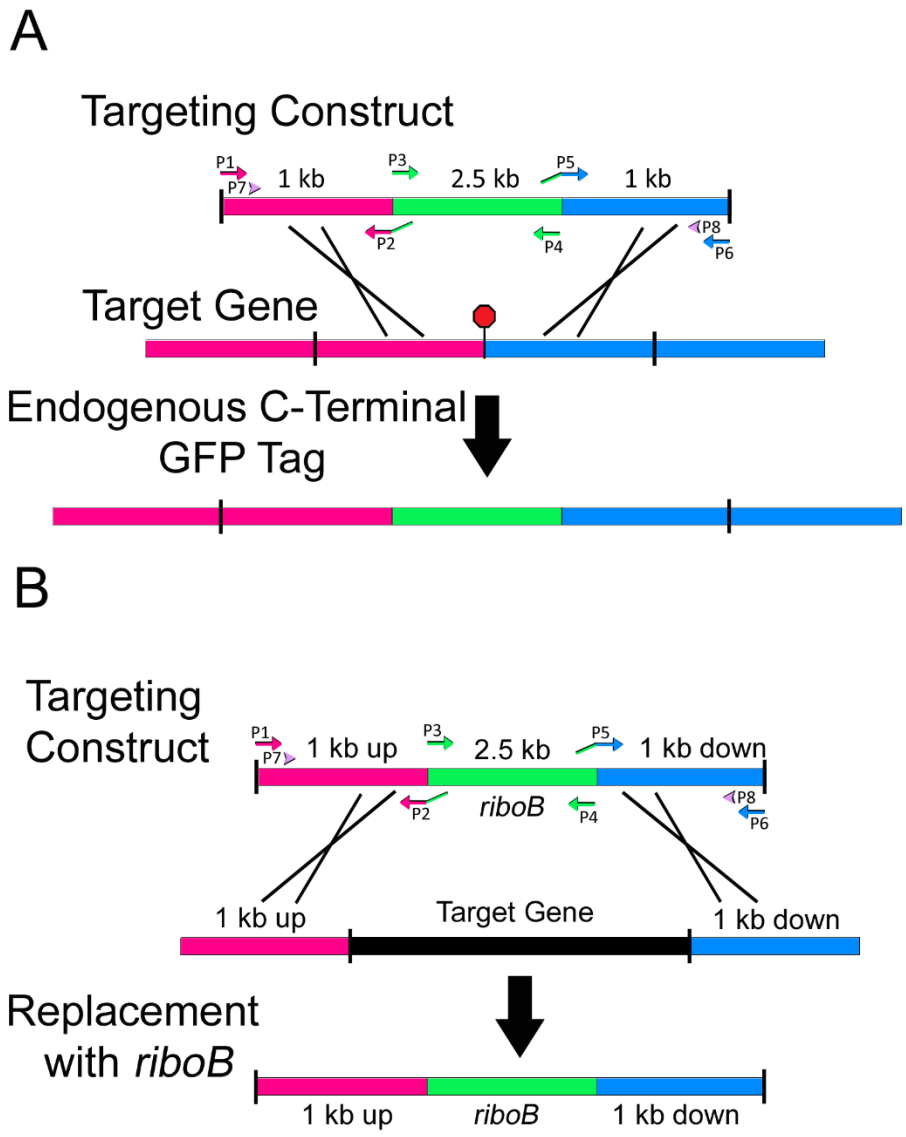

Figure B-1. Primer and Construct Design.
(**A**) Construct design and primer locations for GFP Tags, as compared to (**B**) deletion strains. In deletion constructs, GFP primers P6 and P8 are used again as the third fragment (blue) is the same for each construct. Complements utilized ΔP1/P7 and GFP-P6/P8.

Polyethylene-glycol mediated transformation was performed according to a previously described protocol (Szewczyk et al., 2007) using protoplasts of strain TN02A7 in order to replace the gene of interest. A homokaryon was established for each transformation experiment by single-spore streaking each transformant. A minimum of eight transformants was recovered and confirmed via PCR using primers P1 and P6 to compare the total size of the insert with the known size of the gene. The presence of two bands (one for each the deletion construct and the gene of interest) indicated a heterokaryon and the strain was discarded. One elite strain was then selected and used in all subsequent experiments. Template DNA was acquired by following standard phenol-chloroform procedures with lyophilized mycelium (Sambrook and Russell, 2001).

Microscopy & Slide Preparation

Imaging was performed using an Olympus BX51 microscope (Olympus America, Inc., Melville, NY, USA) outfitted for DIC optics and the Olympus DSU (Disk Scanning Unit) spinning disk confocal imaging system as previously described (Schultzhaus et al., 2016; Upadhyay and Shaw, 2008) and further detailed in CHAPTER II. Strains were grown for a minimum of 24 hours at 30°C prior to imaging. Agar blocks roughly 1 square inch in size were excised from the plate and placed upright on a slide. A minimum of 20 µL of liquid MM was then pipetted on top of the growth, and the coverslip was gently applied. All slides were incubated at 30°C for approximately 15-20 minutes prior to imaging.

GENE DELETIONS

Δ*ecoA* (AN2492)

One phenotype observed in Δ*ecoA* was the inability to maintain a consistent hyphal diameter and shape (**Figure B-2**). This irregular cell shape developed at the forefront of hyphae as the curvature of the apex fluctuated. Once a hypha is established or mature, the diameter does not change to reflect intercalary growth.

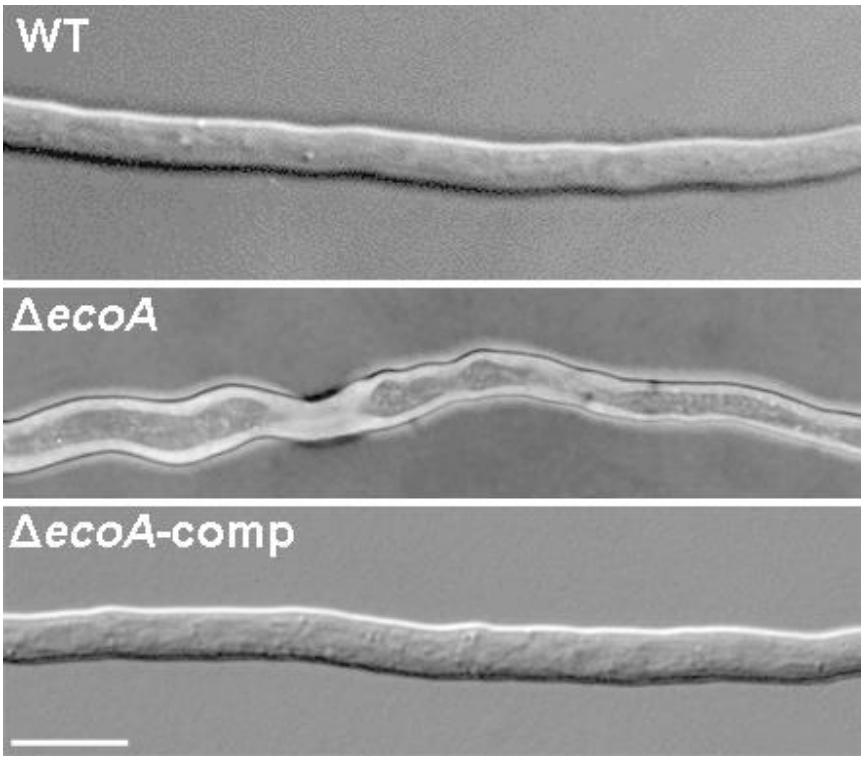

Figure B-2. Inconsistent Hyphal Diameter in Δ*ecoA*.
The diameter of a wild-type (WT) hypha varies only fractions of a micron over time, while Δ*ecoA* is unable to maintain a consistent cell shape or hyphal diameter. Middle panel is a maximum projection of a Z-stack. Phenotype is restored in Δ*ecoA*-complementation strain (bottom). Scale bar is 5 μm.

Another phenotype observed in Δ*ecoA* pertained to lysis at the hyphal apices. Roughly 25-30% of the hyphae observed had either swollen to create a balloon-shaped apex (**Figure B-3**), or ruptured at the apex during growth. This was not a result of adding the coverslip, as was initially hypothesized. The hyphal "ballooning" and lysis could be observed in Δ*ecoA* when plates were viewed on a dissecting microscope, and was evident in varying focal planes within the media both in intact colonies and in prepared slides. This deletion phenotypes is consistent with the localization of EcoA::GFP observed in the sub-apical collar. It is likely that the integrity of the cell wall is compromised at the sub-apical collar of Δ*ecoA*, and that the swelling or lysis therefore occurs at the sub-apical collar and not the actual hyphal apex. This hypothesis is supported by **Figure B-3**, in which a small point is observed at the forefront of each swollen tip. The *Saccharomyces cerevisiae* paralog of EcoA is Pal1, which is involved in the regulation of polar cellular morphology (Swartzman et al., 1996), and is named based on the "*p*ears *a*nd *l*emons" phenotype observed when the gene is deleted. The Δ*pal1* null phenotype is similar to what is observed at the hyphal apices in Δ*ecoA*.

The strain containing Δ*ecoA* was crossed with a strain containing both DnfA::GFP and DnfB::mCherry to evaluate the apical localization of each when a collar-localizing protein was deleted. Little to no disruption in either DnfA::GFP or DnfB::mCherry was noted in this strain (**Figure B-4**).

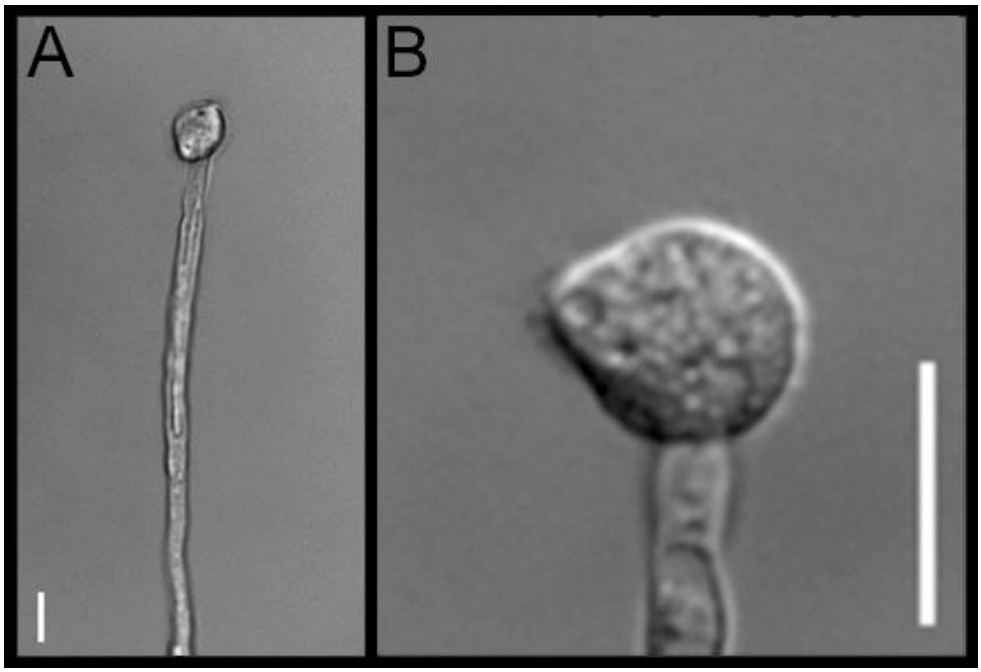

Figure B-3. Cell Lysis Phenotype in Δ*ecoA*.
(**A**) Hyphae in **Δ*ecoA*** exhibit a cell lysis phenotype in which the cytoplasm initially pools at the apex, followed by the cell wall rupturing and cytoplasm emptying. Scale bar is 5 µm. (**B**) Close-up image of a swollen hyphal tip. Scale bars are each 10 µm.

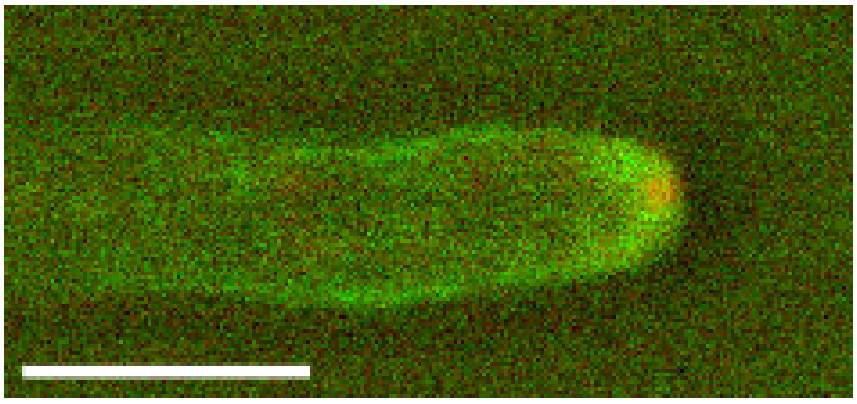

Figure B-4. DnfA::GFP and DnfB::mCherry in Δ*ecoA*.
A hypha with DnfA::GFP and DnfB::mCherry apical localization in Δ*ecoA*. Localization of each of the proteins does not appear to be disrupted. Scale bar is 5 µm.

This strain also quickly created an abundance of cleistothecia (data not shown). Wild type *A. nidulans* produces cleistothecia in an average of 2-3 weeks, whereas Δ*ecoA* typically begins producing them within two days of plating. It is possible that the over-production of cleistothecia is a survival strategy that the strain developed to compensate for the lysis during vegetative growth.

Δ*taoA* (AN0594)

The Δ*taoA* mutant displays anomalous growth, as hyphae frequently leave the axis of polarity (**Figure B-5**). These meandering hyphae likely exhibit a disorganization at the apex, as TaoA::GFP localizes to the apical crescent. This phenotype was restored to WT upon complementation (**Figure B-6**).

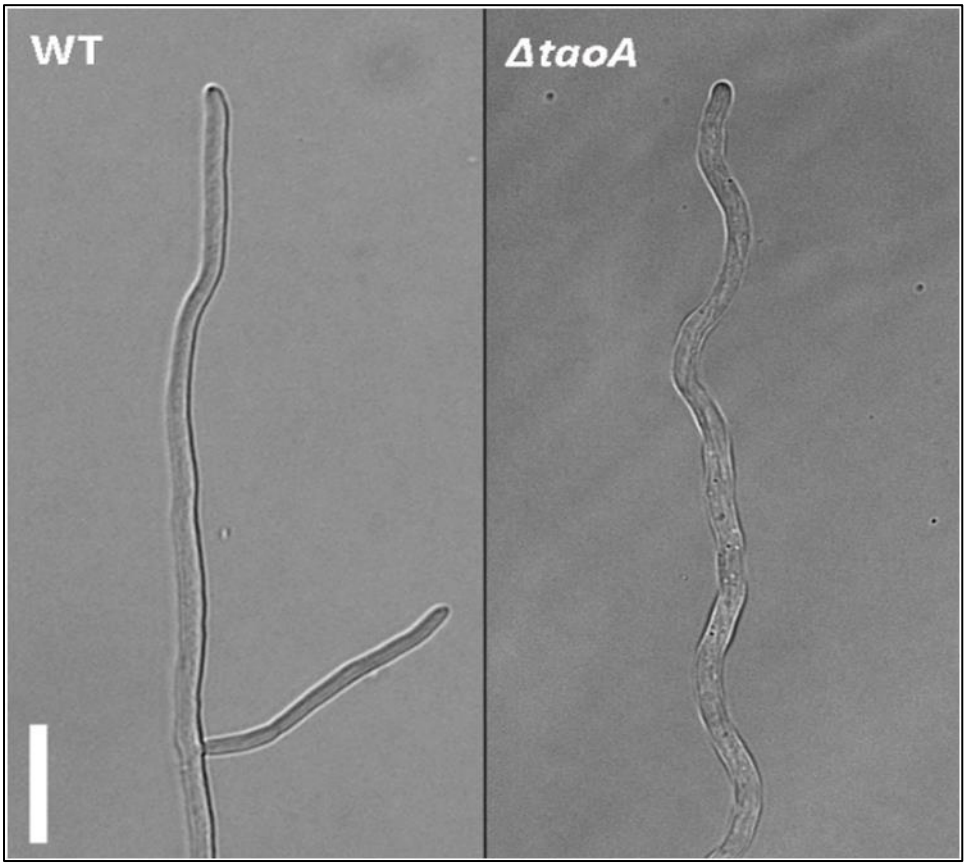

Figure B-5. Meandering Hyphae in Δ*taoA*.
Wild type (WT) hypha (left), compared with a hypha of Δ*taoA* (right). Hyphae in Δ*taoA* were frequently observed leaving the axis of polarity, or meandering. Scale bar 10 μm.

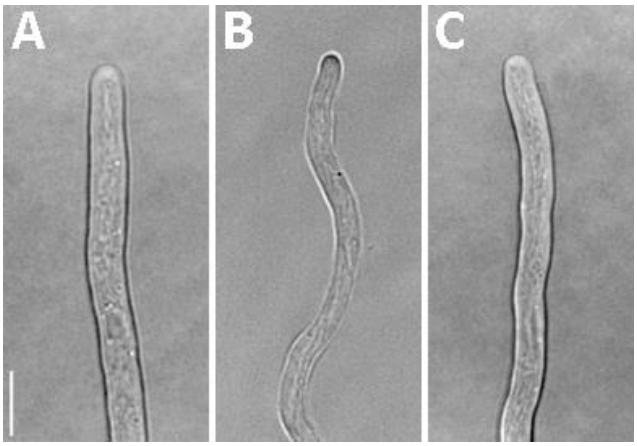

Figure B-6. Meandering Phenotype in Δ*taoA* is Restored by Complement.
(A) Wild type hypha, compared with (**B**) a hypha of Δ*taoA* and (**C**) Δ*taoA*-comp. Hyphae in the complement no longer veered from the axis of polarity. Scale bar is 5 μm.

Cell differentiation and separation are also disrupted during Δ*taoA* vesicle and conidiophore development. Swollen vesicles are frequently observed, as well as metula that revert back to hyphal growth (**Figure B-7**). Septa can also be observed both in conidiophore stalks, as well as in the metula once in hyphal form (**Figure B-7, right**). This phenotype was restored to WT upon complementation (**Figure B-8**). FM4-64 uptake was diminished in conidiophores as well (**Figure B-9**).

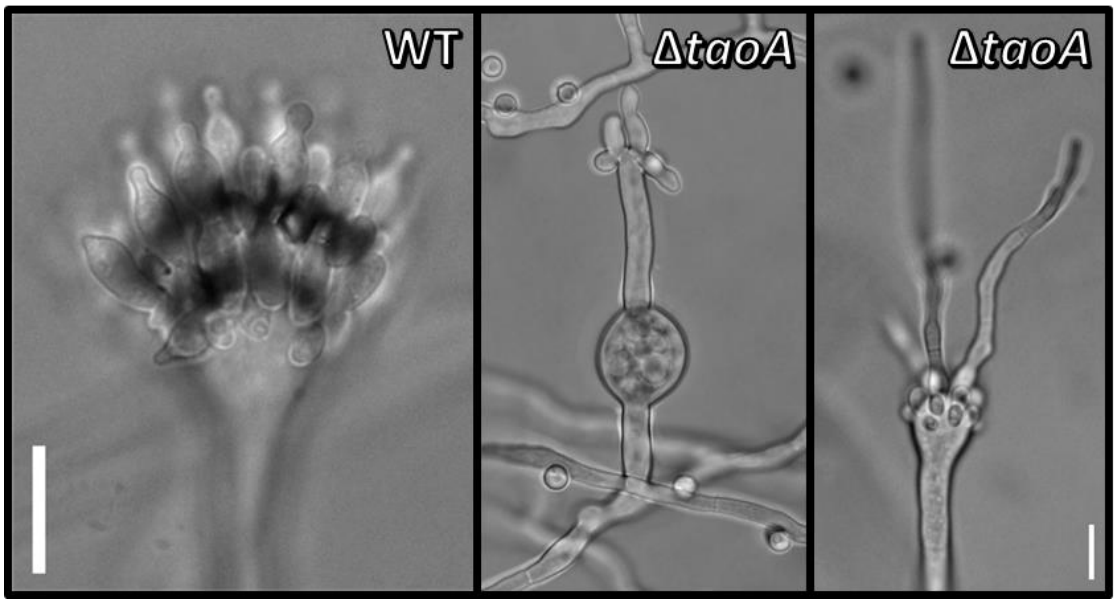

Figure B-7. Conidiophore Defects in Δ*taoA*.
Wild type conidiophore (left) and Δ*taoA* conidiophores exhibiting swollen vesicle (middle) and metula that have reverted back to hyphal growth (middle, right). Cell differentiation from metula is delayed in some conidiophores (middle), and abolished altogether in others (right), in which case septa can be observed in hypha-like metula. Scale bars are each 5 μm.

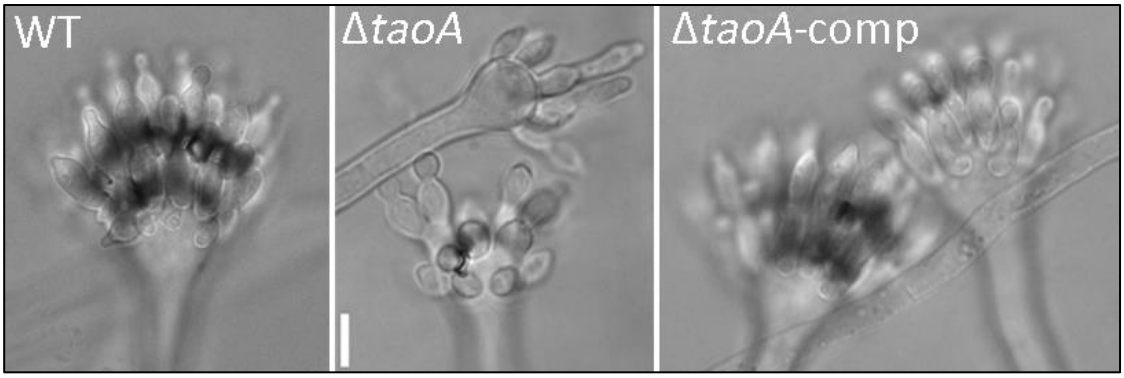

Figure B-8. Conidiophore Defects in Δ*taoA* were Restored to WT.
Wild type conidiophore (left) compared with Δ*taoA* conidiophore (middle) and Δ*taoA* complement. Cell differentiation is asymmetrical and delayed in Δ*taoA* conidiophores, but this phenotype was restored to WT upon complementation (right). Scale bar is 5 μm.

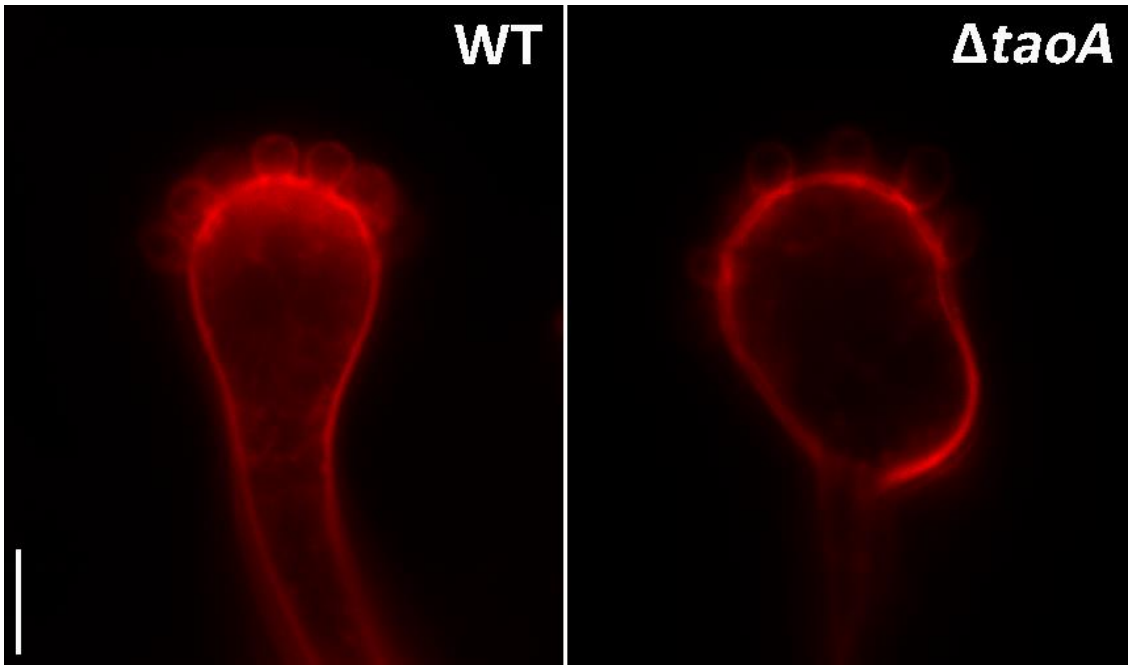

Figure B-9. FM4-64 Uptake in Δ*taoA* Conidiophores.
Uptake and internalization of FM4-64 was clearly diminished in Δ*taoA* conidiophores (right) as compared to WT (left). Scale bar is 5 μm.

Additionally, the formation and the spacing of septa in Δ*taoA* were both irregular (**Figure B-10**).

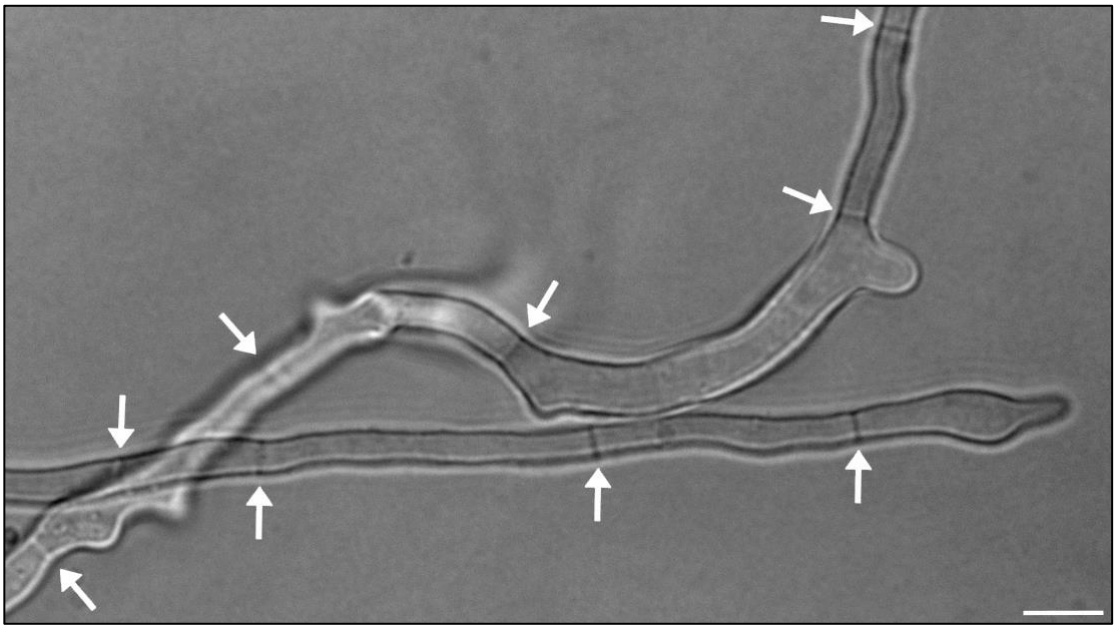

Figure B-10. Formation and Spacing of Septa in Δ*taoA*.
Septa (**arrows**) are overproduced and observed near the hyphal apex here. Septa are also irregularly spaced throughout the mycelium, and branches continue to emerge after septa have been formed. Scale bar is 5 μm.

Δ*ecoC* (AN0594)

The strain containing Δ*ecoC* produced very small, tight-knit colonies. Hyphae exhibited extreme hyper-branching (**Figure B-11**). In yeast, ortholog Syp1 negatively regulates the WASp-Arp2/3 complex activity during endocytic patch formation (Boettner et al., 2009). Accordingly, Syp1 helps to determine the precise timing of actin assembly during endocytosis, and the WASp-Arp2/3 complex acts to create new branches. It makes sense, then, that when *ecoC* is deleted, negative regulation of branch formation is diminished, and branching then becomes excessive.

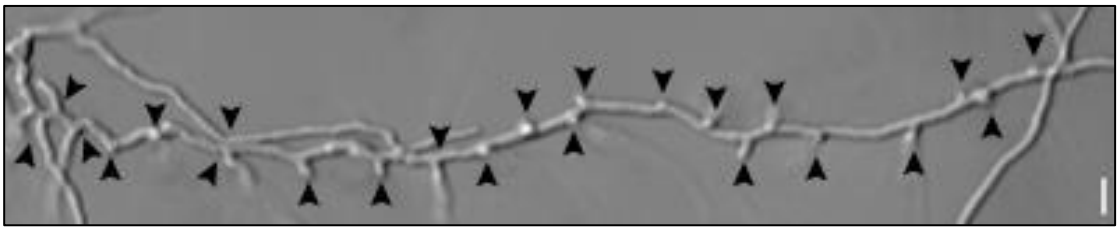

Figure B-11. Δ*ecoC* Hyper-branching Phenotype.
Individual hypha (germinated from the spore in the upper left corner), with sites of branch formation marked (**arrowheads**). Excessive hypher-branching is observed in the very small Δ*ecoC* colonies. Scale bar is 10 μm.

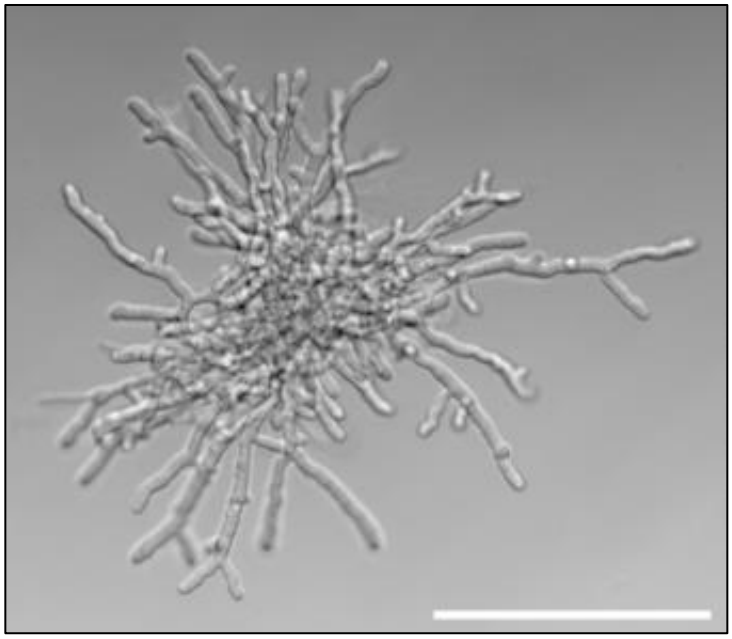

Figure B-12. Δ*hapA* Colony Morphology.
Δ*hapA* colonies were not viable and could not be transferred. Here, an entire colony is imaged after one week of growth. Scale bar is 100 μm.

APPENDIX C

COLOCALIZATION EXPERIMENTS

Strains containing TaoA::GFP, EcoA::GFP, and CorA::GFP were each colocalized with FimA::mCh. Results of colocalization experiments are presented here.

No colocalization was observed between TaoA::GFP and FimA::mCh, as the localization of TaoA::GFP to the apical crescent did not extend far enough to reach the sub-apical collar (**Figure C-1**).

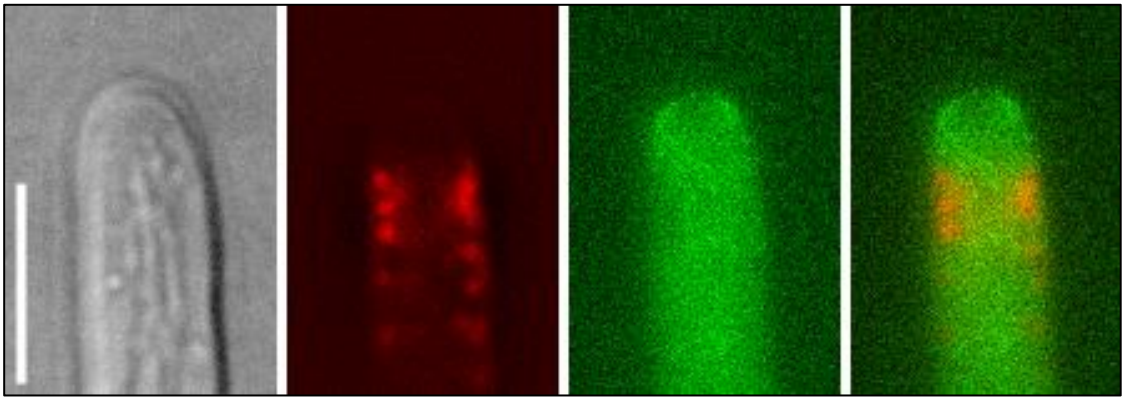

Figure C-1. Colocalization of TaoA::GFP and FimA::mCh.
No colocalization was observed between TaoA::GFP and FimA::mCh. Panels shown (in order from left to right) are BF, FimA::mCh, TaoA::GFP, and merged. Scale bar is 5 μm.

Alternatively, colocalization of EcoA::GFP and FimA::mCh was observed strictly in the sub-apical collar of growing hyphae. Localization of FimA::mCh continued to line the membrane distal to the apex; however, EcoA::GFP localization was restricted to the collar and was not observed in any area distal to the collar (**Figure C-2**).

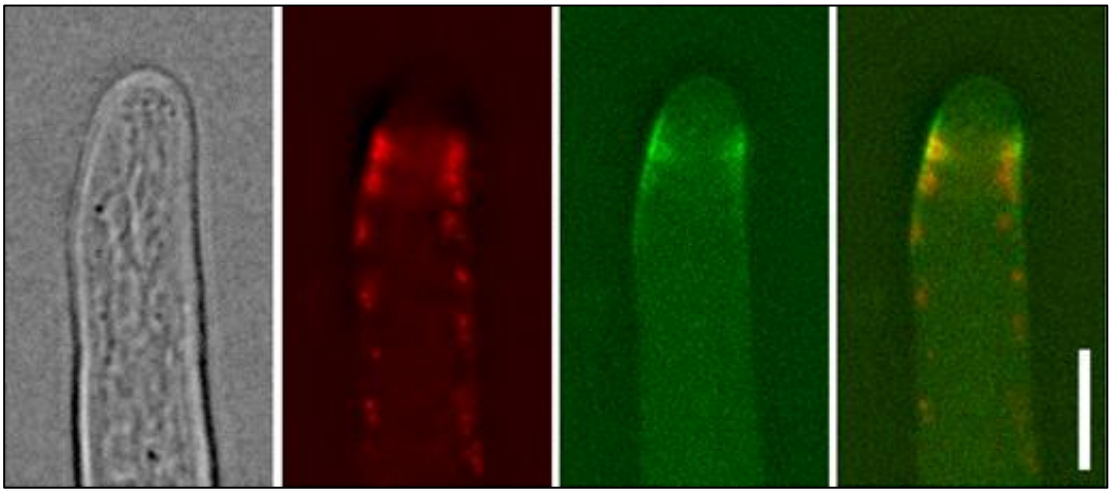

Figure C-2. Colocalization of EcoA::GFP and FimA::mCh.
Colocalization of EcoA::GFP and FimA::mCh was observed strictly in the sub-apical collar of growing hyphae. Panels shown (in order from left to right) are BF, FimA::mCh, EcoA::GFP, and merged. Scale bar is 2.5 µm.

A strain containing both CorA::GFP and FimA::mCherry was also constructed (**Figure C-3**), since each of the proteins is predicted to play a role in cross-linking actin. On the Olympus BX-51 microscope, a smear of red-yellow-green fluorescence was observed in many areas, including the sub-apical collar and individual puncta distal to the collar. It appeared as though the two proteins colocalized, but that the camera could not capture the colocalization perfectly due to the delay in filter rotation. To test this and confirm the colocalization, the strain was then imaged on a microscope with a much shorter time between frame captures.

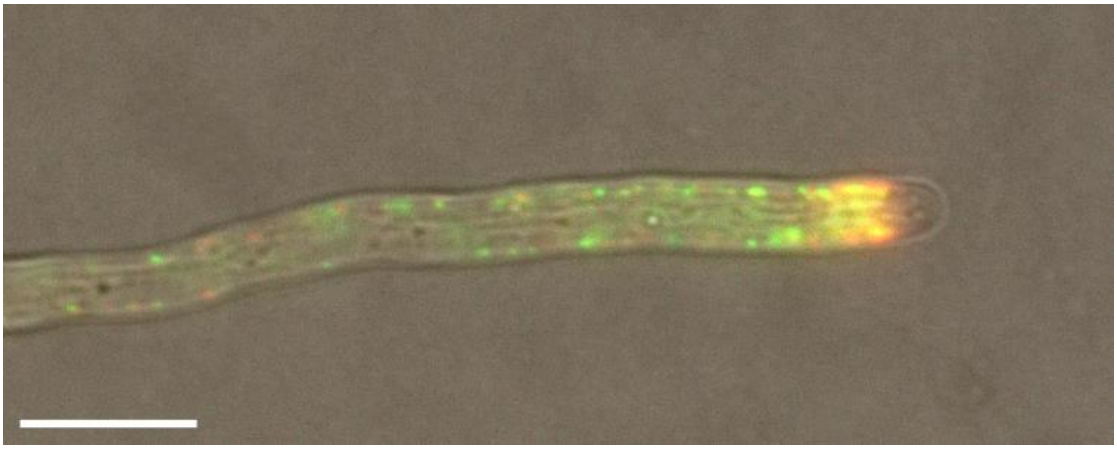

Figure C-3. Colocalization of CorA::GFP and FimA::mCh.
Colocalization of CorA::GFP and FimA::mCh was observed in the sub-apical collar of growing hyphae, and trailed distal to the apex. BF overlay is also shown. Scale bar is 5 µm.

Once the two proteins were able to be imaged with a shorter image acquisition time, it was clear that there was only 25-50% colocalization. This is of important consideration in live-cell imaging, especially when observing proteins which are predicted to be involved in a rapid event like endocytosis. When imaged on a Zeiss Stallion microscope at the TAMU Vet School, it was clear that FimA::mCherry occupied an area of the sub-apical collar closer to the apex of each hypha (**Figure C-4**). The middle of the collar showed colocalization between FimA::mCherry and CorA::GFP, and the late-collar was occupied only by CorA::GFP. Based on this, it is possible that CorA::GFP is localizing to or marking a late-endosome, or a structure tethered to them.

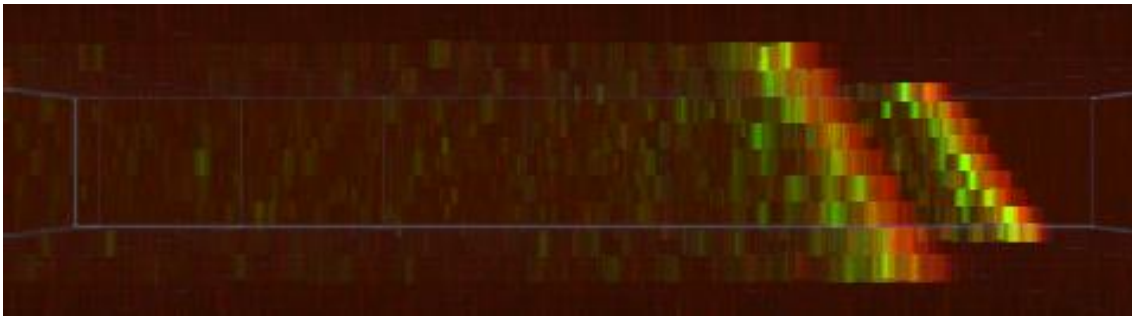

Figure C-4. Time Composition of CorA::GFP and FimA::mCh.
Figure represents a 2D time-lapse converted to a 3D projection image in which the medial planes of two growing hyphae were imaged (the apex of each is growing toward the right side of the image, with one hypha toward the back of the image). The first time-point is represented by the uppermost plane or slice of fluorescence, and subsequent time-points are in order below the first. CorA::GFP and FimA::GFP partially colocalized in the sub-apical collar. Localization of CorA::GFP was observed slightly more distal than FimA::mCh. This suggests that the two proteins may share a similar function, and are potentially tethered to one another, but do not occupy the exact same space. Grid represents 10 μm. Time-lapse frames (horizontal slices) are represented by 10 second sections.

Here, two hyphae were imaged during growth (apices are both facing the right side of the image, with one hypha farther toward the back) to investigate possible colocalization. The endocytic collar was labeled with FimA::mCherry at the most apical end, followed by an area of colocalization, and then an area of only CorA::GFP. Images were collected with exposure times of 250 ms on each channel using an inverted microscope after a 15-minute incubation period. Agar blocks were prepared as previously described (Schultzhaus et al., 2015) and inverted onto a coverslip with 25 μL liquid minimal media prior to imaging. Wild-type, as well as strains expressing only GFP or only mCherry were utilized as controls to ensure there was no fluorescence bleed-through prior to imaging. This figure shows that CorA::GFP and FimA::GFP partially colocalize in the sub-apical collar. Localization of CorA::GFP was observed slightly more distal than FimA::mCh. This suggests that the two proteins may share a similar function, and are potentially tethered to one another, but do not occupy the exact same space.

A strain with CorA::GFP and FimA::mCherry localization was also crossed with the Δ*taoA* strain. Normal localization of each of the tagged proteins is to the sub-apical collar, and neither appears to be disrupted or altered in Δ*taoA* hyphae (**Figure C-5**), which typically displays anamolous growth.

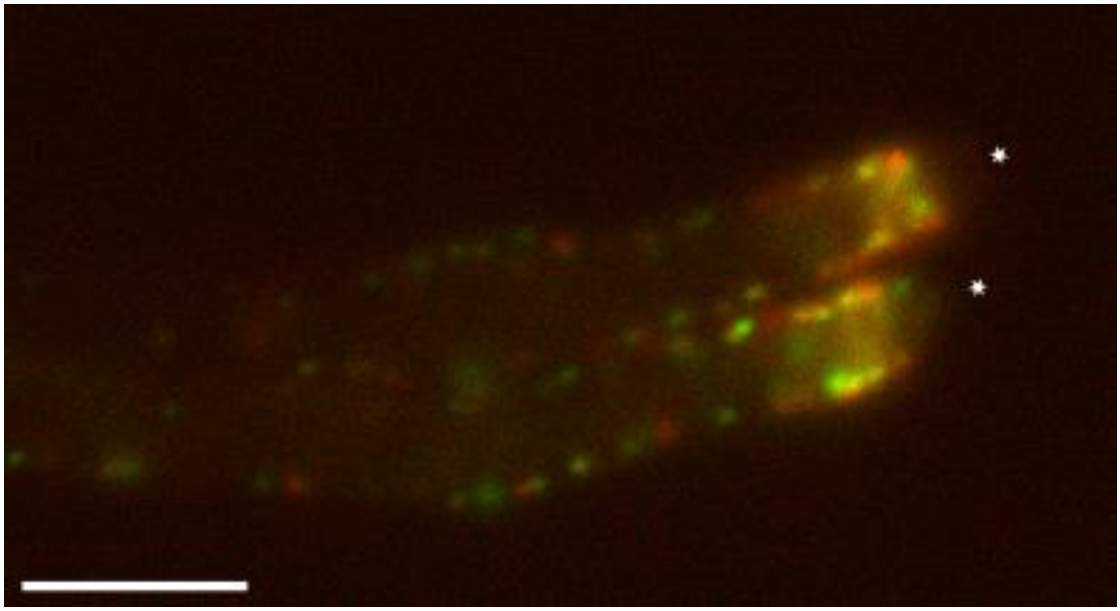

Figure C-5. CorA::GFP and FimA::mCherry in Δ*taoA*.
A hypha with CorA::GFP and FimA::mCherry localization in Δ*taoA*. Normal localization of each of the proteins is to the sub-apical collar, and does not appear to be disrupted or altered in Δ*taoA* hyphae. Apices are marked with asterisks. Scale bar is 5 µm.